

May 2014

Sedimentology and Paleoecology of Fossil-bearing, High-latitude Marine and Glacially Influenced Deposits in the Tepuel Basin, Patagonia, Argentina

Kathryn N. Pauls

University of Wisconsin-Milwaukee

Follow this and additional works at: <https://dc.uwm.edu/etd>

 Part of the [Climate Commons](#), [Ecology and Evolutionary Biology Commons](#), and the [Geology Commons](#)

Recommended Citation

Pauls, Kathryn N., "Sedimentology and Paleoecology of Fossil-bearing, High-latitude Marine and Glacially Influenced Deposits in the Tepuel Basin, Patagonia, Argentina" (2014). *Theses and Dissertations*. 420.
<https://dc.uwm.edu/etd/420>

This Thesis is brought to you for free and open access by UWM Digital Commons. It has been accepted for inclusion in Theses and Dissertations by an authorized administrator of UWM Digital Commons. For more information, please contact open-access@uwm.edu.

SEDIMENTOLOGY AND PALEOECOLOGY OF FOSSIL-BEARING, HIGH-LATITUDE
MARINE AND GLACIALLY INFLUENCED DEPOSITS IN THE TEPUEL BASIN,
PATAGONIA, ARGENTINA

by

Kathryn N. Pauls

A Thesis Submitted in
Partial Fulfillment of the
Requirements for the Degree of

Master of Science
in Geosciences

at

The University of Wisconsin-Milwaukee

May 2014

ABSTRACT

SEDIMENTOLOGY AND PALEOECOLOGY OF FOSSIL-BEARING, HIGH-LATITUDE MARINE AND GLACIALLY INFLUENCED DEPOSITS IN THE TEPUEL BASIN, PATAGONIA, ARGENTINA

by

Kathryn N. Pauls

The University of Wisconsin-Milwaukee, 2014
Under the Supervision of Dr. John Isbell and Dr. Margaret Fraiser

The glacial and non-glacial intervals of the Late Paleozoic Ice Age (LPIA) are of great interest because they are our best deep time analogue for Pleistocene climate change. The changes and adaptations of the biota, as seen in the rock record, can serve as a proxy for understanding future trends in Earth's climate system. Most of the known LPIA marine faunal data come from low-latitudinal regions, and thus have been used as a global proxy. However, modern organisms in the low-latitudes (far-field basins) respond differently to a changing climate relative to marine organisms in the polar regions (near-field basins). In high-paleolatitude regions, glacial and non-glacial communities were ecologically dissimilar and may have had a dissimilar response to climate change relative to contemporaneous fauna at low-paleolatitudes. It is important to understand the how different global climate regimes affected the adaptability of the fauna that lived within them.

This study focuses on a high-latitude fauna from the Tepuel-Genoa Basin in Chubut Province in Patagonia, Argentina in order to better understand the responses of a high-latitude fauna to changing environmental conditions, and to develop a more robust understanding of climate change and its impacts on the biosphere. The Pampa de Tepuel

Formation records Mississippian to Permian depositional history within the Tepuel Basin. Based on current age models for the basin, the analyzed section reported here occurs in the upper portion of the *Lanipustula* biozone, likely from the late Bashkirian to the early Moscovian. Field work consisted of counts of six fossil beds and a 276-meter stratigraphic section was measured and described in order to identify the lithofacies that indicate changes in depositional environments. The fossil count data was analyzed using various methods such as relative abundance comparisons, diversity indices and multivariate tests in order to determine and better define the paleoecology of the *Lanipustula* biozone and its fauna, which has not been accomplished to date.

This particular section of the Pampa de Tepuel Formation in the Sierra de Tepuel is representative of at least two depositional sequences, with evidence of a late highstand and falling stage systems tract in the lower portion of the section followed by a transgressive systems tract at the top of the section. There is also the appearance of slump and slide blocks throughout the section and clinoforms in the middle of the section suggesting that clastics periodically made it into the deeper parts of the basin. Much of the strata described in this study can be related to normal marine processes acting on the outershelf and slope of the Tepuel Basin rather than having occurred in a glacial marine setting. There are only minor glacial signatures observed within this portion of the formation. However, other parts of the Pampa De Tepuel Formation did accumulate in a glaciomarine setting. The paleoecology data suggest that there may be a new faunal composition near the top of the section that does not fit into the *Lanipustula* biozone, although there is no statistically significant difference taxonomically based on the relative abundance values and diversity indices. Results of the multivariate analyses of the

paleocommunities seem to reflect that changes in the local depositional and environmental settings may be the cause for any changes seen in the faunal assemblages within the previously established *Lanipustula* biozone. By continuing research on the LPIA, we may be better able to understand the fundamental factors of species and ecosystem instability because of the substantial environmental and climatic shifts that occurred.

© Copyright by Kathryn N. Pauls, 2014
All Rights Reserved

TABLE OF CONTENTS

LIST OF FIGURES	viii
LIST OF TABLES	xi
ACKNOWLEDGEMENTS	xii
Chapter 1: Introduction	1
Problem	1
Hypothesis	4
Goals	5
Geologic Setting	6
Tepuel Basin	7
Stratigraphy of the Tepuel Group	11
Paleoecology of the Tepuel Group	14
Chapter 2: Methods	18
Sedimentological Analysis	18
Paleoecological analysis	21
Chapter 3. Lithofacies Analysis	25
Fossil-bearing Mudrock Facies Association	31
Description	31
Interpretation	33
Deformed sandstone and mudstone bodies facies association	35
Description	35
Interpretation	38
Horizontally laminated sandstone and mudrock facies association	41
Description	41
Interpretation	44
Rippled cross-laminated facies association	45
Description	45
Interpretation	48
Description	49
Interpretation	52
Massive diamictite facies association	53
Description	53

Interpretation	55
Discussion	56
Chapter 4: Paleoecology Analysis	62
Diversity and Richness.....	64
Trophic and Tiering Analysis.....	69
Multivariate Analyses	72
Discussion	74
Paleoecology of the Lanipustula fauna.....	77
Paleoecology of a potentially new fauna.....	79
Chapter 5. Discussion	82
Chapter 6. Conclusion.....	93
References.....	96
Appendix A.....	123
Appendix B.....	152

LIST OF FIGURES

Figure	Page
Figure 1. Traditional and Recent reconstructions of maximum glaciation during the late Paleozoic Ice Age. A) Traditional reconstruction showing a massive ice sheet. B) Reconstruction of Gondwana during maximum glaciation during the Gzhelian to early Sakmarian (Pennsylvanian–Early Permian) based on recent data and ice flow directions. Ice flow directions are from various studies. C) Location map for selected Gondwana basins and highlands for the Carboniferous and Permian mentioned in the text. From Isbell et al., 2012.	2
Figure 2. Stratigraphic cross section of the Patagonia terrane during the Pennsylvanian. From Ramos, 2008.	6
Figure 3. Plate reconstruction of Gondwana during the late Paleozoic at 310 Ma.	8
Figure 4. Map of Tepuel-Genoa Basin located in central Patagonia, Argentina. Modified from González and Díaz Saravia (2010).	9
Figure 5. Stratigraphy of the Tepuel Group (Jaramillo, Pampa de Tepuel, and Mojón de Hierro Formations) from the Sierra de Tepuel locality. From Freytes, 1971.	10
Figure 6. Stratigraphic cross-section of the Tepuel Basin. From Suero, 1948.	13
Figure 7. Lithostratigraphy and biostratigraphy of the late Paleozoic in the Tepuel Basin. Modified from Taboada, 2008, 2010.	16
Figure 8. Map of Tepuel-Genoa Basin located in central Patagonia, Argentina. Modified from Dineen et al., 2012; González and Díaz Saravia, 2010.	19
Figure 9. Google Earth map showing the location of the study area (indicated by yellow star) relative to the approximate outline of the Tepuel Basin (in red).	20
Figure 10. Google Earth images of the Sierra de Tepuel section, including outline of measured section, and shell bed localities (red circles).	20
Figure 11. Aerial image of the Sierra de Tepuel study area with the measured section (highlighted with red arrows) and the surrounding outcrops. Yellow indicates slide blocks. Orange indicates shelf deposits. Green indicates slide blocks and slumps along the slope.	26
Figure 12. Generalized and simplified stratigraphic column (276m) displaying the facies identified and described in this chapter. Note in Figure 11, that the shell beds (1-5) occur lateral to the measured section and are contained within thick mudrock deposits. Abbreviations of the different facies associations are as follows: Mlm, the mudrock facies; Sdf, deformed sandstone and mudrock, Shl, horizontally laminated sandstone and mudrock; Srl, ripple cross-laminated; Chm, channel-form; Dmm, massive diamictite. See Table 1 for a description and interpretation of the facies associations.	30
Figure 13. Profile view of outcrops displaying the expanse of the mudrock facies association with shell beds labeled (#1-6).	32
Figure 14. Bullet-shaped clast in upper mudrock subfacies.	33

Figure 15. Aerial image of teardrop shape of deformed sandstone bodies.....	36
Figure 16. Small centimeter-scale faults in upper severely deformed sandstone facies association.....	37
Figure 17. Fold nose in upper deformed sandstone subfacies, part of the third and uppermost sand body.	38
Figure 18. Horizontally laminated unit underlying channel-form facies association.	42
Figure 19. Horizontally laminated interbedded sandstone and mudrock facies association.	42
Figure 20. Interfingering wave-rippled facies with horizontally laminated interbedded facies.	43
Figure 21. Interference ripples. Note the mud drape over the rippled surface.	46
Figure 22. Symmetrical ripples and wave ripple laminations. Note the mud drape on top of the symmetrical ripples.....	46
Figure 23. Hummocky cross-stratification interstratified with wave-ripple cross-laminations.	47
Figure 24. Deformed ripples near the top of the ripple cross-laminated facies association.	47
Figure 25. Channel-form facies association, outlined are the channels as amalgamated lenticular bodies. The lenticular bodies of the amalgamated channels have been outlined in yellow. The structural dip of the section is into the photo; whereas, the depositional dip is off to the right.	50
Figure 26. Water escape structures and flame structures seen in the channel-form facies association in the Pampa de Tepuel Formation.	51
Figure 27. Massive diamictite facies association, weakly stratified with pebbles and cobbles suspended in a sandy-muddy matrix.....	54
Figure 28. Pebbles protruding from top of a surface in the massive diamictite facies association.....	54
Figure 29. Aerial image of the Sierra de Tepuel study location. The measured section is marked by the red arrows. The shelf sandstones and slide blocks have been highlighted in bright yellow, and the slumps that are located above the clinoform (here indicated as “Slope”) are highlighted in the lighter yellow; shell beds sampled from are marked by blue circles. The generalized stratigraphic column has been lined up to correspond to the locations of the major sandstone bodies measure in the field.....	57
Figure 30. Sierra de Tepuel field section with the six shell beds (SB #1-6) demarcated. The major stratigraphy features have been highlighted as they relate to the environments in which each paleocommunity was living.	63
Figure 31. Relative abundances of individuals in each shell bed (SB). Shell Beds #1-6, Total = 1261 individuals. SB #1, 308 individuals. SB #2, 89 individuals. SB #3, 330 individuals. SB #4, 387 individuals. SB #5, 92 individuals. SB #6, 53 individuals.....	66

Figure 32. Mean rank-order and Breadth of distribution values of the different faunal Classes recorded in Shell Beds #1-6 in the Pampa de Tepuel Formation. Mean rank-order allows for the ordering of the taxa according to their general abundances, with values closer to 1 indicating the most abundant taxa. Breadth of distribution values measure the proportions of shell beds in which the taxon was present, values equal to 1 indicates that a taxon was present in all shell beds, where values that equal 0.5 indicate a single taxon present in only half of those shell beds.....	67
Figure 33. Comparison of the relative abundance of the individuals in each shell bed (#1-6) displaying various feeding habits as a potential indicator for increase in turbidity throughout the measured section of the Pampa de Tepuel Formation.....	70
Figure 34. Comparison of the relative abundance of the individuals in each shell bed (#1-6) displaying changes in the tiering levels as a potential indicator for environmental stresses in the measured section of the Pampa de Tepuel Formation.	70
Figure 35. Comparison of the relative abundance of the individuals in each shell bed (#1-6) displaying changes in organism mobility as a potential indicator for environmental stresses in the measured section of the Pampa de Tepuel Formation	71
Figure 36. Multivariate analysis for the Pampa de Tepuel Formation, Tepuel-Genoa Basin. Detrended correspondence analysis (DCA) plot showing the relationship of the 6 shell beds studied.	72
Figure 37. Multivariate analysis for the Pampa de Tepuel Formation, Tepuel-Genoa Basin. Non-metric multidimensional scaling (NMS) plot using Chord distance.	73
Figure 38. Multivariate analysis for the Pampa de Tepuel Formation, Tepuel-Genoa Basin. Non-metric multidimensional scaling (NMS) plot using Bray-Curtis index.....	73
Figure 39. Lateral stratigraphic column from the measured field section for this study (276 meters). Note that Shell Beds #1-3 actually occur below the start of the measured portion.	75
Figure 40. Various environmental factors that are known to affect benthic organisms based on their position within a marine environment. Modified from Brenchley and Harper, 1998.	76
Figure 41. The systems tracts of this section of the Pampa de Tepuel Formation, Sierra de Tepuel. The lower half of the measured section represents a late highstand and falling stage systems tract and the upper portion of the section is representative of a transgressive systems tract.	84
Figure 42. A model for sedimentation in this section of the Pampa de Tepuel Formation, Sierra de Tepuel, Argentina. A. Lowstand deposits consist of mass transport processes in which clastics make it into the deep basin. B. Highstand and transgressive systems tracts deposits when the slope and basin floor experience sediment starvation.	86

LIST OF TABLES

Table	Page
Table 1. Facies descriptions and interpretations of this section of the Pampa de Tepuel Formation in the Sierra de Tepuel.	29
Table 2. Comparative table with alpha diversity values for shell beds in the Pampa de Tepuel Formation from a past study (Dineen, 2010) and this current study. Shell Beds #1-6 (with #1 being the lowest stratigraphically and #6 being the highest stratigraphically) in the Pampa de Tepuel Formation. Alpha diversity is the total number of species present within each shell bed.	65
Table 3. Simpson Index of Diversity ($1/D$), Shannon Index (H'), evenness (e), and dominance (d) values for shell beds #1-6 (with #6 as the stratigraphically highest shell bed) of the Pampa de Tepuel Formation. Simpson values range from 0 to 1, with 1 having highest diversity. H' values range from 0 to a maximum of $1/\text{number of groups of organisms}$, with higher values indicating higher diversity. Evenness (e) values range from 0 to 1, with the higher numbers indicating more evenly distributed groups of individuals throughout the shell bed. Dominance (d) values range from 0 to 1, with higher values indicating a dominance of groups of individuals throughout the shell bed.	68
Table 4. Diversity index values from previously published study. Modified from Dineen, 2010.	69

ACKNOWLEDGEMENTS

I would like to express my deepest and sincerest gratitude to Dr. John Isbell and Dr. Margaret Fraiser. Without them, this project would not have been possible. Their continuous support and encouragement over the past two and a half years has taught me to be more confident in myself and my ideas, and I owe a lot of who I am as a scientist today to them. It has been both an honor and a privilege to work closely with these two great scientists, both of whom I look up to. I am also grateful to Dr. Erik Gulbranson for his insight both in the field and while serving on my committee.

I would also like to extend my gratitude to our Argentine colleagues, Dr. Alejandra Pagani and Dr. Arturo Taboada for their expertise in the identification of invertebrate fossils within the field, as well as their assistance in matters of biostratigraphy within the Tepuel Basin. Additional thanks goes to Dylan Wilmeth for his assistance in counting fossils in the field, as well as to Ashley Dineen, who has put up with my incessant list of questions and ideas over the past two and a half years.

I am grateful to the National Science Foundation, the Society for Sedimentary Geologists and the UW-M Geosciences Department for their financial support, as well as to the Edigio Feruglio Paleontologic Museum (Trelew, Argentina) for allowing us to accompany their scientists in the field.

Finally, I would like to thank my parents, Kari and Dennis, and my sister, Emily, for your constant support. Mom, thank you for always reminding me to breathe. Denny, thank you for your constant tech support. And to Emma, thank you for always keeping my sanity in check. Without all of you, I would not be who or where I am today.

Chapter 1: Introduction

Problem

The Late Paleozoic Ice Age (LPIA), which lasted roughly 90 million years during the Carboniferous and Permian, is one of the most important climatic events in Earth's history. The end of the LPIA is the only example in the rock record during which a biologically complex Earth shifted from an icehouse (possibly bipolar) to a greenhouse state (Gastaldo et al., 1996; Isbell et al., 2003, 2012; Soreghan, 2004; Montañez and Soreghan, 2006; Montañez et al., 2007; Fielding et al., 2008a, 2008b). Because of this, the LPIA serves as an analogue for possible changes in climate occurring today (e.g. IPCC, 2007).

Much research concerning the LPIA focuses on determining the timing and extent of the glaciations in Gondwana, the supercontinent that existed during the Paleozoic and Mesozoic, which was composed primarily of Africa, South America, Australia, India, and Antarctica. Past hypotheses implied that there was one large ice sheet that covered Gondwana, and that it persisted for the 70-80 Ma duration of the LPIA (Figure 1) (Frakes, 1979; Scotese, 1999). More recent regional evidence has shown that there were multiple smaller ice centers located across the continent with numerous glacial intervals of several million years separated from non-glacial intervals of equal duration (Crowell and Frakes, 1970; Visser, 1997; Isbell et al., 2003, 2012; Fielding et al., 2008a, 2008b; Gulbranson et al., 2010; Taboada, 2010). These glaciations most likely occurred on smaller scales and in different local regions of Gondwana, which is supported by proxy-based reconstruction of atmospheric CO₂ that suggest atmospheric carbon dioxide levels

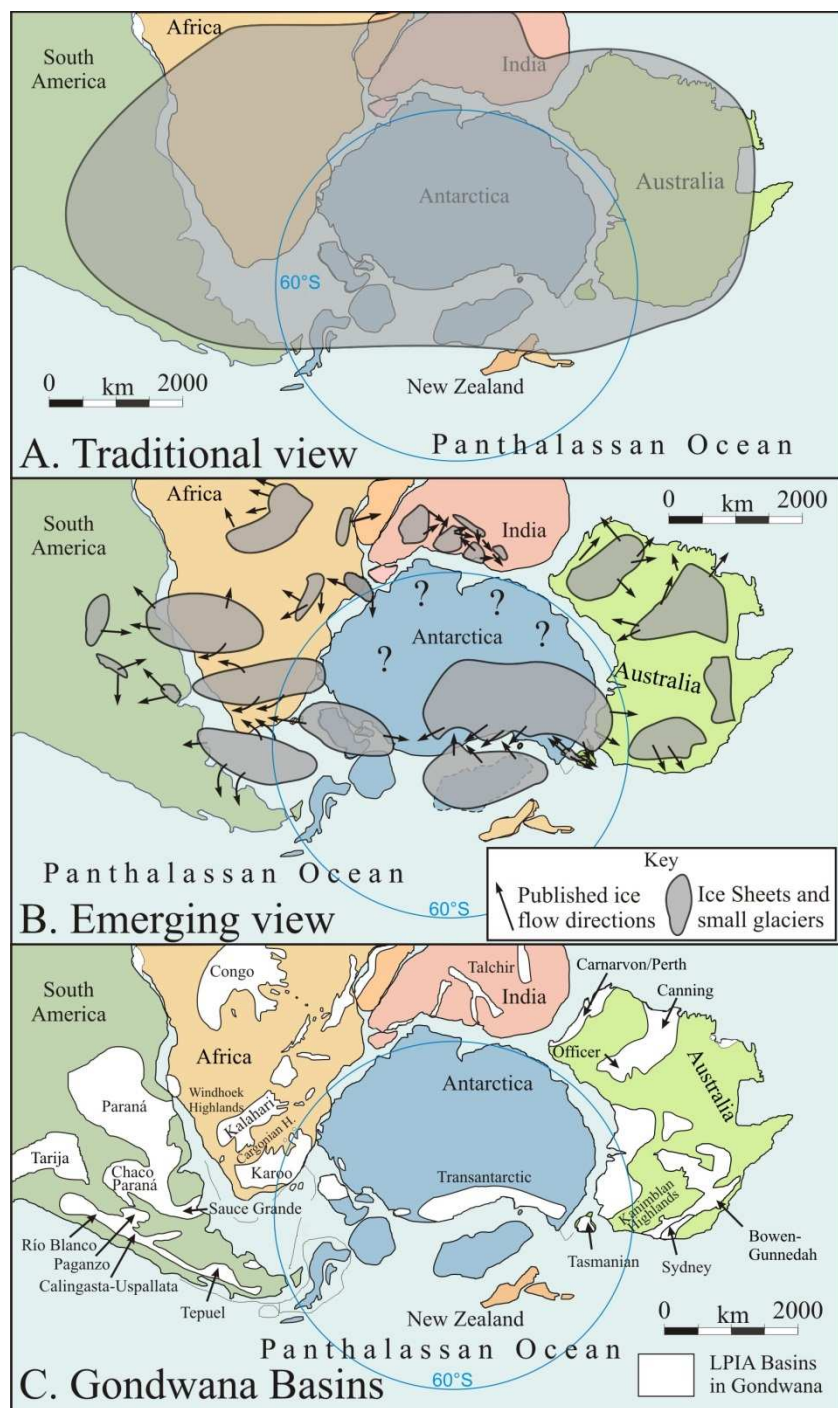


Figure 1. Traditional and Recent reconstructions of maximum glaciation during the late Paleozoic Ice Age. A) Traditional reconstruction showing a massive ice sheet. B) Reconstruction of Gondwana during maximum glaciation during the Gzhelian to early Sakmarian (Pennsylvanian–Early Permian) based on recent data and ice flow directions. Ice flow directions are from various studies. C) Location map for selected Gondwana basins and highlands for the Carboniferous and Permian mentioned in the text. From Isbell et al., 2012.

were low (less than 500 ppm) and modeling studies that indicate that at such low atmospheric CO₂ concentrations only multiple smaller ice sheets would be stable (Royer et al., 2004; Montañez et al., 2007; Poulsen et al., 2007; Montañez and Poulsen, 2013). Thus, an emerging perspective of the LPIA is forming from these studies, providing new insight into the glaciation-climate relationship and the forcing and feedback mechanisms that drive such global change (c.f. Heckel, 1994, 2008; Isbell et al., 2003, 2008; 2012; Royer et al., 2004; Montanez et al., 2007; Davies, 2008; Rygel et al., 2008; Horton and Poulsen, 2009; Gulbranson et al., 2010). Furthermore, there are many paleoenvironmental and paleoecological aspects of the LPIA that are unknown.

Most of what is understood about the biotic effects of the LPIA comes from paleoecological studies of ‘far-field’ (e.g. low-latitude sites, such as North America, Europe and parts of Asia) successions, as opposed to ‘near-field’ records (e.g. high-latitude sites, such as South America, southern Africa, Antarctica, and Australia) which contain glacial deposits. These studies have reported that the LPIA was characterized by low rates of faunal turnover, suggesting instead that faunal and paleoecological compositions persisted and that this was the normal condition during times of high-amplitude and high-frequency glacioeustasy (Stanley and Powell, 2003; Powell, 2005; Bonelli and Patzkowsky, 2008; Heim, 2009; Dineen et al., 2012). It appears that genera with larger geographic ranges due to broader physiological adaptations and habitat preferences came into dominance during the LPIA (Bonelli and Patzkowsky, 2008; Clapham and James, 2008). The results from these far-field studies are often taken to be the example for the whole globe. However, newer evidence has shown that the near-field biota of Gondwana did not respond in the same manner as low-latitude faunas

(Waterhouse and Shi, 2010). In contrast to these far-field studies, a recent study conducted on two LPIA near-field basins from western Argentina, the Paganzo Basin and the Río Blanco Basin, has shown that marine invertebrates were living in ecologically complex and diverse faunal assemblages (Dineen et al., 2012). Even though these two basins are at a similar paleolatitude, there were recorded differences in the changes of the faunal compositions, such as an increase in ecological diversity in one location while there was a decrease in diversity in another location. These differences were most likely due to different positions that they occupied within glacial depositional environments due to the proximity to marine-ending glaciers (Dineen et al., 2012). Further studies are needed in order to add to our understanding of how the biota are affected within these changing high-latitude depositional systems. A study of the Pampa de Tepuel Formation within the near-field Tepuel-Genoa Basin (also Tepuel Basin) and the *Lanipustula* biozone will add to this understanding as there has not yet been a complete paleoecological analysis of the *Lanipustula* biozone and its fauna.

Hypothesis

The ultimate goals of this research project are to understand the depositional environments in a near-field setting during the LPIA, such as the Pampa de Tepuel Formation within the Tepuel Basin, and to determine the relationship of faunal diversity and abundance as a function of paleoenvironment by specifically determining the ecology of the fauna composing the *Lanipustula* biozone. The hypothesis to be tested states that changes in depositional environments at high-paleolatitudes, whether in glacially-influenced or open marine conditions, will affect the biota that live there and may create changes within paleocommunity compositions. The *Lanipustula* biozone in the Tepuel

Basin in southern Argentina provides the means for an in-depth study of a local high-latitude LPIA ecosystem, which can then be linked back to global ecological patterns (e.g., Stanley and Powell, 2005; Clapham and James, 2008; Bonelli and Patzkowsky, 2008; Powell, 2008). Although the *Lanipustula* fauna is endemic to the Tepuel Basin, the patterns and trends determined in the paleoecology can be used as a proxy for fauna living in similar conditions later in the rock record. The LPIA is important for understanding the fundamental factors of ecosystem instability because of the substantial environmental and climatic shift that occurred. By continuing research on the LPIA and its changing climate, we may be better able to understand how the biota responded to changing environmental conditions.

Goals

The overall goals for this project are to determine the composition of the paleocommunities within a measured section of the Pampa de Tepuel Formation, and to assess the relationship of ecosystem composition to depositional environments and how those changed through time, using aspects such as relative abundance, diversity, and guild organization. In addition to that, I am looking at the depositional processes via the construction of a stratigraphic column and identification and interpretation of the lithofacies throughout the section in order to aid in the understanding of the environmental transitions in this near-field basin during the LPIA. The data developed from this project will further help to define the overall impact of environmental change on marine faunal communities during the LPIA.

Geologic Setting

Present-day southern Argentina was part of the southwestern margin of Gondwana which experienced a complex geologic history due to tectonic, sea-level and climate changes that occurred during the LPIA (Figure 2). Patagonia, which is the southernmost region of Argentina, had a tectonic history during the late Paleozoic that is still to be resolved. There are several hypotheses regarding the paleogeography of the Patagonian terrane, including two opposing viewpoints: one proposes that Patagonia was previously accreted to Gondwana by the Devonian (e.g., Dalla Salda et al., 1990), and another proposes that Patagonia was an allochthonous terrane (Pankhurst et al., 2006; Ramos 2008; Rapalini et al., 2010). Recent paleomagnetic dating and geophysical studies suggest that Patagonia accreted to the Antarctic Peninsula during the Carboniferous, and then later accreted to South America during the Permian (Pankhurst et al., 2006; Ramos, 2008; Rapalini et al., 2010; Henry et al., 2012).

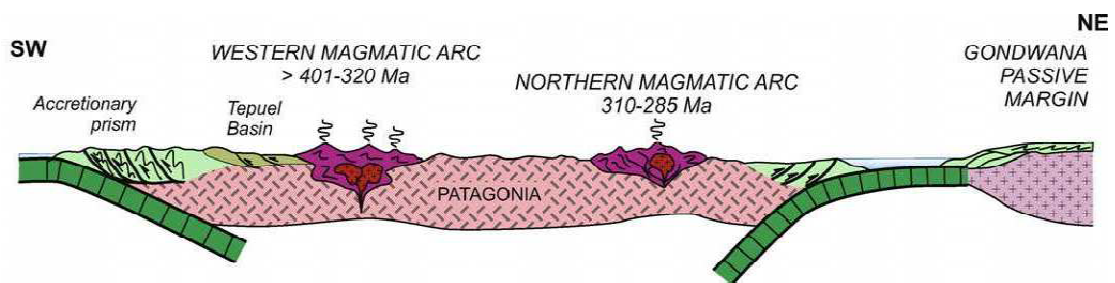


Figure 2. Stratigraphic cross section of the Patagonia terrane during the Pennsylvanian. From Ramos, 2008.

Tepuel Basin

The Tepuel Basin, also referred to as the Tepuel-Genoa or the Langiñeo-Genoa Basin (i.e. López Gamundí, 1987, 1989; Gonzalez, 1993), is today located in western Patagonia. During the LPIA, the Tepuel basin was located near or within the South Polar Circle at approximate 70-80°S paleolatitude (Gonzalez-Bonorino, 1992; Figure 3). Owing to the two different hypotheses over the accretionary processes of the Patagonian terrane, the Tepuel Basin has been interpreted as both a forearc and a foreland basin (Limarino and Spalletti, 2006; Ramos, 2008; Taboada and Shi, 2011). However, recent work suggests that the Tepuel Basin was a foreland basin, which formed adjacent to a magmatic arc during the accretion of Patagonia to the Antarctic Peninsula (cf. Pankhurst et al., 2006; Ramos, 2008; Rapalini et al., 2010; Henry et al., 2012). In either scenario, the basin was a rapidly subsiding embayment along the Panthalassan margin of Gondwana.

In comparison to other basins in Gondwana (e.g., Paraná, Calingasta-Uspallata, Karoo, Transantarctic, Tazmanian), the Tepuel Basin contains perhaps the only continuous succession of strata due to high subsidence rates, with strata ranging from the Early Mississippian to the Early Permian (Tournasian to Artkinsian) (cf. López Gamundí, 1997; Limarino and Spalletti, 2006; Rocha-Campos, 2008; Fielding et al., 2008; Isbell et al., 2003, 2012). The basin consists of nearly 5,000 meters of glaciogenic marine rocks, which comprise the Tepuel Group (i.e. the Jaramillo Formation, the Pampa de Tepuel Formation, and the Mojón de Hierro Formation) in the Sierra de Tepuel and El Molle; the Río Genoa Formation in the Río Genoa Valley; and the Las Salinas Formation in Langiñeo Hills (Figure 4 and 5; Keidel, 1922; Piatnitzky, 1933, 1936; Suero, 1948,

1953, 1958; Freytes, 1971; Lesta and Ferello, 1972; Franchi and Page, 1980; Andreis et al., 1987, 1996; Lopéz Gamundí, 1989, 1997).

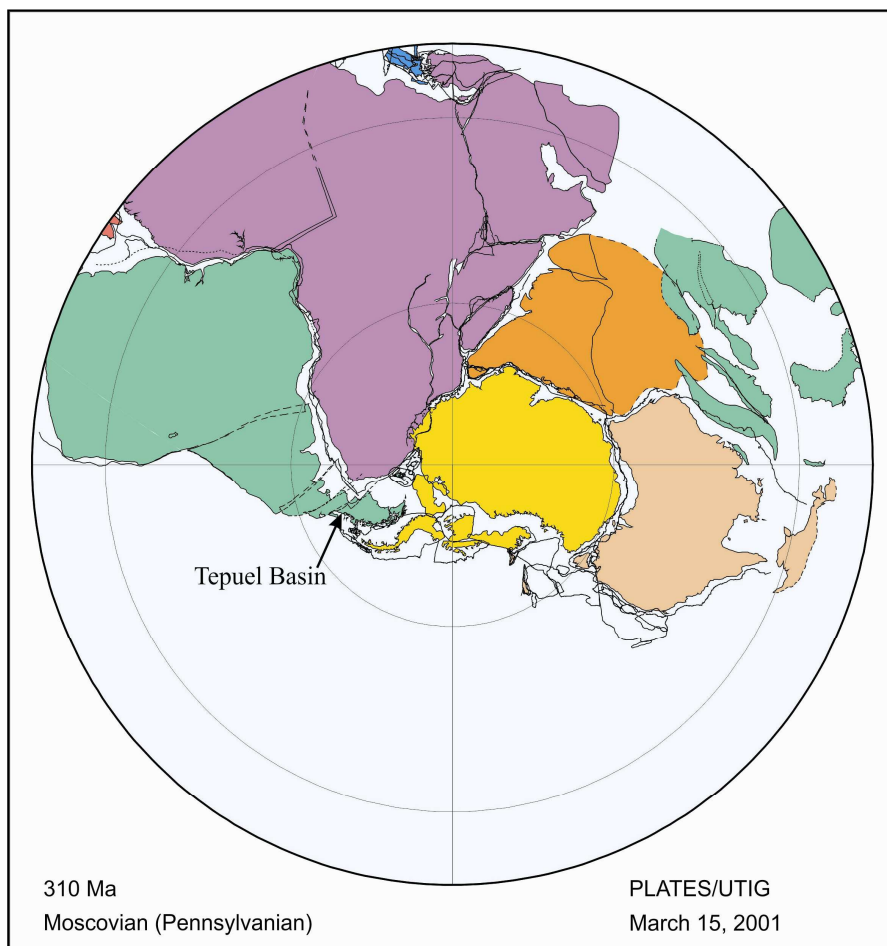


Figure 3. Plate reconstruction of Gondwana during the late Paleozoic at 310 Ma.

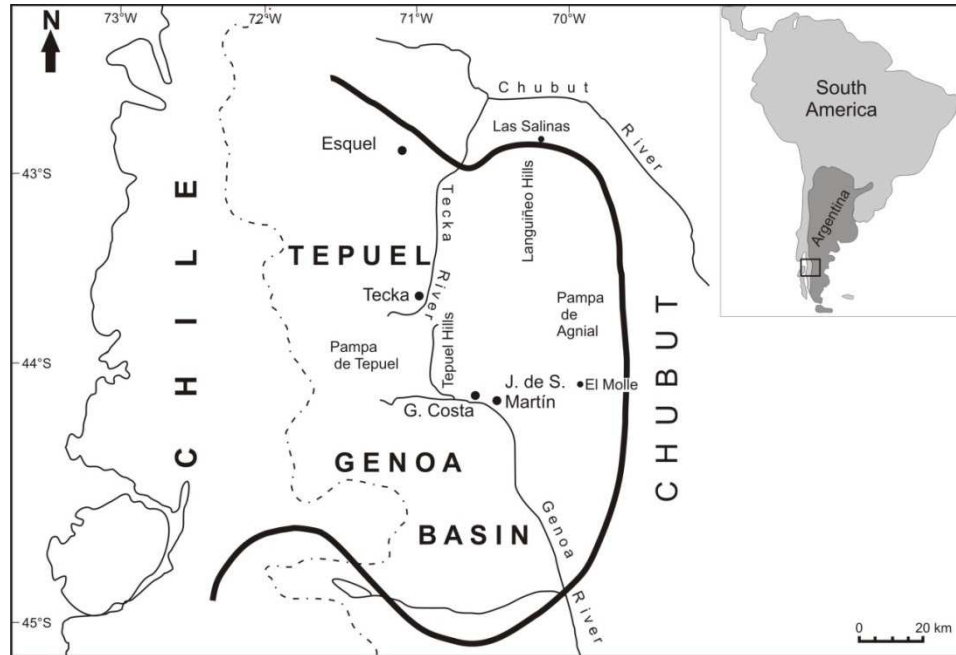


Figure 4. Map of Tepuel-Genoa Basin located in central Patagonia, Argentina. Modified from González and Díaz Saravia (2010).

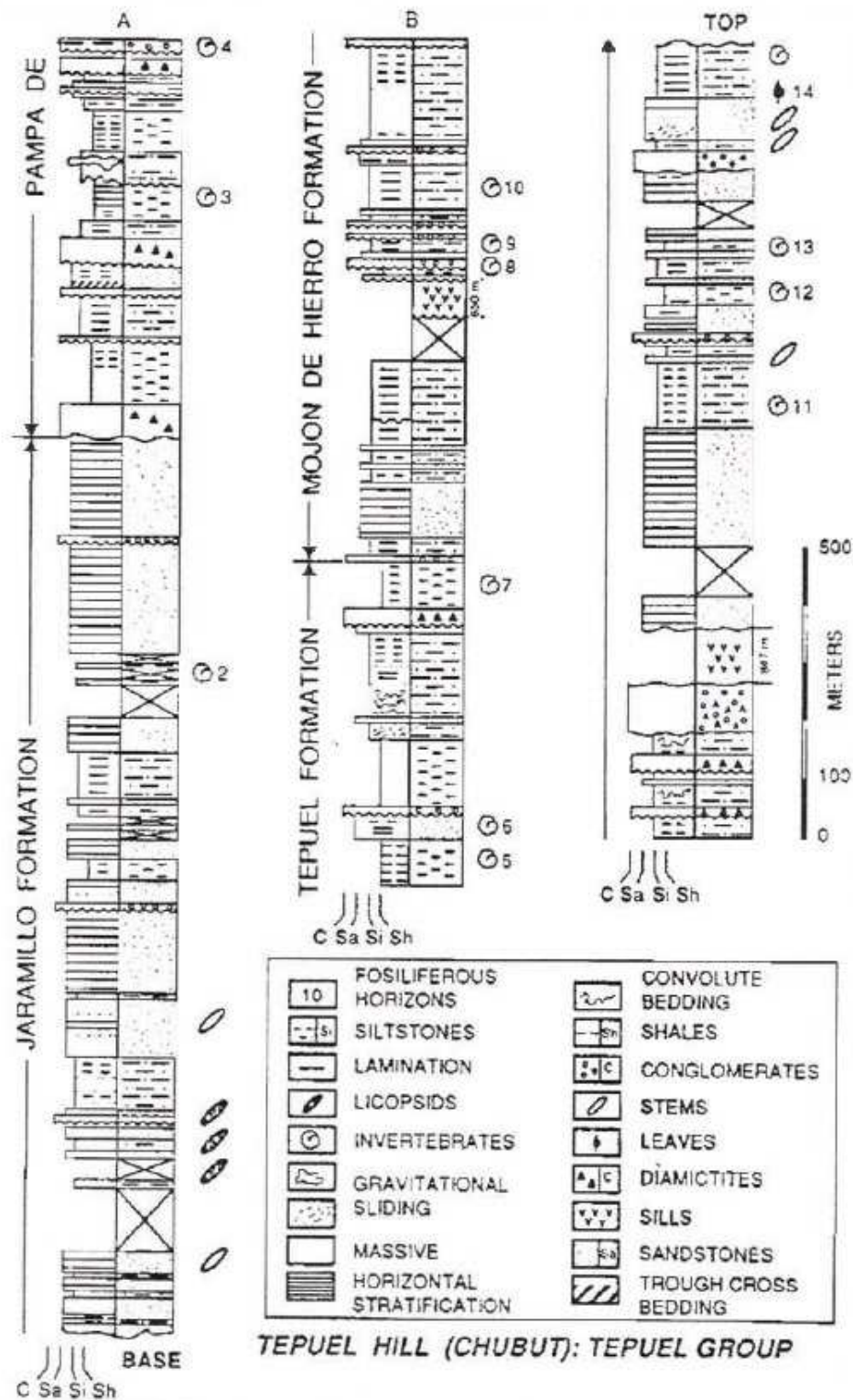


Figure 5. Stratigraphy of the Tepuel Group (Jaramillo, Pampa de Tepuel, and Mojón de Hierro Formations) from the Sierra de Tepuel locality. From Freytes, 1971.

Stratigraphy of the Tepuel Group

The Tepuel Group comprises more than 5,000 meters of the strata within the basin, and is divided into three main formations, the Jaramillo, the Pampa de Tepuel, and the Mojón de Hierro (Page et al., 1984; Pagani and Taboada, 2010). The Jaramillo Formation was deposited during the Viséan and consists of approximately 1,000 meters of littoral sandstone deposits in open shelf environments (Figure 6). This succession represents the depositional environments before the onset of glaciation into the basin (Pagani and Taboada, 2010). The thickest succession in the basin, at over 2,900 meters, is the Pampa de Tepuel Formation, deposited during the Middle Carboniferous to Early Permian (Visean to middle Asselian), and is characterized by mudstone, sandstone, conglomerate, and diamictite (Gonzalez Bonorino et al., 1988; Taboada, 2010). The interpretations of the depositional environments of the Pampa de Tepuel Formation have been controversial. The formation was originally interpreted as a glacially-influenced marine deposit (Suero, 1948), which was further supported by later studies (Frakes et al., 1969; Frakes and Crowell, 1969; López Gamundí and Limarino, 1984; Page et al., 1984; López Gamundí, 1987; González Bonorino et al., 1988; González Bonorino, 1992). It has also been previously regarded as a more continental succession that was deposited by glaciers at the shoreline or in the littoral zone as the glaciers advanced and retreated within the basin (González, 1972, 2002; González and Glasser, 2008; González and Díaz Saravia, 2010). Within the Pampa de Tepuel Formation, there are six diamictites that have been identified by Taboada (2010) as potentially representing six different glacial events. However, the diamictites may have also resulted, in part, from other depositional processes, including: debris flows associated with submarine channels and fans, shallow

marine gravity flows, and direct influence of grounded glaciers (Frakes et al., 1969; Frakes and Crowell, 1969; Page et al., 1984; López Gamundí and Limarino, 1984; López Gamundí, 1987; Gonzalez Bonorino et al., 1988, 1992; González, 1972, 2002). The Pampa de Tepuel Formation also contains several fossiliferous horizons which are used to biostratigraphically date the formation (Pagani and Taboada, 2010; Taboada and Shi, 2011). The youngest portion of the Tepuel Group is the Mojón de Hierro Formation, which was deposited during the Permian (Asselian-Artinskian) and consists of marine blue-black shale at the base, which may represent a short-lived rise in sea level that grades into more continental sandstone and conglomerate near the top, as well as diamictites and sandstones (Gonzalez Bonorino, 1992; López Gamundí, 1997; Díaz Saravia and Jones, 1999).

Paleoecology of the Tepuel Group

There have been several marine biostratigraphic zonations used over the years to describe the units within the Tepuel Basin. The first and most widely-used scheme was introduced by Amos and Roller (1965) and was based on the identification of two brachiopod taxa, *Levipustula levis* and *Cancrinella farleyensis*. The biozones have since been modified several times (e.g. Amos et al., 1973; González, 1981; Archangelsky and Marrquez Toigo, 1980; Simanaukas and Sabbattini, 1997; Taboada, 2001; Pagani and Sabbattini, 2002; Taboada et al., 2006; Taboada and Shi, 2008; Taboada and Pagani, 2010), and thus creating the controversy over the exact age and timing of the depositional environments within the basin. The depositional environments in the basin appear to shift from littoral deposits of the Jaramillo, to glaciomarine deposits of the Pampa de Tepuel, and finally to marine and glacially influenced marine deposits of the Mojón de Hierro (López Gamundí, 1989; Gonzalez, 2006; Pagani and Taboada, 2010). The faunal assemblages within the Tepuel Group are thought to reflect these shifts in environments, starting with the lack of an easily identifiable biozone in the Jaramillo Formation (Pagani and Taboada, 2010).

Within the Jaramillo, there have been few, poorly-preserved fossils recovered, but they have been identified as belonging to a brackish water fauna, including gastropods and bivalves along with some plant remains (Díaz Saravia and Jones, 1999; Pagani and Taboada, 2010). The Pampa de Tepuel Formation contains at least two Pennsylvanian-aged marine faunal assemblages composed mostly of cold-water invertebrate organisms (Suero, 1948; Simanaukas, 1996; Simanaukas and Sabbattini, 1997; Taboada et al., 2006; Pagani and Taboada, 2010) (Figure 7). The first and oldest faunal assemblage is

the *Lanipustula* biozone, which was previously categorized as the *Levipustula levis* biozone, which also occurs in western Argentine, Antarctic and eastern Australian basins (Simanaukas, 1996; Simanaukas and Sabbattini, 1997; Taboada, 2001; Taboada et al., 2006; Taboada and Shi, 2008; Pagani and Taboada, 2010). The *Lanipustula* biozone is classified as a cold-water fauna, characterized by *Lanipustula patagoniensis* as well as other brachiopods, bivalves, gastropods, bryozoans, ostracods, corals, and scarce trilobites (Suero, 1948; Simanaukas, 1996; Simanaukas and Sabbattini, 1997; Taboada et al., 2006; Pagani and Taboada, 2010). This biozone has most recently been interpreted to span the middle Carboniferous (Serpukhovian-Bashkirian) or the middle Late Carboniferous (Moscovian-Kasimovian), but appears to be no younger than the Westphalian (Taboada, 2001, 2008; Taboada et al., 2006; Taboada and Shi, 2008; Pagani and Taboada, 2010). The second faunal assemblage in the Pampa de Tepuel Formation is the *Tuberculatella* Zone, which appears about 500 m above the *Lanipustula* Zone and continues to the top of the formation, covering about 700 m of the

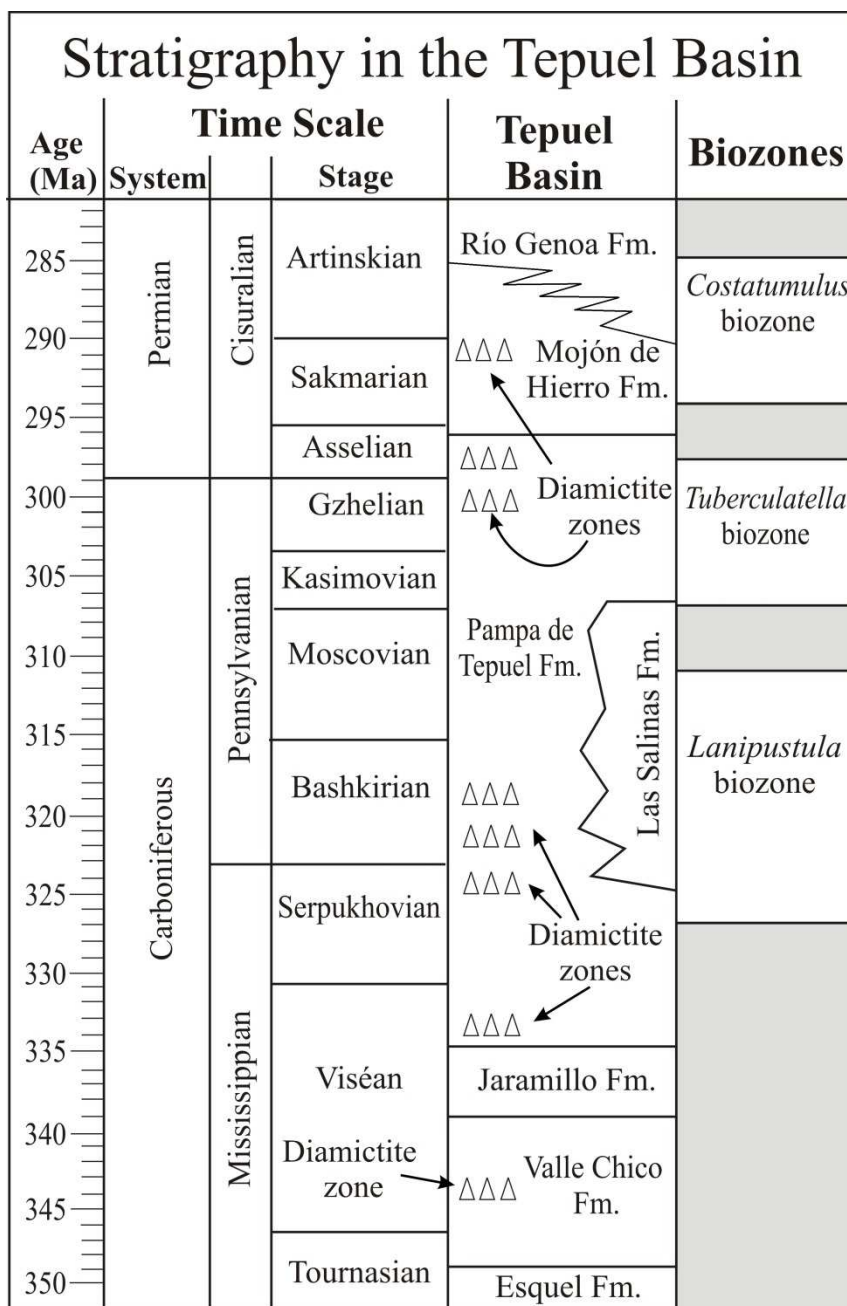


Figure 7. Lithostratigraphy and biostratigraphy of the late Paleozoic in the Tepuel Basin. Modified from Taboada, 2008, 2010.

formation (Taboada, 2001, 2008; Taboada et al., 2006). This fauna is characterized by the brachiopod *Tuberculatella laevicaudata*, and contains a fauna similar to the previous *Lanipustula* assemblage, but is altogether more brachiopod-dominated with the additional appearances of *Verchojania archboldi* sp., *Amosi sueroi* Simanauskas, and *Beecheria patagonica* (Taboada et al., 2006; Taboada, 2008; Pagani and Taboada, 2010). The *Tuberculatella* fauna shifts in the Mojón de Hierro Formation to the warmer-water fauna of the *Costatumulus* Biozone, which coincides with the climate amelioration and sea level rise that occurs during this time (Gonzalez, 2006; Taboada et al., 2006). This faunal assemblage includes brachiopods, including its namesake *Costatumulus amosi* sp., bivalves, gastropods, bryozoans, cephalopods, and crinoids (Suero, 1948; Taboada, 2001, 2008; Taboada et al., 2006; Pagani and Taboada, 2010).

Chapter 2: Methods

I conducted field work in March 2012 in Patagonia, and was aided in the field by Dr. Margaret Fraiser, Dr. John Isbell, Dr. Erik Gulbranson (UWM), Dr. Arturo Taboada (LIEB) and Dr. Alejandra Pagani (CONICET), and Dylan Wilmeth (UWM). This project is part of a more extensive project examining the strata and paleoecology of the LPIA in Patagonia by the members of the field party. Sedimentological and paleoecological methods both in the field and in the laboratory were used to reconstruct the paleoenvironments of the Tepuel-Genoa Basin.

Sedimentological Analysis

For this project I examined the marine strata of the Pampa de Tepuel Formation in the Sierra de Tepuel within the Tepuel-Genoa Basin (locality coordinates, S 41°41'43", W 70°43'46", Figures 9,10). The Sierra de Tepuel locality was chosen because it contains one of the most continuous successions of the Tepuel Group strata (Figure 7). During field work sedimentary and deformational structures, lithology, contacts, and bounding surfaces were described and analyzed using standard sedimentological techniques to measure a stratigraphic section, using a Jacob's staff, abbney level and Brunton compass. This data was then used to create and construct stratigraphic columns as well as to conduct a facies analysis. The sedimentary and soft-sediment deformational and structures were studied reconstruct depositional settings and apparent sea-level change. The facies analysis was used in conjunction with the paleoecological data gathered to 1) interpret the changing depositional environments, 2) record the glacial influence on the system, 3) understand the changes that shelf-slope environments undergo

during sea-level transgressions, and 4) determine the various physical stresses that affect the marine system, which aids in paleoecological studies.



Figure 8. Map of Tepuel-Genoa Basin located in central Patagonia, Argentina. Modified from Dineen et al., 2012; González and Díaz Saravia, 2010.

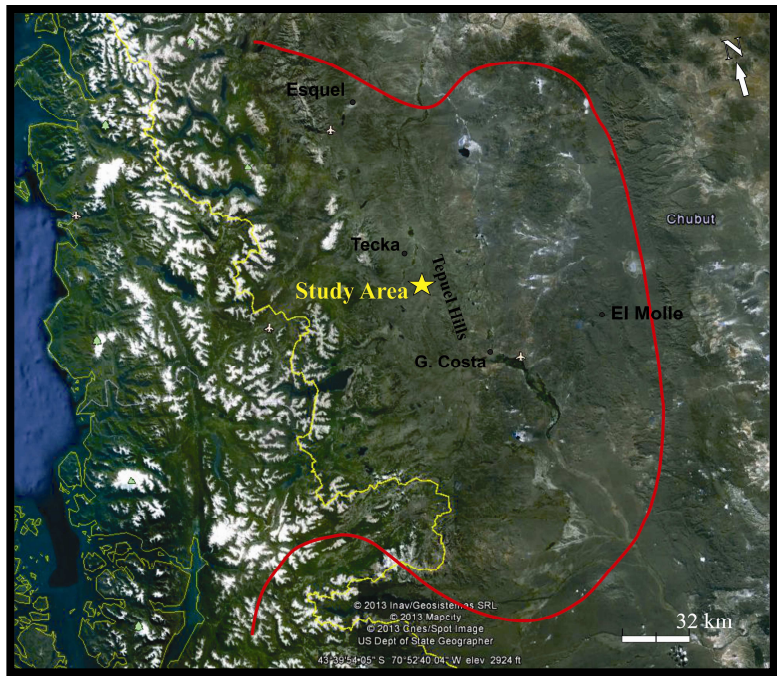


Figure 9. Google Earth map showing the location of the study area (indicated by yellow star) relative to the approximate outline of the Tepuel Basin (in red).

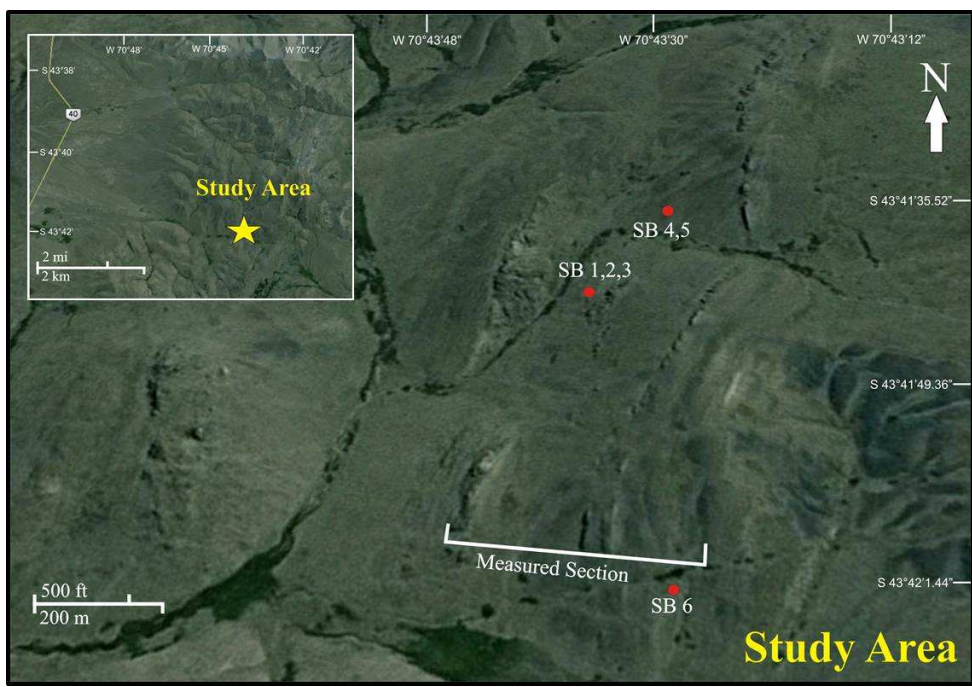


Figure 10. Google Earth images of the Sierra de Tepuel section, including outline of measured section, and shell bed localities (red circles).

Paleoecological analysis

For the paleontological portion of the project, the genera were identified and recorded in order to determine the abundance and diversity of the biota while in the field. In the laboratory, changes in diversity and evenness among the fossil beds were determined using various diversity indices, such as Simpson's index of diversity and the Shannon-Weiner diversity index. The life habits and trophic level information of the specimens were compiled using the paleoecological information available in the Paleobiology Database (<http://paleodb.org>), which aid in the reconstruction of the paleocommunities. Statistical analyses, such as the student's t-test and z-test, were also conducted in order to determine the significance of these changes.

In order to determine a thorough analysis of the paleoecology in a specific locality, it has been suggested that a count of only 50 specimens need be taken (Forcino, 2012). To comply with this rule, at least 50 fossils were counted per shell bed, with three out of the six beds averaging over 300 specimens, one with only 55 specimens and the rest with closer to 250 specimens. As the shell beds were not sampled equally, the data was then rarefied in order to ascertain that a sufficient example of the community was recorded (Hammer and Harper, 2006). A Z-test was then performed in order to determine if there were statistically significant differences among the shell beds (i.e. $p < 0.05$, where $p < 0.05$ is considered to be statistically significant). The p values for the shell beds ranged from 0.14 to 0.20 and therefore are not considered to be taxonomically statistically significant from one another (for a full table of p values from the Z-test, consult Appendix B).

In order to estimate the biodiversity of a paleocommunity, a variety of biodiversity indices and values were used, including: (1) Simpson's index of diversity; (2) Shannon-Wiener index of diversity; (3) mean rank-order; and (4) breadth of distribution. For each fossil shell bed, calculations were made in order to compare the change in paleocommunities during the change in environments.

For the Simpson's index, both the dominance and diversity values were calculated, but only the index of diversity will be used for comparison. The following equations were used for this index:

$$\text{Simpson's index of dominance: } D = \frac{\sum n(n-1)}{N(N-1)}$$

$$\text{Simpson's index of diversity: } 1-D = 1 - \left(\frac{\sum n(n-1)}{N(N-1)} \right)$$

For both of these equations, D is the index of dominance, n is the number of specimens counted for each phylum, and N is the total number of specimens for the entire level. If there is a shell bed with a dominance index close to one, then this indicates that there is one dominant taxon for that particular fossil horizon (Simpson, 1948; Hammer and Harper, 2006). Instead, though, for this study the author focused on the Simpson's index of diversity, which the opposite of dominance. The index of diversity demonstrates the overall diversity of a shell bed, with values closer to one indicating a higher diversity.

The Shannon-Wiener index was also calculated, using the following equation:

$$H' = \sum p_i \ln p_i$$

where $p_i = n/N$. This index indicates the ability to predict the species of the next collected specimen (Shannon, 1948; Hammer and Harper, 2006). In other words, if the species are evenly distributed, the H' value would be high, so therefore, high H' values represent high diversity. Using both Shannon's index and Simpson's index values

provide useful insights when comparing diversity within a stratigraphic section (Hammer and Harper, 2006).

The relative abundance and dominance of the different specimens in a shell bed were quantified in order to determine any changes in faunal assemblages throughout the measured section. This was done using rank order and breadth of distribution (Clapham et al., 2006). Mean rank-order allows for the ordering of the taxa according to their general abundances. Breadth of distribution values measure the proportions of shell beds in which the taxon was present. Comparing these two values allows for the observation of changes in dominance in a locality (Clapham et al., 2006). Together, these various analyses were powerful tools in demonstrating 1) the changes in biodiversity and abundances throughout this section, 2) the manners in which the paleocommunities responded to glacial stresses, 3) the responses to fluctuating glaciation/non-glaciation environments in a glaciomarine shelf setting.

Multivariate analyses have been done on stratigraphically lower faunal assemblages in the Sierra de Tepuel in the past (c.f. Simanauskas and Sabattini, 1997), but there has not been a comprehensive analysis done on the *Lanipustula* fauna since there have been changes made to the faunal assemblage and the redefinition of the new brachiopod species (Pagani and Taboada, 2010). This study attempts to delve deeper into this fossil-rich section of the Pampa de Tepuel Formation in order to determine the paleoecology of the *Lanipustula* fauna as it is currently understood in the literature. I used two multivariate analyses, a detrended correspondence analysis and two types of cluster analysis (Bray-Curtis and Chord distance), using the PAST software package in order to better determine the similarities between the shell beds as time progresses

through the section (Hammer et al., 2001). A detrended correspondence analysis (DCA) attempts to group similar compositions of fauna in similar positions together on a plot (Hammer et al., 2001). These groupings can then be used to interpret environmental conditions. A non-metric multidimensional scaling, such as the Bray-Curtis and Chord distance cluster analyses, attempts to group faunal compositions from field counts into a two- or three-dimensional coordinate system in order to show spatial and ecological comparisons between paleocommunities based on similarity coefficients for each pair of samples (Hammer et al., 2001; Dineen et al., 2012).

Chapter 3. Lithofacies Analysis

Originally, numerous studies determined that glaciation in Gondwana shifted from west to east during the late Paleozoic ice age (LPIA), as the super continent drifted over the South Pole (Caputo and Crowell, 1985; López Gamundí, 1997; Isbell et al., 2003). Although it was previously thought that there were three major glacial phases (e.g. López Gamundí and Martinez, 2000; Isbell et al., 2003; Fielding et al., 2008a, 2008b), it now appears that the timing and location of glaciation waxed and waned diachronously across the supercontinent (Fielding et al., 2008b; Isbell et al., 2012, 2013). Therefore, localized near-field projects, such as this one, are important in understanding the bigger picture of the LPIA.

The depositional settings within the Tepuel Basin remain controversial (Frakes and Crowell, 1969; Gonzalez Borino et al. 1988, 1992; López Gamundí, 1997; Gonzalez 1997, 2010). The controversy revolves around the depositional setting and the proximity of the glaciers within the basin through time. Interpretations of the Pampa de Tepuel Formation, in particular, are contentious. Originally, the formation was interpreted as a glacially-derived marine deposit (Suero, 1948). Later studies also support this interpretation (Frakes and Crowell, 1969; Page et al., 1984; López Gamundí, 1987; González Bonorino et al., 1988; González Bonorino, 1992). In contrast to these interpretations, the Pampa de Tepuel Formation has also been regarded as a more continental succession that was deposited by glaciers at the shoreline, or in the littoral zone with marine transgressions as the glaciers advanced and retreated within the basin (González, 1972, 2002; González and Glasser, 2008; González and Díaz Saravia, 2010). This present study takes a closer look at the middle portion of this formation and presents

a modified interpretation of the depositional setting through the identification and subsequent interpretation of the lithofacies in this portion of the formation.

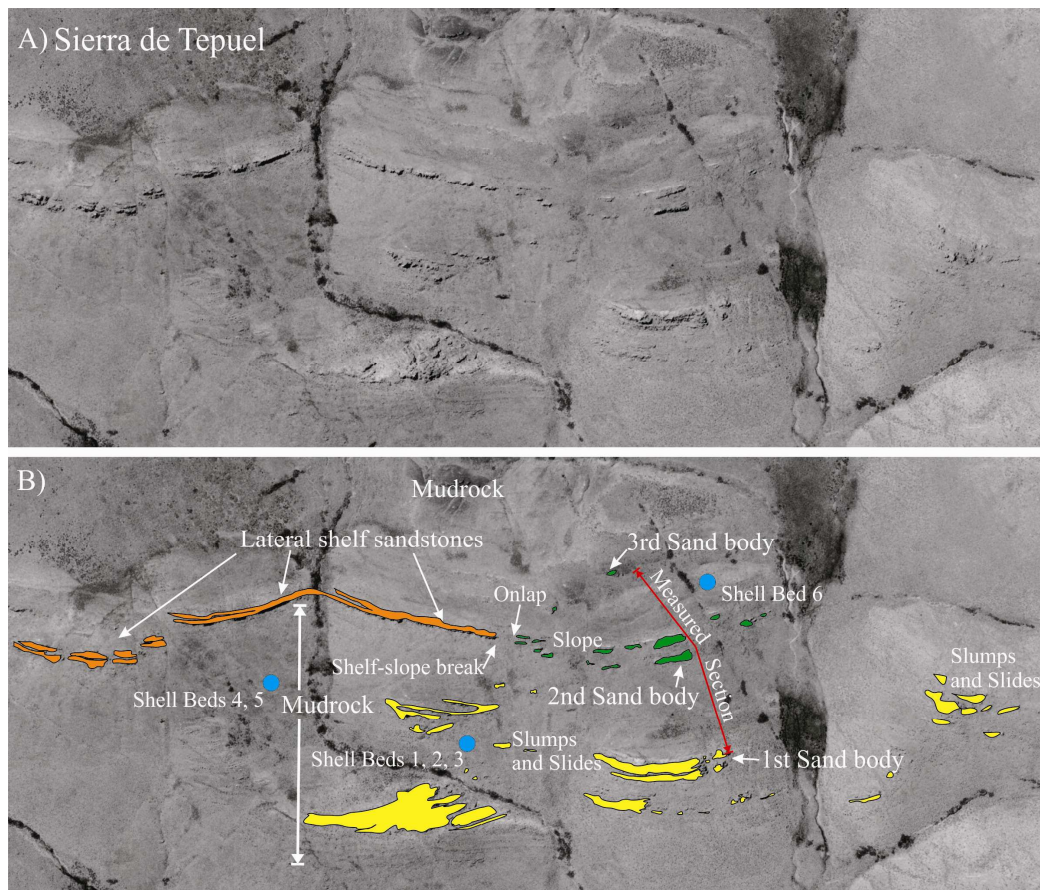


Figure 11. Aerial image of the Sierra de Tepuel study area with the measured section (highlighted with red arrows) and the surrounding outcrops. Yellow indicates slide blocks. Orange indicates shelf deposits. Green indicates slide blocks and slumps along the slope.

The measured section occurs to the south of a thick succession of mudrock that in the upper middle portion of the exposure contains a continuous sandstone body that can be traced for over 1 km across the exposure. Approximately 400 m from the measured section, this sandstone changes apparent orientations across a nodal point and begins dipping at 1 to 5 degrees depositional dip. Beyond this nodal point, the sandstone becomes discontinuous and contains the lenticular sandstone body described above.

Together, these sandstones, the continuous sandstone and the discontinuous sandstone bodies in the middle of the section, define what Isbell et al (2013) identified as a “clinoform set” that is on a scale of hundreds of meters (Figure 11; cf. Henriksen et al., 2011). They interpreted the continuous sandstone to have been deposited on a shelf within the basin, the nodal point to represent the shelf-slope break and the dipping discontinuous sandstone bodies to have been deposited on the upper part of the slope. Therefore, the measured section represents a stratigraphic section recording sediment deposited beyond the shelf slope break.

In basins with sufficient sediment supply and adequate accommodation space, the basinward progradation of clastic wedges results in the deposition of clinoforms on delta and shoreface scales (e.g. tens of meters), as well as on shelf margin scales (e.g. hundreds of meters or more) (Pirmez et al., 1998; Steel and Olsen, 2002; Henriksen et al., 2009; Henriksen et al., 2011). These clinoforms at the shelf margin scale can be used to determine shelf-edge trajectories, which can give insight into fluctuating sediment supply and accommodation in deeper parts of the basin (Steel and Olsen, 2002; Henriksen et al., 2011). As the shelf progrades into the basin, sediment on the slope moves down along the dipping clinoform, where it is subject to gravity-driven mass transport processes (Swift and Thorne, 1991; Steel and Olsen, 2002). Within this area of the Tepuel Basin (Sierra de Tepuel), it seems as though there are a series of clinoforms present (Figure 11; Isbell et al., 2013a). Identifying clinoforms within a basin and understanding that clinoforms represent regressive-transgressive successions can lead to creating a more complete depositional history (Steel and Olsen, 2002).

Strata of the Pampa de Tepuel Formation at the measured section in the Sierra de Tepuel are divided into six facies associations: 1) fossil-bearing mudrock facies association, 2) deformed sandstone and mudrock facies association, 3) thin interbedded sandstone and mudrock facies association, 4) rippled cross-laminated facies association, 5) channel-form sandstone facies association and 6) massive diamictite facies association (Table 1). The facies associations and the resulting depositional processes are described and interpreted within this chapter (Figure 12). The entire stratigraphic column for the measured section (276 meters) is available in Appendix A. The strata at the Sierra de Tepuel locality dip 36° towards the East (structural dip). Tilting of the strata occurred during the Cenozoic uplift of the Andes.

Facies association	Lithologies	Sedimentary structures	Bed thickness	Interpreted mechanisms	Depositional environment
Fossil-bearing mudrock (Mlm)	Mudrock containing clay and silt, very-fine sand	Horizontal laminations, fossiliferous beds, and rare dropstone horizons; sheared zones containing boudins, occur in mudrock beneath deformed sandstone and mudrock facies associations	Mudrock: 25-120cm Sandstone: 0.5-1m	Settle-out of suspension, dropstones represent sedimentation from iceberg rafting, and shearing occurs beneath mass transport deposits	Slope and basin floor setting
Deformed sandstone and mudrock (Sdf)	Fine-grained sandstone, mudrock containing silt and clay	Folded bodies with well-developed fold noses, listric-shaped faults, normal faults	Sandstone: 10-15cm Mudrock: 1-10cm	Mass transport (Slide and slump) of material down a slope	Distal marine, upper slope
Horizontally laminated sandstone and mudrock (Shl)	Very-fine to medium-grained sandstone, mudrock containing silt	Horizontal laminations, ungraded to graded, load structures, gutter casts	Sandstone: 1-10cm Mudrock: 1-10cm	Underflows, turbidity currents	Outer shelf and slope setting (near and beyond the shelf-slope break)
Rippled cross-laminated sandstone and mudrock (Srl)	Very-fine to medium-grained sandstone, mudrock containing silt	Symmetrical ripples and wave ripple cross-laminations with mudrock drapes, occasional deformed ripples; hummocky cross-stratification and interstratified mudrocks at base	Sandstone: 1-10cm Mudrock: 1-5cm	Storm-wave activity, rapid settle-out	Outer shelf and upper slope near shelf-slope break, below normal wave base but above storm wave base
Channel-form (Chm)	Medium-grained sandstone	Lenticular bodies, channel incisions, normal grading, dewatering structures, load structures	Sandstone: 1.5-2m	Scouring, rapid deposition, dewatering due to liquefaction and mass transport	Slope beyond shelf-slope break
Massive diamictite (Dmm)	Massive to weakly stratified diamictite, matrix containing medium-grained sandstone and mud	Outsized clasts, small to medium-sized folds and slumps, mud drapes	Bedded massive diamictite: 10cm-2m beds	Debris flows, flow resedimentation	Outer shelf and upper slope

Table 1. Facies descriptions and interpretations of strata in the Pampa de Tepuel Formation, Sierra de Tepuel, Argentina, described in this thesis. See Figure 12 for the vertical distribution of the facies associations within the measured section.

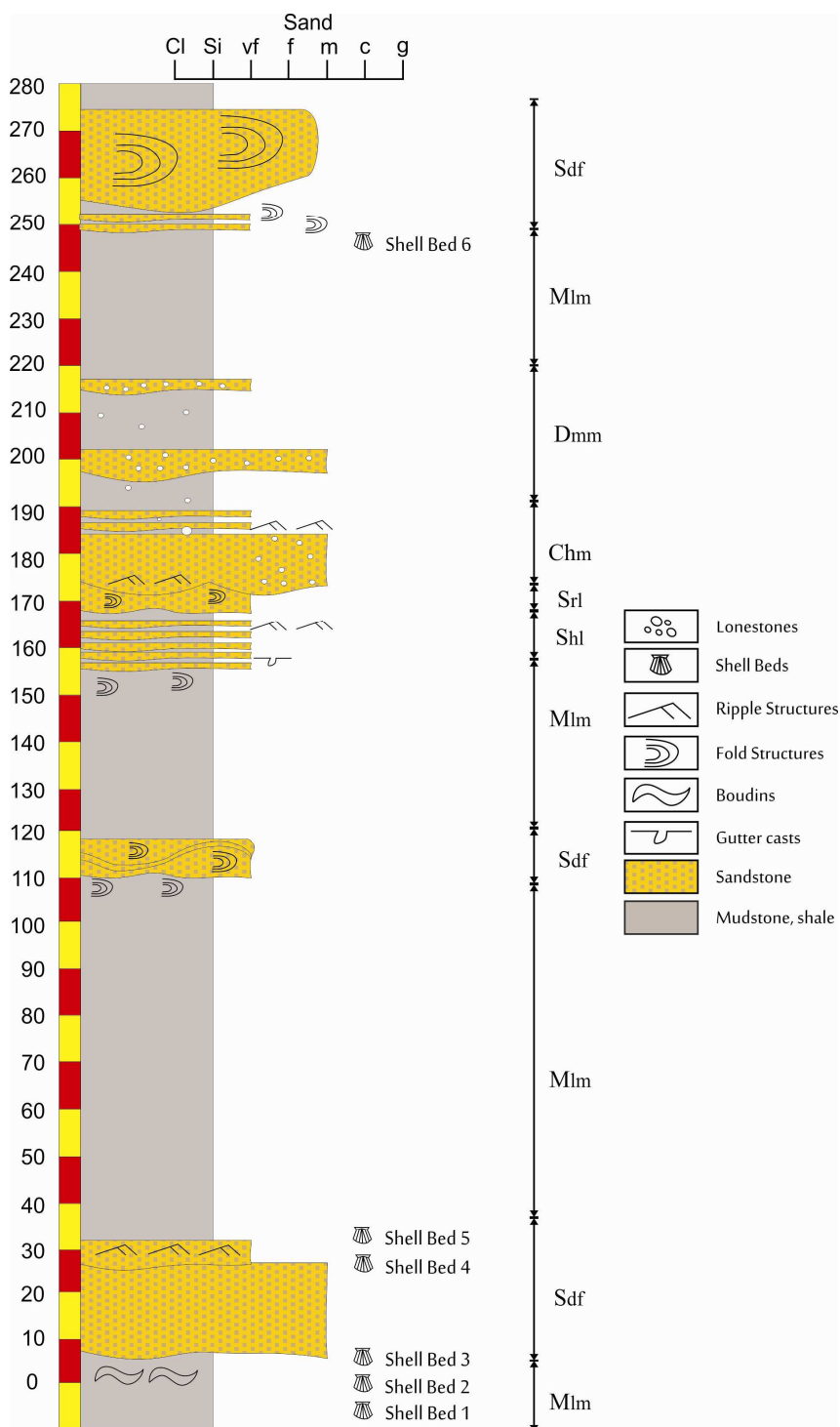


Figure 12. Generalized and simplified stratigraphic column (276m) displaying the facies identified and described in this chapter. Note in Figure 11, that the shell beds (1-5) occur lateral to the measured section and are contained within thick mudrock deposits.

Abbreviations of the different facies associations are as follows: Mlm, the mudrock facies; Sdf, deformed sandstone and mudrock, Shl, horizontally laminated sandstone and mudrock; Srl, ripple cross-laminated; Chm, channel-form; Dmm, massive diamictite. See Table 1 for a description and interpretation of the facies associations.

Fossil-bearing Mudrock Facies Association

Description

The fossil-bearing mudrock facies association is common throughout the measured section. There are two main mudrock facies association occurrences, separated into subfacies associations, a lower mudrock facies and an upper mudrock facies. The lower mudrock facies spans approximately 120 meters of the measured vertical section and extends below the start of the measured section as well. Strata of this lower mudrock subfacies envelopes the lowermost lenticular sand body, where there is evidence of shearing within the mudrock that lies below this sand body, and an abrupt return to the mudrock at the top of the sand body. The lower subfacies contains numerous fossiliferous horizons (Shell Beds 1-5), most of which are located lateral to the measured section, and were located in clusters (e.g. 1, 2, and 3 are located near each other; 4 and 5 are located close together). The marine invertebrate fossils recorded in the fossiliferous beds included brachiopods, bivalves, ostracods, crinoids, gastropods, scaphopods, hyoliths, bryozoans, and corals, most of which are associated with and included in the *Lanipustula* biozone (Pagani and Taboada, 2010). This lower mudrock subfacies is abruptly overlain, by a 25-meter thick deformed zone containing highly fissile mudrocks and sandstone boudins, which in turn is overlain by the interbedded sandstone and mudrock facies association, and finally by the second sand body (Figure 11, 12, and 13).

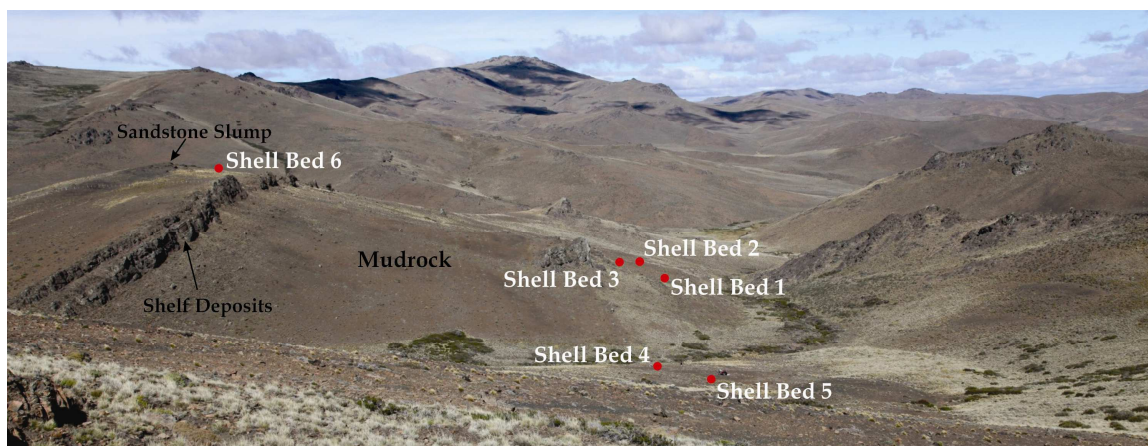


Figure 13. Profile view of outcrops displaying the expanse of the mudrock facies association with shell beds labeled (#1-6).

The upper mudrock facies spans approximately 55 meters between the two upper major sandstone bodies. The grain size within this facies observed at these localities consists of laminations of very fine sand to silt and clay-sized particles, and is dark grey to brown in color. There is one identified fossil horizon (Shell Bed 6) located within this upper mudrock succession which consists mostly of bivalves, ostracods, gastropods, crinoids, and scaphopods. There are also rare pebble- to cobble-sized lonestones found within the strata as well. The lonestone are rounded and are usually quartzite in composition, with one large cobble displaying a possible bullet-like shape (Figure 14). This lonestone-bearing mudrock transitions into a lonestone-free mudrock near the uppermost appearance of this facies association. The uppermost mudrock succession is overlain by another deformation zone, which contains evidence of fissile mudrock and boudins at the base of another horizontally laminated sandstone and mudrock facies association.



Figure 14. Bullet-shaped clast in upper mudrock subfacies.

Interpretation

The absence of glacial indicators within the mudrock facies association in the lower portion of the stratigraphic column suggests that these mudrock facies were deposited under non-glacial open marine conditions or deposited distal to an active ice front. The depositional processes of this facies are mainly due to settling-out of hemipelagic material suspended within the water column. Marine conditions are indicated by the presence of the marine fossils found within the six shell beds (Figure 13). The lower mudrock subfacies association was deposited in a lower energy environment, probably along the lower basin slope. An absence of sedimentary structures in the mudrock produced by wave activity indicates deposition well below storm-wave base. The shearing and boudinage structures seen at the contact between the

mudrock and the lowermost sand body most likely occurred due to mass movement of this sand body along a glide plane from a shallower, more clastic-rich environment onto the basin slope, where the mudrock facies association was being deposited. This would also account for the abrupt return to mudrock at the top of this sand body, as settle-out processes would have continued after the slide block/slump ceased moving, which would have resulted in the sharp contact between the two bodies. Other deformed sandstone bodies also occur lateral to the measured section.

The upper mudrock subfacies contains scattered lonestones, which may have been deposited by a combination of settling from suspension from the distal portions of a meltwater plumes and rain-out from floating ice, in a process termed “two component mixing” (Powell and Domack, 2002). This process occurs when finer-grained particles, such as clay and silt, settle from suspension within the water column at the same time that gravel-size material is being deposited from melt-out from sea ice or icebergs (Thomas and Connell, 1985; Gilbert, 1990). The presence of bullet-shaped clasts and deposition in deep water suggest that rafting was due to icebergs rather than sea ice or as outsized clasts in debris flows (Carto and Eyles, 2012; Isbell et al., 2011, 2013b). However, because the strata contain rare lonestones that are here interpreted as dropstones, this could also have been the result of ice rafted debris being deposited in association with deposition of hemipelagic muds on the basinal slope and basin floor during a relative sea level high stand or during the early part of a falling stage system track (Powell, 1984; Powell and Domack, 2002). The transition from lonestone-bearing mudrock to a lonestone-free mudrock probably indicates a cessation of ice-rafted debris deposition and a return to more clastic-starved conditions during a possible glacial retreat. The upper

contact of this upper mudrock subfacies with the interbedded sandstone and mudrock facies shows similarities to the lower mudrock subfacies, in that there are fissiled and boudinage structures present. A sheared upper contact with the overlying interbedded sandstone and mudrock facies may also be the result of development of a glide plane, along which the next facies association was transported onto the basin slope.

Deformed sandstone and mudstone bodies facies association

Description

The folded and internally deformed sandstone facies association occurs mainly in the lower and upper portions of the measured section (2-27m and 255-261m), with the occasional occurrence of smaller deformed sand bodies found encased in the mudrock facies association (117-118m). The grain size of this facies is mainly fine-grained sandstone contained in bedding up to 10 to 15 centimeters thick, although it consists of some interbedded mud layers up to 10 centimeters in thickness. This facies also consists of two subfacies associations, a subfacies that shows little deformation and a highly deformed sand body subfacies.

The slightly deformed subfacies is found in meter-scale to 20 meters-thick blocks that are 10-100 meters in length (found mostly from 2-27m in the measured section). These blocks rest on fissile and boudin-bearing mudrock intervals that measure up to 50 cm in thickness. The blocks tend to occur along with smaller blocks that are concentrated in zones that are elongate and teardrop-like in appearance over distances of tens to a hundred meters (Figure 15). The sand bodies of this subfacies show very little internal deformation throughout the blocks, but may contain listric-shape reverse faults in the

thicker, or frontal, portions of the blocks. Multiple faults may also occur within the horizon, or possibly within a single sandstone body (Figure 16). The upper contact is usually sharp in relation to the mudrock that overlies it, and can have rare wave ripples preserved on the top of the sandstone blocks.

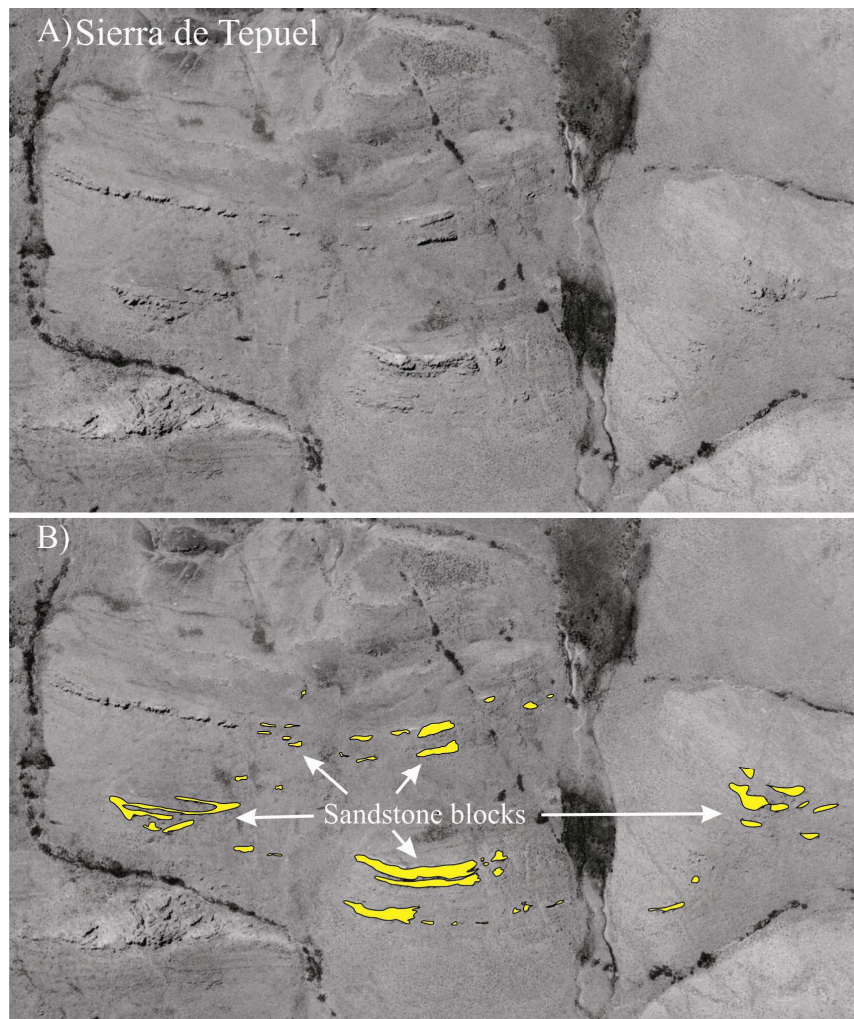


Figure 15. Aerial image of teardrop shape of deformed sandstone bodies.

The highly deformed sand body subfacies (117-118m; 255-261m) display major internal deformation features, which includes fold noses and small-scale faulting. This subfacies, like the previous subfacies, also rests on fissile and boudin-bearing mudrock, which occurs in smaller intervals of a few to a few tens of centimeters thick. The sand bodies are mostly discontinuous, usually a few meters to 10-meters thick and a few tens of meters long. The sandstone body at the top of the measured section also contained overturned fold noses, which are a few meters thick, at the front, or leading-end, of the sand body, as well as internal fault structures, which display a few millimeters offset, and some brecciated intervals within the sandstone bodies (Figure 17).

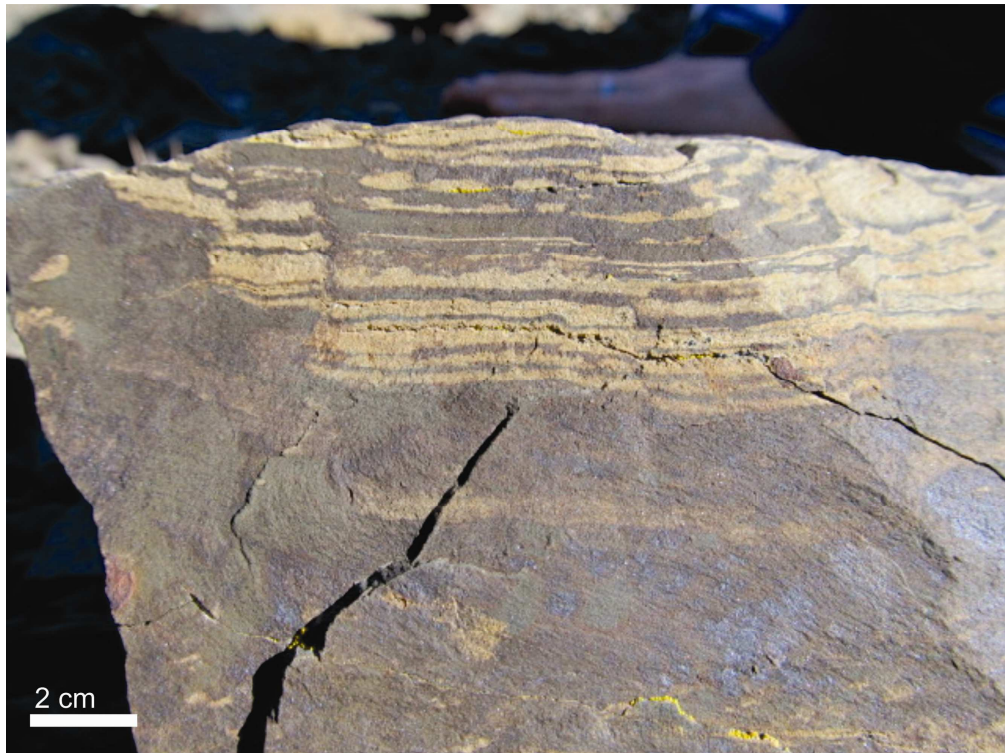


Figure 16. Small centimeter-scale faults in upper severely deformed sandstone facies association.

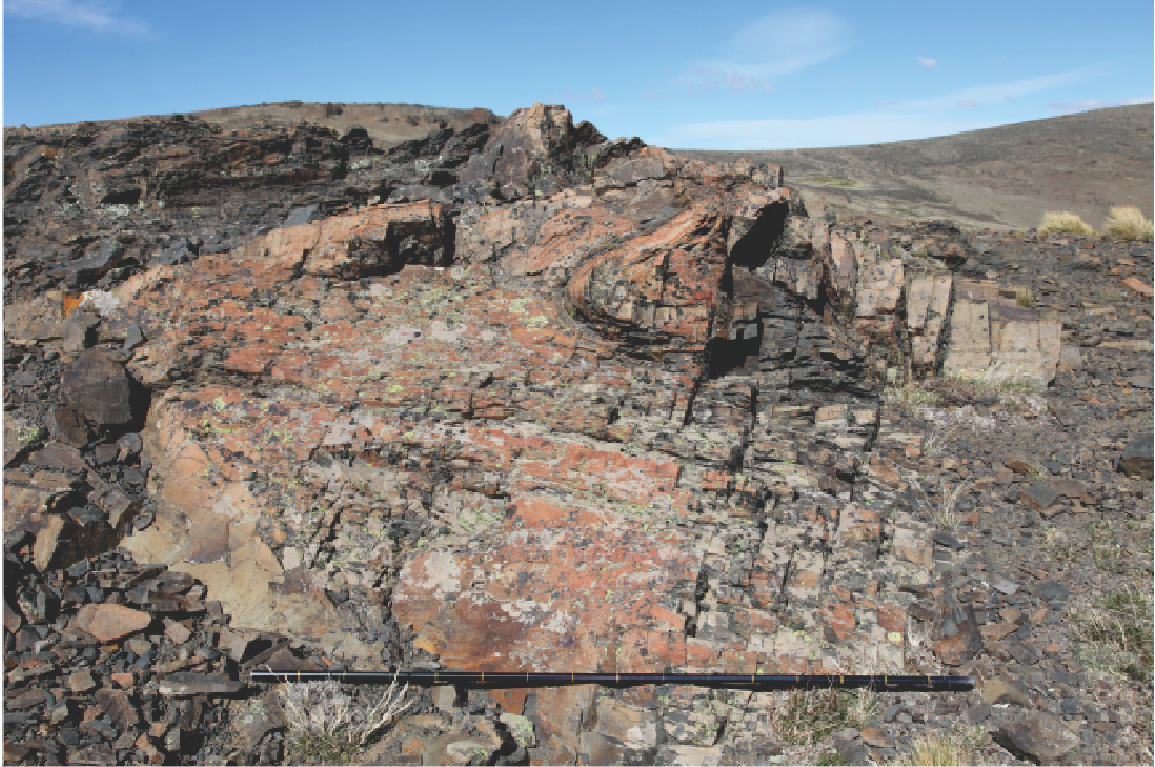


Figure 17. Fold nose in upper deformed sandstone subfacies, part of the third and uppermost sand body.

Interpretation

The lowest sand body (sand body #1 in Figure 11) of the measured section is interpreted here as a slide block, where a slide is a mass movement of a coherent block of strata transported downslope along a glide plane, or shear surface, without internal deformation and may have travelled some hundreds of meters to hundreds of kilometers down slopes (Elliot and Williams, 1988; Shanmugam et al., 1994; Laberg and Vorren, 1995; Dimakis et al., 2000; Shanmugam, 2006). The fissile and boudin-bearing mudrock served as the glide plane, or *décollement*, along which these slightly deformed sand bodies were moving. As the slide blocks moved downslope, they truncate the underlying mudrock, and created a shear zone which is evidenced by the fissile and boudinage

structures seen at the base of the sand bodies. The thicker portions of the sand bodies are interpreted as the front, or leading-end, of the slide blocks. As the movement decreased in velocity, and eventually stopping, the front of the slide block would cease movement first, followed by the material behind it. This differential cessation of movement would have created a “back-up” effect, causing the still-moving material to ramp up onto the sandstone at the front of the sliding body, creating the listric-shaped reverse faults seen in many of these slide blocks (Allen, 1985; Collinson and Thompson, 1989; Ricci Lucchi, 1995; Ben and Evans, 1998; Isbell, 2010). These reverse faults are also similar to those found in the mass transport deposits of the Jejenes Formation at Quebrada de Las Lajas in the Paganzo Basin in western Argentina (Dykstra et al., 2006). The upper surfaces of some of these sand bodies display ripple structures, which would not occur in the deeper environments of the slope, as it is well below storm-wave base. The fact that these are preserved seems to indicate that these sand bodies were not originally deposited at this location, but are instead the product of remobilization of shelf edge deposits after primary deposition occurred (Strachan, 2002).

The upper sand body (sand body #3 in Figure 11) is interpreted as a slump, which is defined as a rotational mass movement of a coherent block of strata along a concave-up glide plane, or shear surface, with internal deformation within the body (Elliot and Williams, 1988; Shanmugam et al., 1994; Laberg and Vorren, 1995; Dimakis et al., 2000; Shanmugam, 2006). Much like for the lower sand bodies of the slightly-deformed subfacies, the fissile and boudin-bearing mudrock serves as the décollement for this highly deformed subfacies. The upper sand body may have started as a slide block like the ones of the slightly-deformed subfacies, but as movement continued down the

clinoform and further into the deeper basin environments, the block became internally folded resulting in an internally chaotic slump block.

The presence of folds observed in relation to evidence of shear zones and glide planes at the lower contacts of these sand bodies indicates that these internally deformed sandstones were deposited due to mass movement/mass transportation processes. The sharp upper contact, as opposed to a gradational contact, with the mudrock facies association for both the lower and upper sandstone bodies further supports the interpretation of these sand bodies as mass transportation deposits, as the mudrock facies seems to encase the discontinuous blocks, where a gradational contact would indicate a transitional change in depositional environments. Deformation of these sandstone beds most likely occurred as a result of slope failure followed by the downslope movement and transportation of the bodies, which caused the folding, sliding, slumping, and boudinage structures observed in the field (Prior, 1984; Norem et al., 1990; Mulder and Cochonat, 1996; Strachan, 2002; Lee et al., 2007). The causes of these mass movements were most likely due to the buildup of excess pore pressure due to high sediment input, or the oversteepening of deposits at the shelf-slope break (Laberg and Vorren, 1995; Dimakis et al., 2000; Lee et al., 2007).

A third cause of the mass movements may have been due to slope instability created by earthquakes, as continental slopes are 5-degrees or less and are usually stable and there is a lessened influence of storm-wave activity beyond the shelf-slope break (Lee and Edwards, 1986; Lee et al., 2007). The former two scenarios are more likely the case as the sediment input changed within the Tepuel Basin due to either fluctuations in the position of glaciers, changes in sea level at the shelf slope break, or due to tectonic

activity in the form of earthquakes potentially produced during Patagonia's accretion to South America as suggested by Ramos (2008).

Horizontally laminated sandstone and mudrock facies association

Description

The thin interbedded sandstone and mudrock facies association mainly occurs near the middle of the measured section (159-169m), in between the lower thick fossil-bearing mudrock facies and the overlying channel-form facies (Figure 18). The interbedded sandstone and mudrock facies association are continuous across the outcrop. This horizontally laminated facies consists of interbedded sandstone beds that range from a few centimeters to a few tens of centimeters in scale (Figure 19). The sandstone layers are interbedded with laminated mudrock, which is made up of both mudstone and siltstone, and range in thickness from a few centimeters to around 10 centimeters. The lower contacts of sandstones units in this subfacies tend to be erosional to sharp, and occasionally display load structures or gutter casts. The sandstone layers are usually ungraded to graded, and range in grain size from very-fine to fine-grained sandstone. A few of these beds display some internal folding with well-developed fold noses. These interbedded layers have a sharp to gradational upper contact with the rippled cross-laminated facies, and can be found to intercalate with the rippled cross-laminated facies (Figure 20).



Figure 18. Horizontally laminated unit underlying channel-form facies association.



Figure 19. Horizontally laminated interbedded sandstone and mudrock facies association.

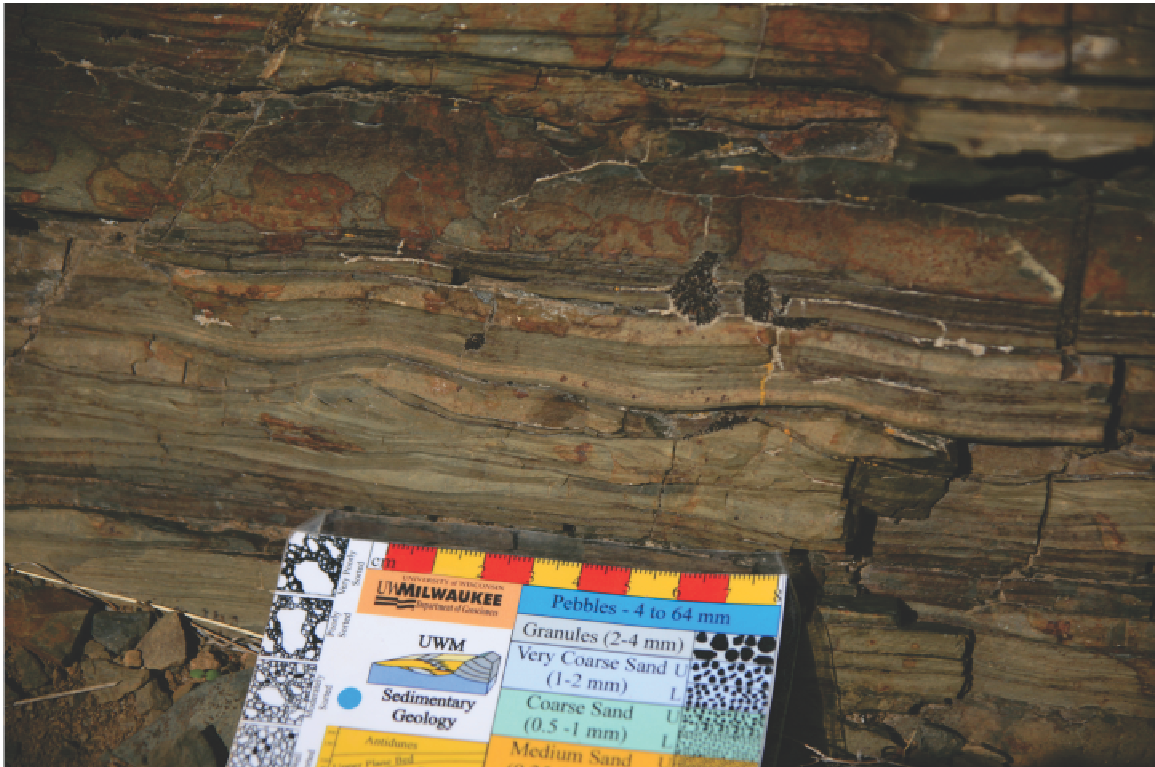


Figure 20. Interfingering wave-rippled facies with horizontally laminated interbedded facies.

Interpretation

The presence of the thin planar and interbedded sandstone and mudrock facies association indicates a rapid and fluctuating change in environmental and depositional energy, which commonly occurs in shelf break environments, turbidites, and in wave dominated coastlines below normal wave base, but above storm wave base (Powell and Cowan, 1986; Boulton, 1990). The appearance of horizontally laminated layers is consistent with the definition of the T_D turbidite interval as described by Talling et al. (2012). Talling et al. (2012) describes this interval to be deposited from relatively low-density turbidity currents that are fully turbulent near the bed. Horizontally laminated sandstones are also deposited by geostrophic currents that represent return flow of water along the sea bottom away from coastlines during storm surges. Such events result in deep water deposition from episodic underflow currents (Basilici et al., 2012). The fine-grained horizontally laminated sandstone beds were most likely deposited by turbidity currents or possibly underflows, and could have possibly been triggered by slope failure or storm activity (Dott and Bourgeois, 1982; López Gamundí, 1997; Gani, 2004; Posamentier and Walker, 2006; Winsemann et al., 2007; Talling et al., 2012). The erosional lower contacts recorded in the directly underlying mudrock facies is most likely due to the scouring caused by the underflow currents (Powell and Cowan, 1986; Boulton, 1990; Powell and Domack, 2002).

Rippled cross-laminated facies association

Description

Like the horizontally laminated facies, this rippled cross-laminated subfacies is also laterally continuous across the outcrop. The basal contacts of this facies may be interbedded with the horizontally laminated facies, as previously mentioned (Figure 20). The facies becomes more abundant farther to the north where it is contained in a coarsening upward facies associated within the continuous sandstone body as part of the topset of the clinoform set studied by Isbell et al. (2013a). These rippled units start with interbedded sandstone and mudstone/siltstone layers at the base and coarsen upward through the succession to very-fine to medium-grained sandstone beds. Upward, the mudrock interbeds are lost entirely. For the most part, wave-ripple cross-laminations dominate (Figure 21), with the occasional appearances of symmetrical interference ripples preserved on some bedding planes (Figure 22). There are a few interbeds of the horizontally laminated mudrock units that are a few centimeters thick. A few beds in this facies display internal deformation, such as folding with well-developed fold noses and deformed ripples (Figure 23), while other beds display loaded bases. Rare beds of hummocky cross-stratification also occur (Figure 24). The upper contact of this facies is erosional when it is overlain by massive sandstone bodies and sharp when it is overlain by the mudrock facies association.



Figure 22. Symmetrical ripples and wave ripple laminations. Note the mud drape on top of the symmetrical ripples



Figure 21. Interference ripples. Note the mud drape over the rippled surface.



Figure 24. Deformed ripples near the top of the ripple cross-laminated facies association.

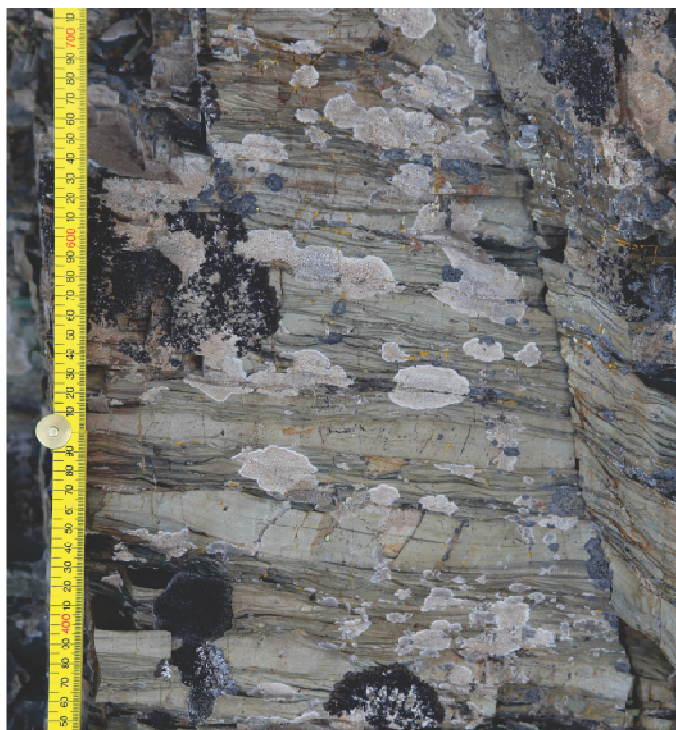


Figure 23. Hummocky cross-stratification interstratified with wave-ripple cross-laminations.

Interpretation

The internal deformation, such as deformed ripple structures, suggest deposition and movement along a depositional slope, which suggest rapid deposition by processes that trap high water content within the sand, and which supports the interpretation that these deposits were remobilized after deposition as small-scale slumps. The massive diamictite facies directly overlies this interbedded sandstone and mudrock facies association, and suggest that these events were related in time and space as potentially linked events depositing debrites and turbidites.

This facies association also contains ripple structures/ wave ripple cross-laminations that are symmetrical and can be identified as wave ripple cross-laminations. The interlaminations of the mudrock indicate a depositional environment that is below normal wave base, as any mud would be winnowed away due to the constant wave activity. Therefore, it can be inferred that these ripples record storm wave activity (Baird, 1962; Reineck and Singh, 1980). The rare preservation of hummocky cross-within this facies are anomalous as such interbedded sandstones and mudstone typically contain abundant hummocky cross-stratification. Their rarity in this succession suggests that wave energy/storm energy may have been dampened in this section. Dowdeswell et al. (2000), Clifton (2006), and Murray (2013) report dampened wave activity in polar settings to be the result of possible sea ice cover. The scarcity of the hummocky cross-stratification could also indicate an absence of big storms. Since these structures occur at what is interpreted here to be the shelf-slope break, big waves would be expected to break as they encounter the shallower shelf waters, and so there should be a greater presence of these structures here.

Channel-form sandstone facies association

Description

The channel-form sandstone facies association occurs near the middle of this measured section (160 m) and occurs on one of the discontinuous sandstone bodies on the dipping clinoform (Figures 11, 15, and 25). The amalgamated channel complex overlies the horizontally laminated sandstone and mudrock facies with an erosional surface, and it underlies the mudrock and massive diamictite facies associations. The grain sizes of the channel facies association is medium-grained sandstone, and contains occasional intermittent outsized clasts, some of which are close to 10 cm in diameter. There are also soft sediment deformation features, such as water escape and large-scale load structures observed in the lower portion of this facies (Figure 26). Grading appears to be normal throughout this facies association.

The channel complex sand body is located lateral to and above the wave-rippled cross-laminated sandstone facies assemblage recorded in this portion of the measured section (176-181 m). Channel-form bodies consist of two to four large lenticular structures each of which spans about 65 meters in width and about 1.5-2 meters in thickness. There is also one larger lenticular body near the bottom of this sandstone ridge, which spans the length of the outcrop. The base of each channel-form body is loaded into the underlying strata and may contain internal folds.

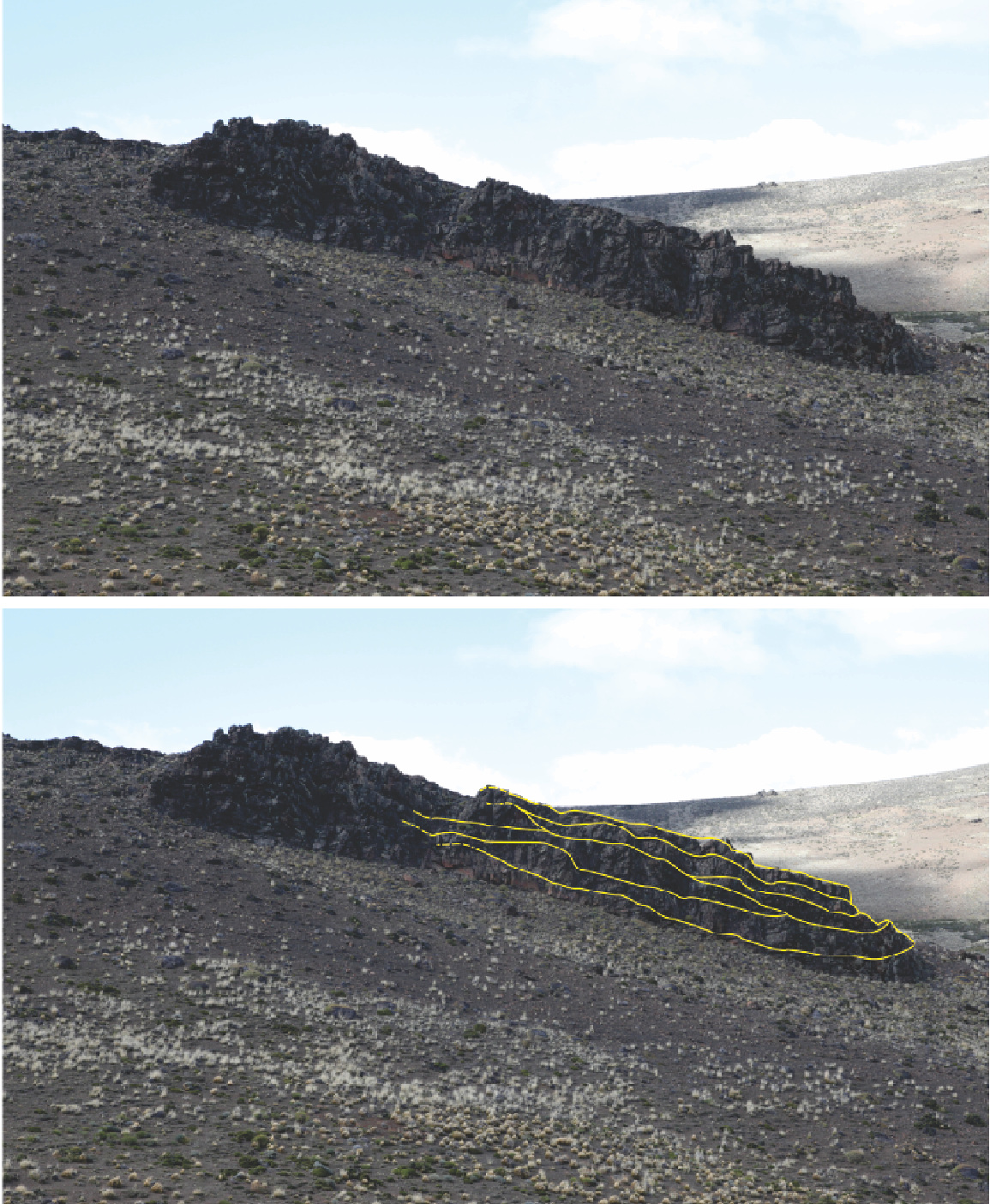


Figure 25. Channel-form facies association, outlined are the channels as amalgamated lenticular bodies. The lenticular bodies of the amalgamated channels have been outlined in yellow. The structural dip of the section is into the photo; whereas, the depositional dip is off to the right.



Figure 26. Water escape structures and flame structures seen in the channel-form facies association in the Pampa de Tepuel Formation.

Interpretation

Submarine channels are known to form and feed sand into the deep basin (Steel et al., 2008; Henriksen et al., 2011). These subaqueous channels can open into the basin and are known to occur on the slope beyond the shelf-slope break and to be sites of turbidites and mass transport activity (Petter, 2005; Steel et al., 2008). The base of the lenticular bodies observed in this massive ridge-forming sandstone (sand body #2 in Figure 11) displays evidence of erosion, which could have been formed by the bypass of sediment over the shelf-slope break onto the upper slope (Bhattacharya and Giosan, 2003; Steel et al., 2008). The interpretation of this facies as an amalgamation of submarine channels seems to fit the overall interpretation that this middle ridge-forming sandstone was deposited in an environment feeding sand into the deeper basin.

Water escape structures, such as the flame structures observed in this facies association (Figure 6), formed as the result of rapid deposition and subsequent dewatering of the deposits due to the compaction and liquefaction of the water-saturated substrates, or possibly due to the loading of a soupy substrate by adding additional sediment as the sediment was making its way over the shelf edge and onto the slope (Henry, 2007). Furthermore, the fact that the lower contacts of this facies are bounded by erosional contacts with probable turbidites (see Horizontally laminated sandstone facies association above) and overlain by debrites (see Massive diamictite facies association below) that are located along the basin slope, supports this interpretation.

Massive diamictite facies association

Description

The massive diamictite facies is located above the channel-form sandstone facies association, which occurs near the top of the second lenticular sandstone body (182-186m, and 198-202m). This facies has sharp planar to undulating lower and upper contacts with the underlying and overlying mudrock facies association. Beds range in thickness from 10 centimeters to a few meters thick (Figure 27). The grain size within this facies is mainly medium sand and some mud, but it also contains numerous outsized clasts, which includes granite to quartzite, that tend to protrude above the bedding at the upper surface (Figure 28). Internally, the diamictite is massive with randomly oriented floating clast set in the finer grained matrix. The clasts are mostly well-rounded pebble to cobble-sized and do not show any clear evidence of striations, faceted faces, or bullet-shape. This facies is associated with small and medium-sized folds and slumps (10-50cm), and in some places drapes over the slump folds

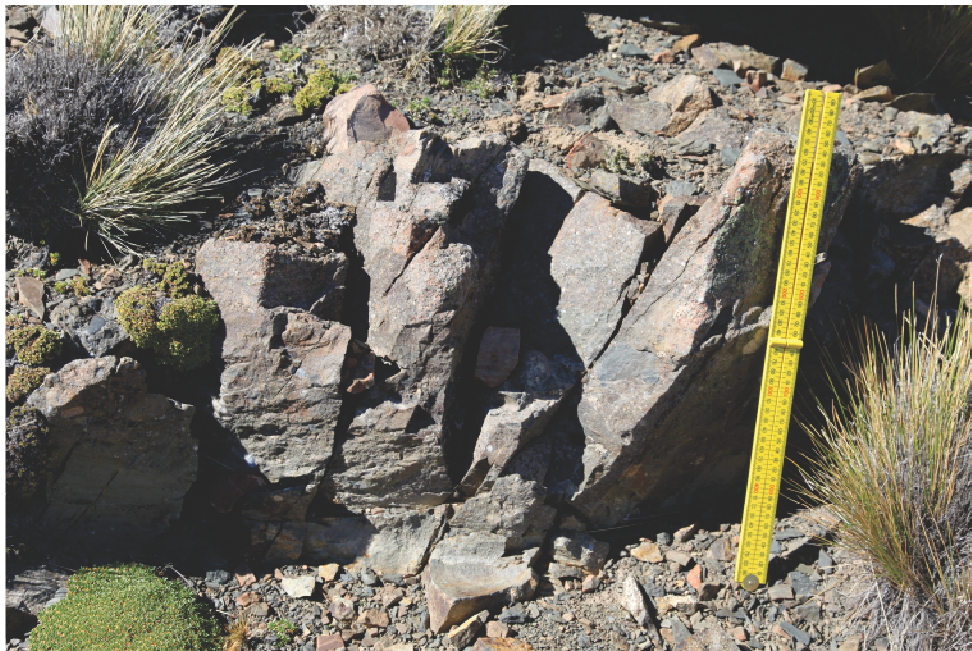


Figure 27. Massive diamictite facies association, weakly stratified with pebbles and cobbles suspended in a sandy-muddy matrix.



Figure 28. Pebbles protruding from top of a surface in the massive diamictite facies association.

Interpretation

Massive diamictites are not uncommon in glaciomarine environments or shelf edge settings and can form from varying depositional processes (Eyles and Eyles, 2000; Mulder and Alexander, 2001; Powell and Domack, 2002; Steel and Olsen, 2002; Henry, 2007). These processes can include 1) rain-out of clay, silt, and sand from meltwater plumes emanating from the terminus of a glacier, 2) melt-out of material from the base of a glacier near the grounding line, 3) rain-out of clay-to boulder-sized material from icebergs, 4) iceberg turbation, and 5) subaqueous debris flow (Anderson et al., 1983; Eyles et al., 1985; Montcrieff and Hambrey, 1990; Hambrey et al., 1991; Woodworth-Lynas and Dowdeswell, 1994; Evans and Pudsey, 2002). The sharp contacts also suggest that this diamictite was not the result of a gradual process such as a meltwater plume depositing the material, nor was it the result of iceberg turbation, as there were no striations recorded on the clasts nor grooved surfaces identified on the underlying sedimentary rocks (Powell and Domack, 2002).

Due to the presence of the mudrock facies association in immediate contact with the massive diamictite (182-202m), its association with slump folds, its sharp upper and lower contacts, the presence of randomly oriented floating clasts, and the occurrence of clasts that protrude from the upper surface of the units, this massive diamictite facies is interpreted to be the result of debris flow depositional process (Carto and Eyles, 2012). These were deposited in association with slump and slide blocks that were likely deposited in deeper water beyond the shelf slope break. Their association with such deposits suggest that they may have been generated as part of the mass movement process where debris flows result from disintegrating of slump and slide blocks

(Maejima, 1988; Eyles, 1990; Noda et al., 2013) Such deposition of these diamictites is consistent with previous interpretations for the Pampa de Tepuel Formation (Frakes et al., 1969; Frakes and Crowell, 1969; Page et al., 1984; López Gamundí, 1987). For this facies association, the term diamictite refers not to a glacial deposit, but a mixture of clasts and matrix that has been redeposited (Dott, 1961; Carto and Eyles, 2012).

Environments in which there are high rates of sediment accumulation may be susceptible to re-sedimentation, especially at the shelf-slope break, and can collapse causing mass movement and debris flows to occur (Eyles, 1990; Powell and Domack, 2002; Carto and Eyles, 2012; Noda et al., 2013). Activity such as storm waves as well as shock and movement from earthquakes can also cause debris flows in marine environments (Powell and Domack, 2002; Talling et al., 2012). The resulting deposits are known as debrites (Mulder and Alexander, 2001; Gani, 2004; Talling et al., 2012; Carto and Eyles, 2012).

Discussion

As previously discussed, the Pampa de Tepuel Formation was originally interpreted as a glacially-derived marine deposit (Suero, 1948; Frakes et al., 1969; Frakes and Crowell, 1969; Page et al., 1984; López Gamundí, 1987; González Bonorino et al., 1988; González Bonorino, 1992). Parts of this formation have also been interpreted as having a more continental origin, with deposition occurring at the shoreline or within the littoral zone by glacial processes (González, 1972, 2002; González and Glasser, 2008; González and Díaz Saravia, 2010). Results presented here suggest that in the measured section from the middle of the Pampa de Tepuel Formation the deposits are primarily marine and were deposited at or near the shelf-slope break. A glacial signature is only

evident by the limestones observed in the section, however, limestones are equivocal evidence of glaciation and can be formed through numerous non-glacial processes such as: floatation, tree rafting, and volcanic eruptions. Moreover, the ubiquitous nature of large slide blocks of sandstone suggests that coarse clastics could have been delivered to this portion of the basin via mass transport during catastrophic failure of coarse clastic debris and mass movement to the shelf-slope break. Thus, the Pampa de Tepuel Formation is more easily explained by deposition associated with the outer shelf, shelf slope break, and deposition on the slope within the Tepuel Basin.

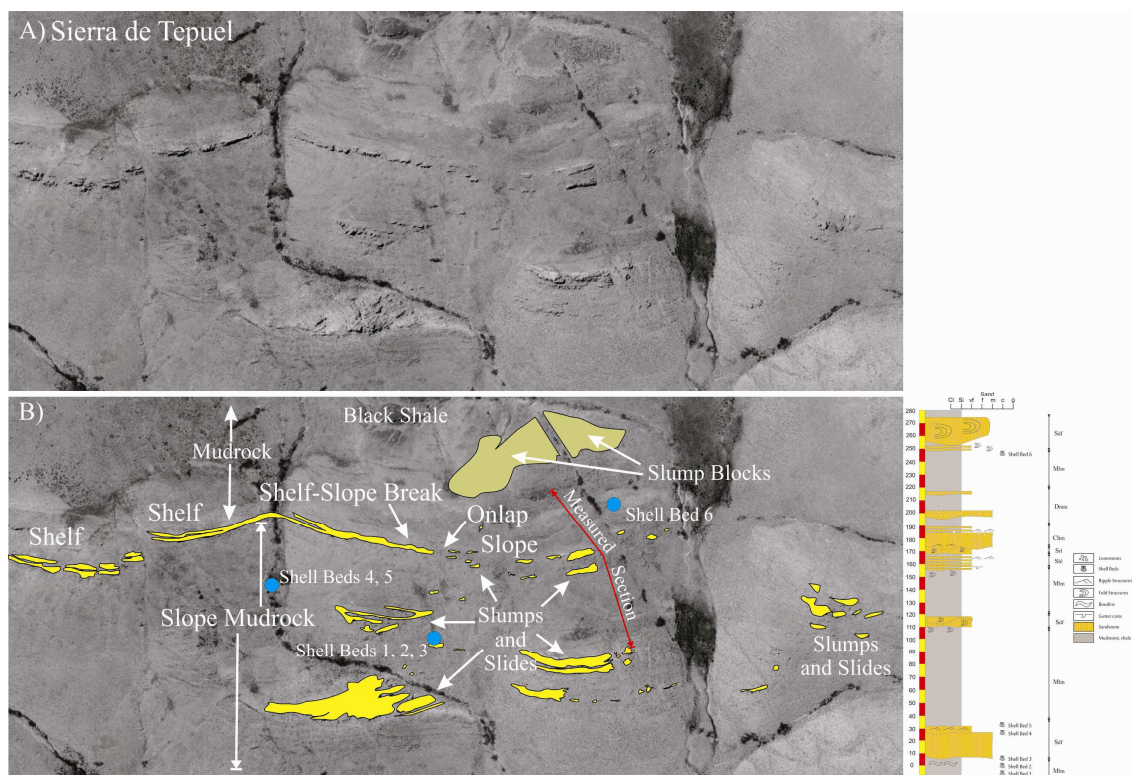


Figure 29. Aerial image of the Sierra de Tepuel study location. The measured section is marked by the red arrows. The shelf sandstones and slide blocks have been highlighted in bright yellow, and the slumps that are located above the clinoform (here indicated as “Slope”) are highlighted in the lighter yellow; shell beds sampled from are marked by blue circles. The generalized stratigraphic column has been lined up to correspond to the locations of the major sandstone bodies measure in the field.

The measured section is located to the south of a nodal point where a continuous sandstone body changes its apparent depositional dip and begins to dip more steeply into the depositional basin (Figure 29). For this portion of the basin fill, Isbell et al (2013a) interpreted this point as the shelf slope break. The shelf is interpreted to lie to the north and discontinuous more steeply dipping (depositional dip) slope and basinal deposits are interpreted to lie to the south of this nodal point. Therefore, the measured section contains sedimentation deposited on the basin slope. The base of the measured section begins with a deep-water mudrock that contains a lenticular sandstone body originally deposited in shallow water near the shelf slope break prior to mass transport into deeper water as a slide block (Elliot and Williams, 1988; Shanmugam et al., 1994; Laberg and Vorren, 1995; Dimakis et al., 2000; Bryn et al., 2005; Rise et al., 2005; Solheim et al., 2005; Shanmugam, 2006). A deep water environment for the mudrock is supported by the absence of wave structures and the occurrence of normal marine fossils. During periods of high sea-level, the outer shelf and basin slope becomes clastic-starved and little sediment make it into the deep basin (Henriksen et al., 2011). Above and adjacent to the slide block, the mudrock continues upward. The presence of established faunal communities within the mudrock indicates that the environment was relatively stable enough to support an abundance of life, which is discussed in the succeeding chapter.

Gravity-driven processes initiated by lowering of sea level and high sedimentation rates are largely responsible for mass movements of sediments into deep-marine environments (Swift and Thorne, 1991; Bryn et al., 2005; Rise et al., 2005; Steel and Olsen, 2002; Solheim et al., 2005; Shanmugam, 2006). This explains the occurrence of large lower and upper sandstone bodies within the measured section. According to the

characteristics previously described, these sandstone facies were originally deposited in a clastic-rich, shallower-water setting, which then failed and slid down the slope where they are encased in deep-water deposits of the mudrock facies associations (Bryn et al., 2005; Rise et al., 2005; Solheim et al., 2005; Shanmugam, 2006; Noda et al., 2013).

Additional episodic slumping and sliding of shallow water sandstones continued down the slope during mudrock deposition as indicated by the occurrence of a small sandstone slump block at 115m above the base of the section and by the occurrence of larger slump and slide blocks located laterally to this part of the measured section. These blocks have fold noses and internal chaotically deformed bedding (as seen in Figure 16, 17).

Mudrock occurs upward until about 159 meters above the base of the section where the fine-grained mudrock coarsens into interbedded sandstones. These interbedded sands and mudrock are interpreted to have been deposited by mass transportation processes, specifically by turbidity currents, which represent a basin-ward progression of the clinoform. Deposition of these units on the slope usually occurs during late high stand or during the falling stage of relative sea level when sediment bypass of the shelf occurs due to a lack of accommodation space (Steel et al., 2008).

Immediately overlying these turbidites are small-scale massive diamictites (169-172m), which are interpreted as debris flow deposits. These debrites, underlying turbidites, and slump/slide blocks are all likely related as part of the mass transport deposits associated with deposition at the edge of a prograding basinal shelf (Steel and Olsen, 2002; Steel et al., 2008; Henriksen et al., 2011). The middle portion of this second sand body contains channelized deposits suggesting development of slope channels that transported coarse sediment away from the shelf edge and onto the distant basin floor.

Throughout this portion of the section, multiple levels of symmetrical wave ripples and interference wave ripples occur lateral to the channel sandstone body. These ripples formed in deeper water, below normal wave base, as they are separated by thin mud layers, indicating episodic wave activity likely generated during storm events as suggested by the occurrence of rare hummocky cross-stratification (Basilici et al., 2012). The upper part of the slope can still be influenced by wave activity especially because waves are bigger as deep water waves strike the upper slope and outer shelf (Basilici et al., 2012). The scarcity of the hummocky cross-stratified structures may be due to an absence of large storms, or possibly due to the presence of sea ice.

Above these channels, large outsized cobbles occur within massive bedded diamictites. These deposits are interpreted as debris flows. These deposits are interspersed with brief sections of mudrock, which were again deposited due to settling from suspension. These strata, which are contained in a dipping clinoform include turbidites, debrites and slump/slide blocks, all of which suggest high sedimentation rates at the shelf edge due to a low-stand of relative sea level. Above this clinoform, a second clinoform composed of lenticular sandstones, turbidites and debrites occurs at approximately 200 m above the base of the section. When traced laterally, this clinoform laps onto the underlying clinoform suggesting a further slight drop in relative sea level.

At the top of the section, a large and internally deformed sand body displays several fold noses on both meter and centimeter-scales (Figures 16, 17). This upper sand body is interpreted as amalgamated slump deposits. The slump located at the very top of this section might be indicative of a short-lived reintroduction of clastics onto the lower slope environments due to the destabilization of the shelf-edge as the transgression

occurred, but further evidence of this is required (Noda et al., 2013). The slumps located here are encased by mudrock. Shell bed 6 is located within this upper mudrock facies, lateral to the slumps, and may be indicative of a return to a deep-water depositional environment in which the fauna was able to establish communities. The system seems to return to a clastic-starved depositional environment due to a major transgression due to the appearance of black shale and mudrock recorded just above the measured stratigraphic section. This mudrock unit quickly grades into very dark black shale as the Pampa de Tepuel Formation continues upward above the measured section. This mudrock unit is several hundred meters thick and ends in another laterally continuous sandstone horizon. The change from the amalgamated slump to the thick dark shale likely represents a major rise in relative sea level and the back stepping of clastics across the shelf to the north.

Combining together the processes of each of these described facies, an overall understanding of the depositional environments and shelf-edge trajectory of this measured portion of the Pampa de Tepuel Formation can be determined. Overall, these facies were deposited in a depositional setting that sits at or near the shelf-slope break (Figure 11). Identifying the clinofolds and their stacking patterns within this section help to identify depositional environments and changing relative sea level within the distal, deep-water portions of the basin.

Chapter 4: Paleocology Analysis

The faunal assemblage at this section of The Sierra de Tepuel is representative of the *Lanipustula patagoniensis* Biozone, which is unique to the Tepuel Basin (Simanaukas and Sabattini, 1997; Azcuay et al., 2007; Taboada, 2010; Pagani and Taboada, 2010, Pagani et al., 2012). There are many fossiliferous horizons in the Pampa de Tepuel Formation at several locations throughout The Sierra de Tepuel (e.g. as listed and described in Suero, 1948 and Freytes, 1971; Pagani and Taboada, 2010), and in the past years these have been revisited and catalogued to gain a better understanding of this *Lanipustula* fauna (Simanaukas and Sabattini, 1997; Pagani and Taboada, 2010). For this particular study, I examined beds described as some of the highest-known stratigraphically in the biozone (Freytes, 1971; Pagani and Taboada, 2010; Pagani et al., 2012). These beds are located lateral to and north of the measured section that was described in the previous chapter (Figure 30), and contain primarily rhynchonelliform brachiopods, bivalves, ostracodes, bryozoans, hyoliths, scaphopods, crinoids, and rare gastropods and corals. Out of the fossiliferous horizons, six shell beds were randomly chosen due to their proximity (within 1 km) to previously identified shell bed horizons (FT1-13 Bed from Freytes, 1971). This part of the section is approximately 1300 meters above the base of the Pampa de Tepuel Formation, and is located stratigraphically above the most fossiliferous locality within the formation (c.f. FT1-13 Bed in Freytes, 1971; Pagani and Taboada, 2010; Pagani et al., 2012). In the past few decades, new material collected from this locality has produced a more diverse fauna than was previously regarded (Simanaukas, 1996; Simanaukas and Sabattini, 1997; Pagani and Taboada, 2010).

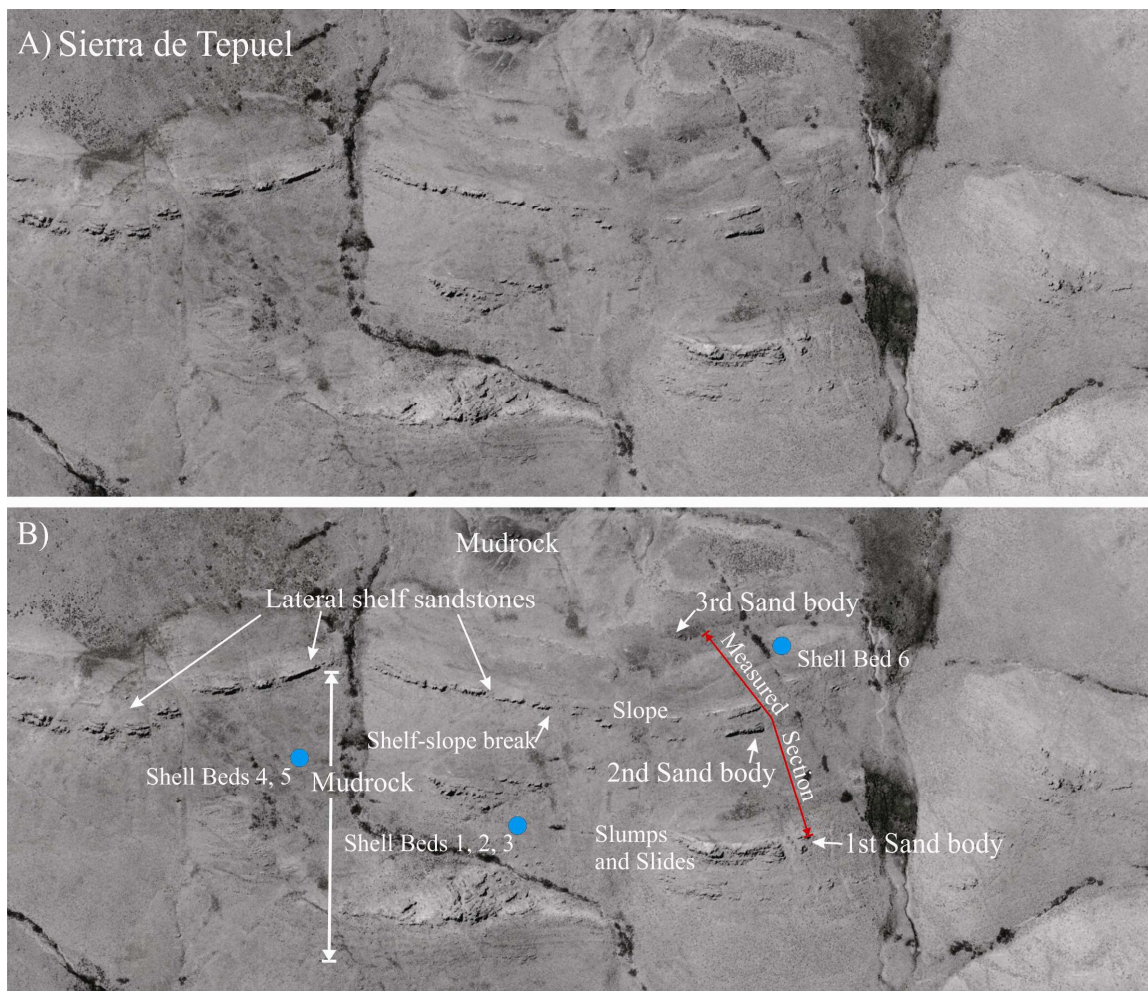


Figure 30. Sierra de Tepuel field section with the six shell beds (SB #1-6) demarcated. The major stratigraphy features have been highlighted as they relate to the environments in which each paleocommunity was living.

Far-field studies have reported that the LPIA was characterized by low rates of faunal turnover, suggesting that ecological persistence was the normal condition during times of high-amplitude and high-frequency glacioeustasy (Stanley and Powell, 2003; Powell, 2005; Bonelli and Patzkowsky, 2008; Heim, 2009; Dineen et al., 2012). Due to these changing conditions, it has been reported that broadly adaptive taxa (eurytopes) increased regionally in subtropical latitudes (Brenchley and Harper, 1998; Bonelli and Patzkowsky, 2008, 2011; Heim, 2009). This pattern may have been caused by the failure of fauna with more limited environmental tolerances to cope with and adapt to the changing conditions during climate fluctuations (Stanley and Powell, 2003; Clapham and James, 2008). The Tepuel Basin, as a near-field Gondwana basin, would have experienced high-frequency fluctuations in glacial influences, which could have led to a variety of disruptions in the ecosystem, and would thus be reflected in the faunal communities. In this portion of the study, I used a variety of quantitative paleoecological analyses in order to determine how the paleocommunities of the *Lanipustula* fauna were influenced, on a local scale, by the changing environmental factors in the Tepuel Basin.

Diversity and Richness

A total of 1261 individual specimens were counted (a full list of taxa available in Appendix B). Alpha diversity varied widely between the shell beds, ranging from 10 to 25 species in at least 12 different Classes. The alpha diversity in Shell Bed 1 is 17 (relatively high in this study) and declines to 10 in Shell Bed 2, which is then followed by a substantial increase in Shell Bed 4 at 25 species and the highest in this study (Table 2). The next two shell beds (5-6) show an increase after a decline from Shell Bed 4 (from 25 species to 12 species), but there is an increase in the number of species at Shell Bed 6 (14

species; Table 2). There is no overall trend throughout the section; rather, the diversity seems to fluctuate from shell bed to shell bed starting at 17 (Shell Bed 1) and ending at 14 (Shell Bed 6). The alpha diversities in this study remained higher in comparison to the alpha diversities recorded from beds sampled in a location that is stratigraphically lower within the *Lanipustula* zone in the Pampa de Tepuel Formation (c.f. Dineen, 2010).

Alpha Diversity			
		Shell Bed 6	14
Shell Bed 5	5	Shell Bed 5	12
Shell Bed 4	4	Shell Bed 4	25
Shell Bed 3	6	Shell Bed 3	12
Shell Bed 2	12	Shell Bed 2	10
Shell Bed 1	9	Shell Bed 1	17
Dineen, 2010		This Study	

Table 2. Comparative table with alpha diversity values for shell beds in the Pampa de Tepuel Formation from a past study (Dineen, 2010) and this current study. Shell Beds #1-6 (with #1 being the lowest stratigraphically and #6 being the highest stratigraphically) in the Pampa de Tepuel Formation. Alpha diversity is the total number of species present within each shell bed.

The relative abundances of the individual organisms were tallied for each shell bed (Figure 31). Figure 2 shows that the abundances of taxa vary from one bed to another, and that the first five shell beds share similar faunal compositions. The abundances of bivalves to brachiopods relative to each other and to other organisms change from one shell bed to another (with a range of 3.9% in Shell Bed 3 to 26.1% in Shell Bed 5 for the brachiopod populations), and it should be noted that there is an absence of any brachiopod specimens recorded in the field counts from Shell Bed 6 (Figure 31). Overall, ostracodes are ranked first at 1.17, followed by bivalves at 2.83 and

brachiopods at 3.17 (Figure 32). Gastropods increase in abundance, though not a statistically significant increase (e.g. p values range from 0.14 to 0.2 through the section), while hyoliths, corals and bryozoans gradually disappear through the section, also not statistically significant (Figure 31, Figure 32). Crinoids decrease in abundance from Shell Bed 1 to Shell Bed 5 and then increase in abundance at Shell Bed 6, but this trend is also not a statistically significant trend (Figure 32).

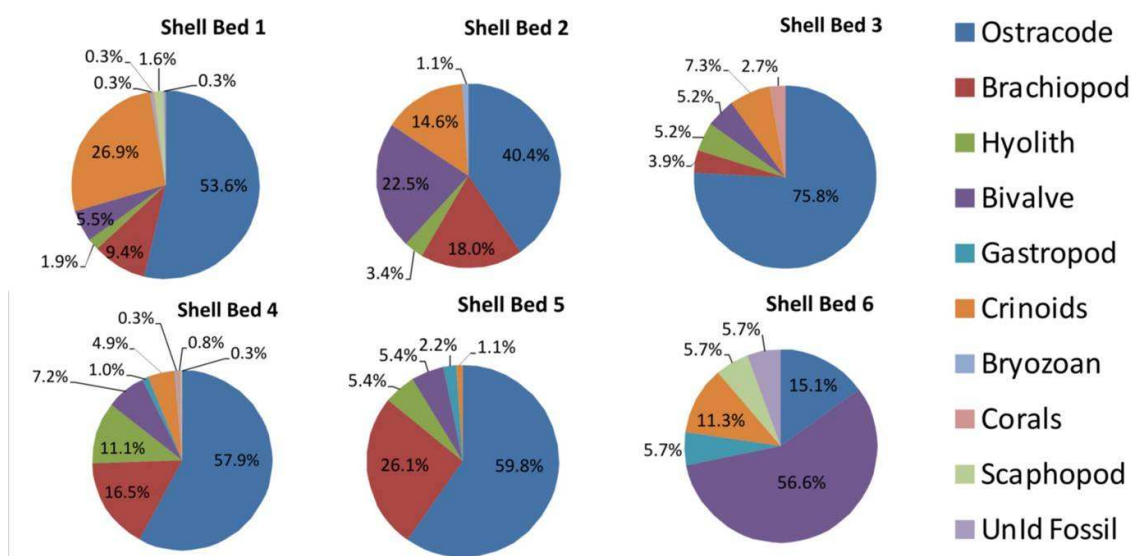


Figure 31. Relative abundances of individuals in each shell bed (SB). Shell Beds #1-6, Total = 1261 individuals. SB #1, 308 individuals. SB #2, 89 individuals. SB #3, 330 individuals. SB #4, 387 individuals. SB #5, 92 individuals. SB #6, 53 individuals.

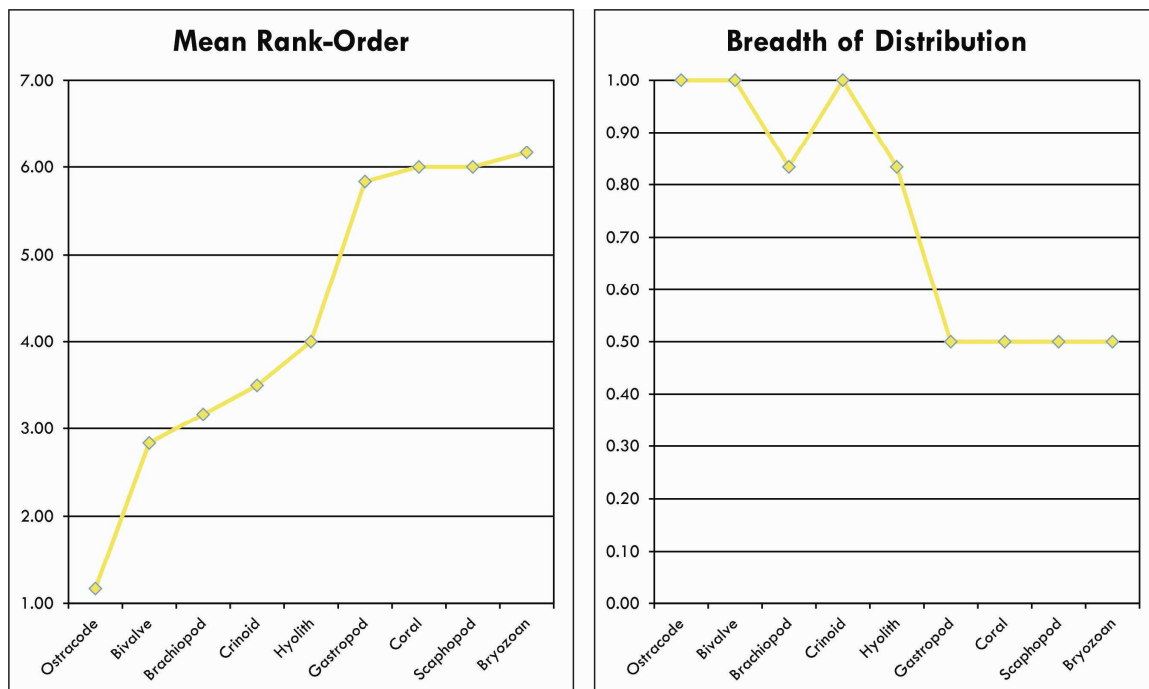


Figure 32. Mean rank-order and Breadth of distribution values of the different faunal Classes recorded in Shell Beds #1-6 in the Pampa de Tepuel Formation. Mean rank-order allows for the ordering of the taxa according to their general abundances, with values closer to 1 indicating the most abundant taxa. Breadth of distribution values measure the proportions of shell beds in which the taxon was present, values equal to 1 indicates that a taxon was present in all shell beds, where values that equal 0.5 indicate a single taxon present in only half of those shell beds.

Based on the Simpson's Index of Diversity ($1/D$) (e.g. the higher the number calculated, the greater the overall paleocommunity diversity) calculations, the beds are more diverse in some levels and less diverse in others. The dominance values range from 0.41 to 0.74 (Table 3). The lowest value, from Shell Bed 3, corresponds to the bed with the most ostracodes counted, which indicates high ostracode dominance within the bed. And, inversely, the two shell beds (Shell Beds 2 and 6) with the highest values are also the beds with the fewest ostracodes counted.

Shell bed	Simpson's Diversity Index (1/D)	Shannon Index (H')	Evenness (e)	Dominance (d)
Shell Bed 6	0.67	1.27	0.74	0.26
Shell Bed 5	0.57	1.11	0.62	0.38
Shell Bed 4	0.62	1.31	0.6	0.4
Shell Bed 3	0.41	0.93	0.52	0.48
Shell Bed 2	0.74	1.46	0.81	0.19
Shell Bed 1	0.63	1.45	0.55	0.45

Table 3. Simpson Index of Diversity (1/D), Shannon Index (H'), evenness (e), and dominance (d) values for shell beds #1-6 (with #6 as the stratigraphically highest shell bed) of the Pampa de Tepuel Formation. Simpson values range from 0 to 1, with 1 having highest diversity. H' values range from 0 to a maximum of 1/number of groups of organisms, with higher values indicating higher diversity. Evenness (e) values range from 0 to 1, with the higher numbers indicating more evenly distributed groups of individuals throughout the shell bed. Dominance (d) values range from 0 to 1, with higher values indicating a dominance of groups of individuals throughout the shell bed.

Another statistic, the Shannon-Weiner Index (H') (e.g. the higher the number calculated, the more evenly the organisms are distributed throughout a paleocommunity) was calculated in order to further assess the abundance and richness in shell beds through time (Shannon, 1948). The results for the six beds ranged from 0.93 to 1.46 (Table 3). In Table 3, both the Simpson's and Shannon-Weiner index trends mimic one another, and again there is a sharp decrease in diversity and evenness at Shell Bed 3, which is then followed by fluctuating values between the remaining shell beds.

For a further look into the distribution of the taxa in the shell beds throughout time, the evenness (e) and dominance (d) was calculated from the Shannon Indices of each bed (Table 3). Overall, the evenness values (e.g. higher evenness numbers indicates that the taxa were evenly distributed in that particular bed, whereas higher dominance numbers would indicate that a particular taxon was more dominant over the others in a shell bed) indicate that the taxa in each shell bed were fairly evenly distributed, with a

drop in evenness at the same Shell Bed 3, as described previously (Table 3). These results are consistent with the shell beds studied previously lower in the Pampa de Tepuel Formation (c.f. Dineen, 2010; Table 4).

Shell Bed	Simpson Index of Diversity (D)	Shannon Index (H')	Evenness (e)	Dominance (d)
Shell Bed 5	0.341	0.727	0.452	0.548
Shell Bed 4	0.5	0.914	0.659	0.341
Shell Bed 3	0.389	0.846	0.472	0.528
Shell Bed 2	0.827	1.889	0.76	0.24
Shell Bed 1	0.68	1.542	0.702	0.298

Table 4. Diversity index values from previously published study. Modified from Dineen, 2010.

Trophic and Tiering Analysis

Shell Beds 1-5 exhibit a numerical dominance of detritivore-grazers, which can be attributed to the dominance of ostracodes (Figure 33). Shell Bed 6 is different from other shell beds in that the number of deposit feeders increases, while the abundance of detritivore-grazers decreases. When comparing the changes in tiering, once again, Shell Beds 1-5 showed similar compositions, with epifaunal and a mostly actively mobile taxa (Figures 34, 35). Shell Bed 6 displayed different characteristics in that there was a decrease in the epifaunal to infaunal organism ratio, as well as the reappearance of some nektobenthic organisms.

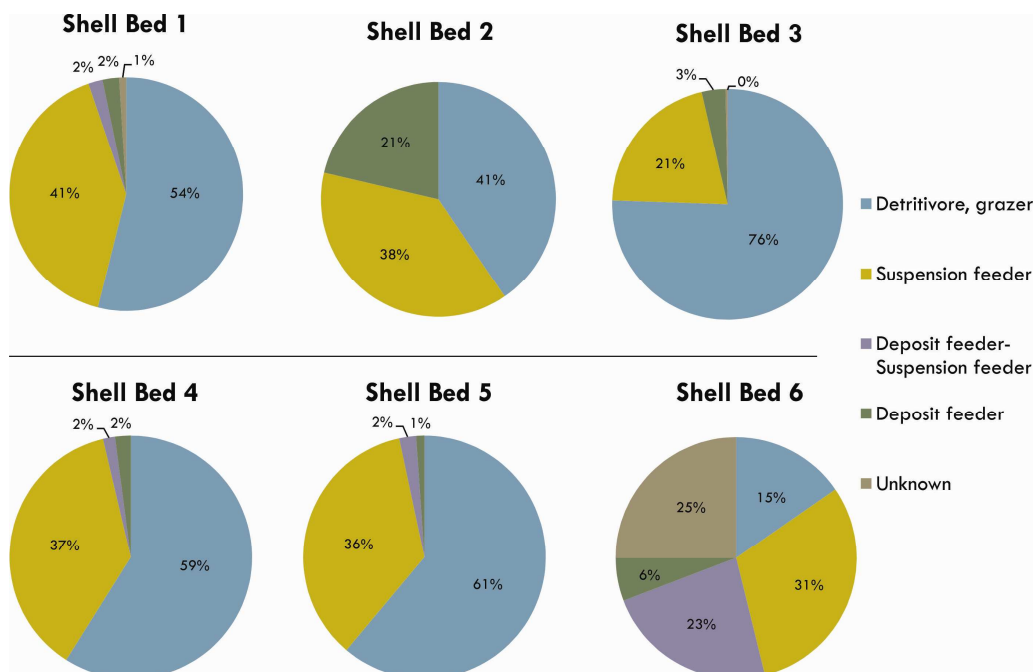


Figure 33. Comparison of the relative abundance of the individuals in each shell bed (#1-6) displaying various feeding habits as a potential indicator for increase in turbidity throughout the measured section of the Pampa de Tepuel Formation.

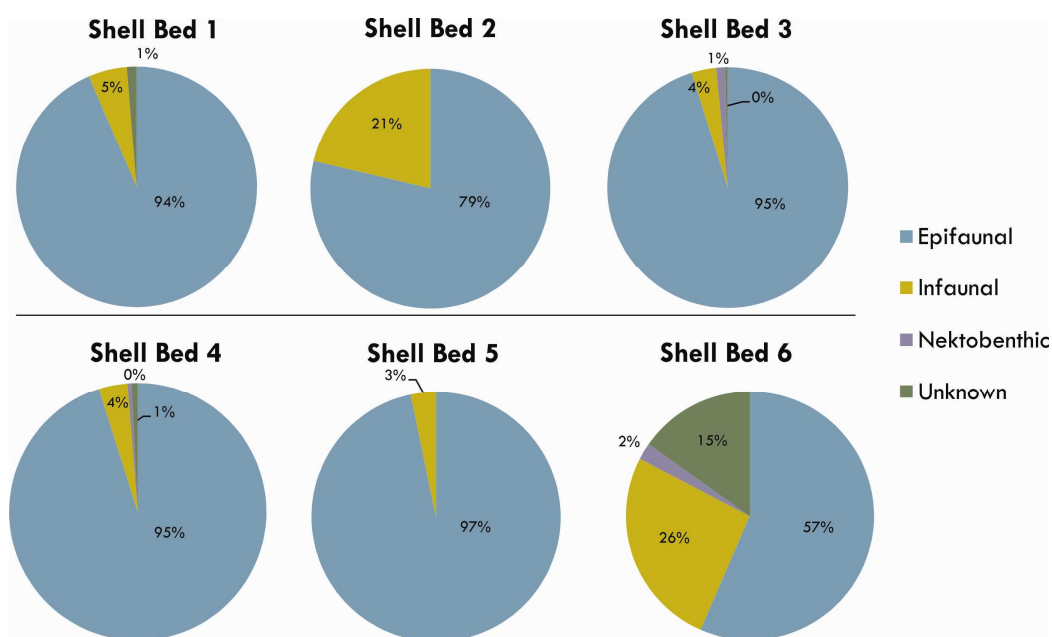


Figure 34. Comparison of the relative abundance of the individuals in each shell bed (#1-6) displaying changes in the tiering levels as a potential indicator for environmental stresses in the measured section of the Pampa de Tepuel Formation.

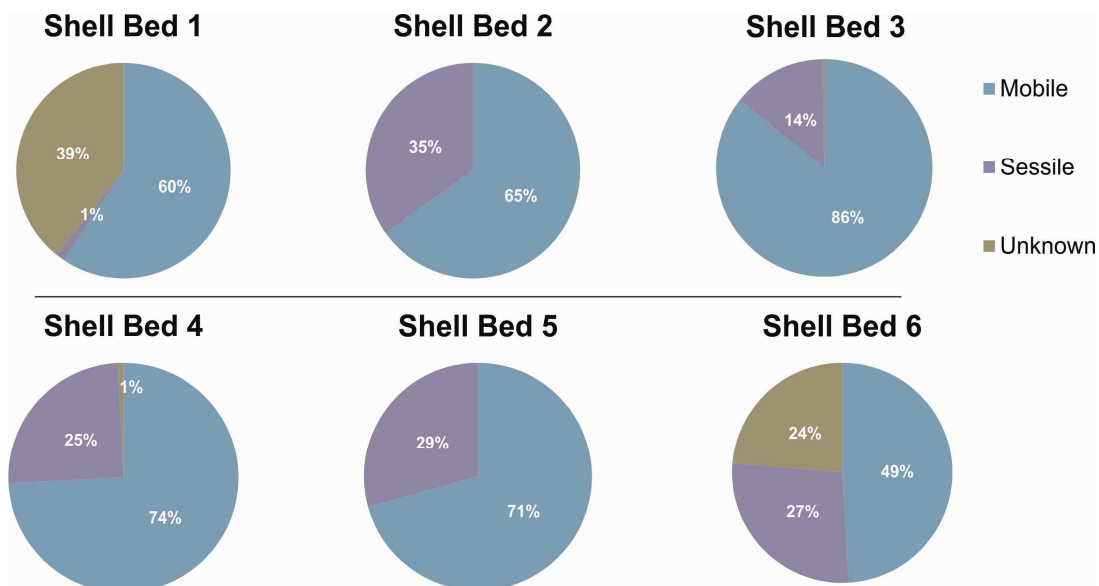


Figure 35. Comparison of the relative abundance of the individuals in each shell bed (#1-6) displaying changes in organism mobility as a potential indicator for environmental stresses in the measured section of the Pampa de Tepuel Formation

Multivariate Analyses

A detrended correspondence analysis (DCA) and a non-metric multidimensional scaling (NMS) were used to evaluate the paleocommunities in relation to one another through the section. The DCA showed that Shell Beds 1 through 5 plotted in a similar location, toward the right side of the axis, while Shell Bed 6 plotted to the left of the axis (Figure 36). To further support these findings, the NMS analysis was performed, measuring for the Bray-Curtis distance, as well as the Chord distance (Figures 37, 38). The findings from these measurements corroborate the DCA output, wherein the Bray-Curtis and Chord distance clusters (cohenetic coefficients 0.9889 and 0.9956, respectively), for Shell Beds 1- 5 show strong similarities, and are thus grouped together apart from Shell Bed 6, once again highlighting the difference in faunal composition found in Shell Bed 6 (Figure 38).

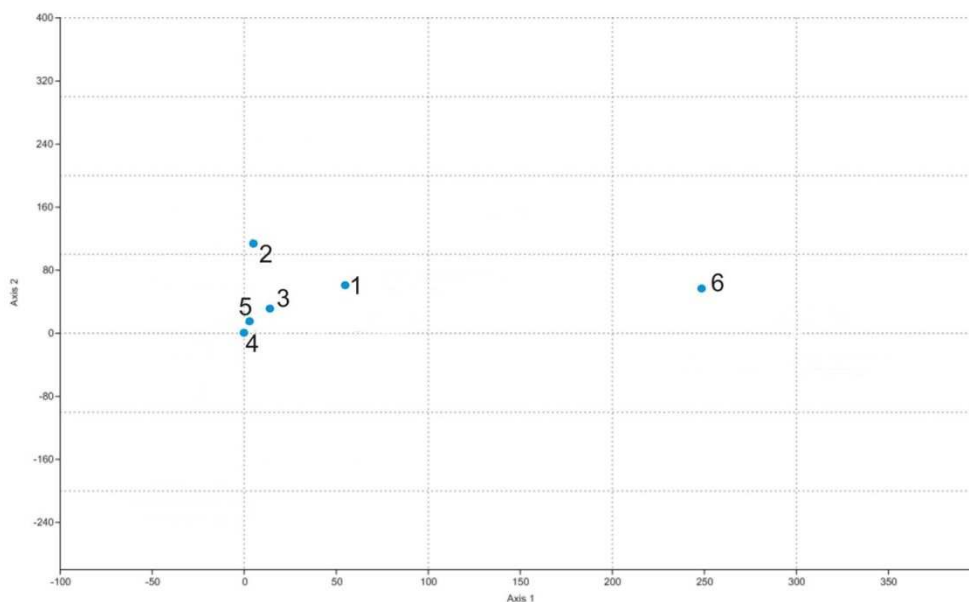


Figure 36. Multivariate analysis for the Pampa de Tepuel Formation, Tepuel-Genoa Basin. Detrended correspondence analysis (DCA) plot showing the relationship of the 6 shell beds studied.

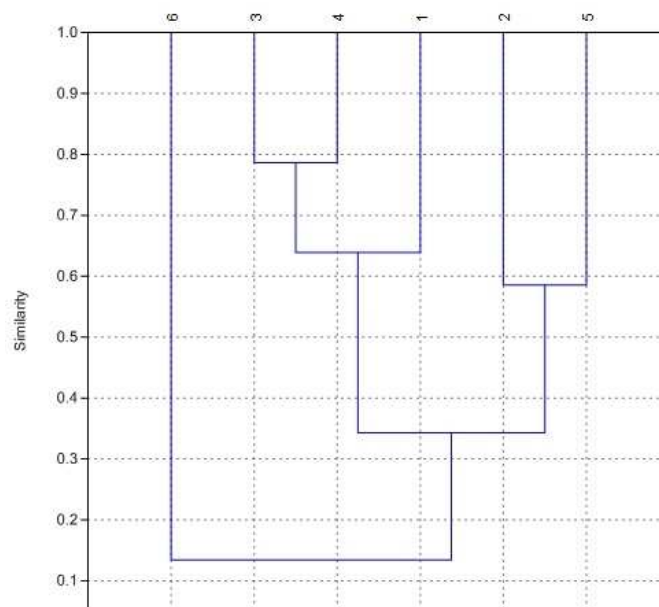


Figure 38. Multivariate analysis for the Pampa de Tepuel Formation, Tepuel-Genoa Basin. Non-metric multidimensional scaling (NMS) plot using Bray-Curtis index.

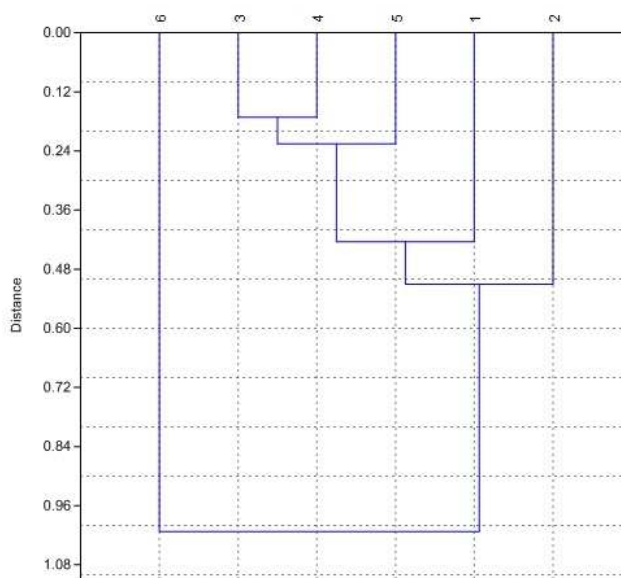


Figure 37. Multivariate analysis for the Pampa de Tepuel Formation, Tepuel-Genoa Basin. Non-metric multidimensional scaling (NMS) plot using Chord distance.

Discussion

At this location in the Pampa de Tepuel Formation, there is evidence of an established faunal composition, the *Lanipustula* fauna (in Shell Beds 1-5), gradually changing to a new faunal composition (in Shell Bed 6) as fluctuations occurred in the depositional conditions, from basin floor environments to shallower upper slope and outer shelf environments, in the Tepuel Basin (Figure 39). The biological activity and processes in this near-field basin are primarily a function of fluctuations in turbidity and sedimentation rates as this marine system changed during the LPIA.

Despite the lack of sedimentologic evidence for glacially influenced stratigraphy in the Pampa de Tepuel Fm., the time interval studied herein contains a record of glaciation in NW Argentina (Henry et al., 2008; Gulbranson et al., 2010) and eastern Australia (Fielding et al., 2008), thus shifting substrates or possible fluctuations in water salinity or oxygen concentrations, could have led to stressful conditions that facilitated paleocommunities that tended to be low in diversity (Figure 40; Brenchley and Harper, 1998; Pörtner, 2001; Peck et al., 2004; Clapham and James, 2008; Badyrka et al., 2013). In normal (i.e. environments without stressors) marine waters during the Paleozoic, one would expect to see brachiopods, corals, echinoderms, ammonoids, and benthic foraminifera (Brenchley and Harper, 1998; Pagani and Taboada, 2010). If stress is introduced into the system, such as a shift in relative sea-level, there may be an increase in opportunistic and eurytopic, or generalist, taxa. Environments that undergo frequent periods of stress (e.g. fluctuations in turbidity, substrate stability, oxygen, and salinity; Figure 40) tend to be characterized by more mobile organisms, which can rapidly move

to and colonize other environments (e.g. opportunistic taxa; Wignall, 1994; Brenchley and Harper, 1998; Sterren and Cisterna, 2010).

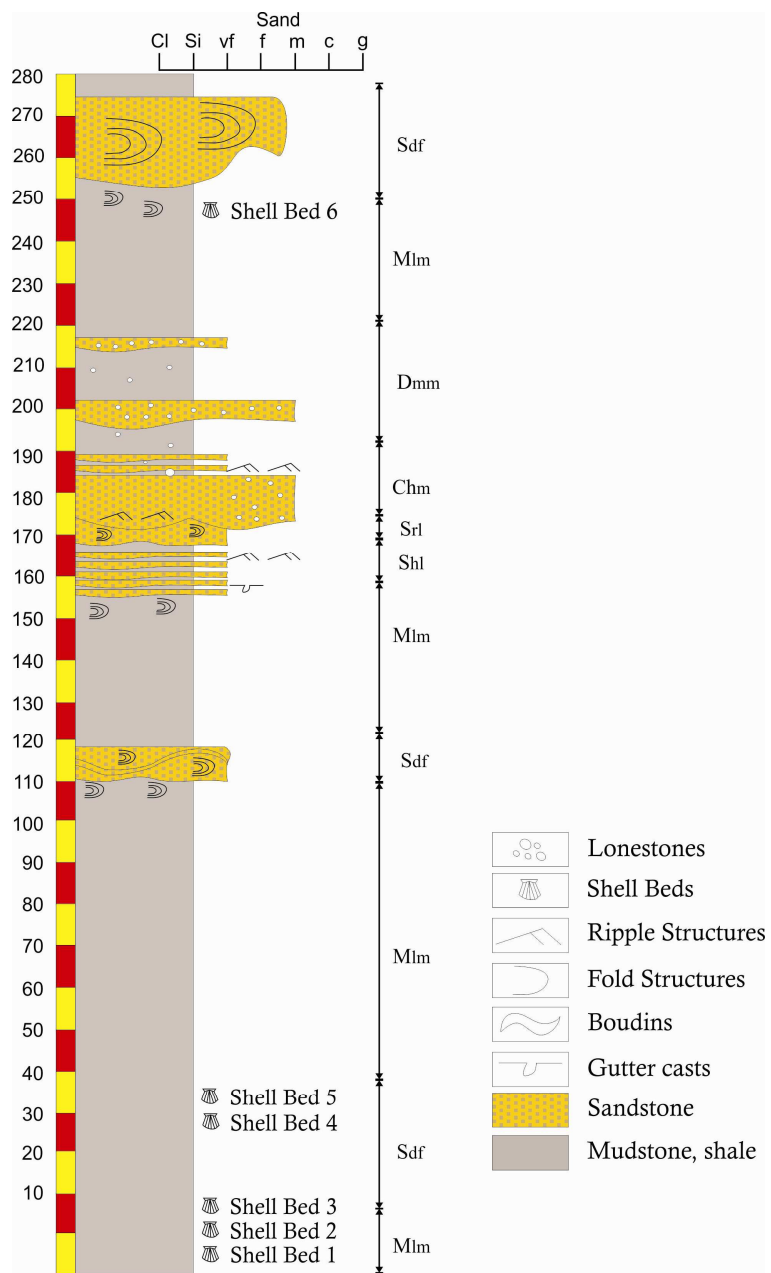


Figure 39. Lateral stratigraphic column from the measured field section for this study (276 meters). Note that Shell Beds #1-3 actually occur below the start of the measured portion.

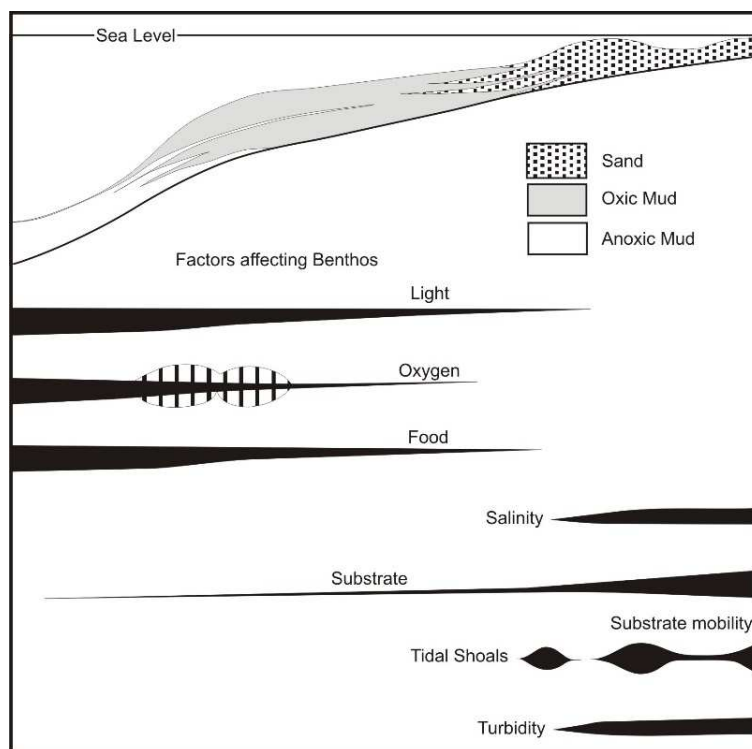


Figure 40. Various environmental factors that are known to affect benthic organisms based on their position within a marine environment. Modified from Brenchley and Harper, 1998.

In the rock record, diversity can appear to increase when there is a mixing of shells from different environments because of physical processes, or it can be skewed when there is an abundance of small taxa, such as the large numbers of counted ostracodes, as seen in Figure 31 (Brenchley and Harper, 1998; Clapham et al., 2006). Diversity and abundance of skeletonized marine invertebrates can also change depending on the specific environments in which a community is located (Brenchley and Harper, 1998; Pörtner, 2001; Peck et al., 2004; Clapham and James, 2008; Badyrka et al., 2013). Fossil abundances vary depending on the environmental setting; i.e. the abundances increase from inner to mid-shelf facies, and then decreases as one moves into deeper shelf facies (Brenchley and Harper, 1998). Changes in the abundances of the different

the feeding habits can indicate the amount of turbidity in the system. Changes in tiering, which refers to the life position of the organism in relation to the substrate, can be used to determine substrate stability. Comparing the fossil abundances, diversity indices and changes in tiering of the shell beds throughout a section, the changes and trends can be used to evaluate environments.

In this study, the diversity remains relatively high throughout the section, although the decrease in diversity seen in Shell Bed 3, as has been stated, is most likely due to the sharp increase in the abundance of the ostracodes at this level. This increase is most likely due to a sampling bias that could have been caused by a possible taphonomic bias, patchy distribution of individuals, or time averaging (Kidwell and Holland, 1991; Bennington, 2003; Dineen et al., 2012). Based on the results from the analyses, the lower five shell beds show a distinct separation from that of the uppermost shell bed (i.e. Shell Bed 6; Figures 36-38, 39). Based on this separation, we can deduce that the paleocommunities of Shell Beds 1-5 were living in similar environments, with similar faunal compositions and can be placed within the *Lanipustula* biozone. Shell Bed 6 comprised a different faunal community and may have been living in different environmental conditions. The fauna of Shell Bed 6 will be discussed in more detail later in this chapter.

Paleoecology of the Lanipustula fauna

As discussed in the previous chapter, the section of the Pampa de Tepuel Formation examined in this study includes facies that were deposited in the outer shelf and upper slope depositional settings (Figure 11). It is likely that the *Lanipustula* fauna

(Shell Beds 1-5) recorded in these beds lived on a fairly stable substrate within the low energy environment of the slope, which is evident as the lower five beds reside well within the expanse of the lower mudrock facies association.

The lower five shell beds show similarities to the beds that have been published previously (c.f. Dineen, 2010). Both the previously studied beds (c.f. Dineen, 2010), and the lower 5 shell beds studied here consist of a relatively diverse fauna composed of dominantly epifaunal organisms. The shell beds studied here differ in that they consist predominantly of actively mobile detritivores due to the statistically abundant ostracodes recorded. This is in contrast to the lower shell beds from a previous study (c.f. Dineen, 2010) that consisted of mostly sessile suspension-feeding organisms, which indicates that these lower paleocommunities lived on a stable substrate and likely experienced little turbidity. Unlike the underlying beds from a previous study (c.f. Dineen, 2010), the paleocommunities in this study contained higher abundances of bivalves rather than brachiopods. The most abundant organism in the shell beds of this study, the ostracod, was also not present in the previous study, which could indicate that the environments may have been shifting.

Ostracodes are a eurytopic taxon and have the ability to live in most environments (Dodd and Stanton, 1986; Brenchley and Harper, 1998; Díaz Saravia and Jones, 1999). In the Tepuel Basin, there are at least eight species of ostracodes that have been identified, but there has been only one species of ostracod that has been positively identified at this field locality, which is *Graphiadactylloides patagoniensis* (Díaz Saravia and Jones, 1999; Pagani and Taboada, 2010). This genus has been recorded in sediments from the shelf-slope break environments of North American and European basins, which corresponds to

the depositional environments interpreted here (Benson and Collinson, 1958; Green, 1963; Blumenstengel, 1975; Gründel, 1975; Lane, 1978; Díaz Saravia and Jones, 1999). The presence of this genus in the Tepuel Basin is the southern-most recorded occurrence, which may indicate that these ostracodes are tolerant to colder water temperatures and were able to adapt to changes within the marine environment (Díaz Saravia and Jones, 1999). In addition to the presence of the ostracodes, there are two bivalve genera found in these shell beds that are considered to be generalist taxa (e.g. *Nuculopsis* and *Phestia*; Kammer et al., 1986; Sterren and Cisterna, 2010). These genera have been linked to dysaerobic and unstable substrate conditions, which can indicate stressed environments (Sterren and Cisterna, 2010). There is not a predominance of either genus in the lower five shell beds, but they do increase in appearance from Shell Bed 4 to Shell Bed 6, though not significantly (e.g. $p = 0.2$ from SB 4 to SB 5 and $p = 0.19$ from SB 5 to SB 6). The appearance of these genera may be connected to the periodic disruptions introduced by the slide blocks that moved down the slope to the basin floor environments where these established and diverse paleocommunities were living, although further investigation is needed to determine if this pattern is significant.

Paleoecology of a potentially new fauna

The paleocommunity of the uppermost shell bed (6) in this study is unlike the faunal compositions in the lower five beds, and it is also different from the study conducted by Dineen (2010). The most notable difference in the fauna of this shell bed is that there were no brachiopods positively identified from field counts, although after some study of the site material in the lab, a portion of the unidentified fossils counted here were later identified as brachiopods, but there was a distinct lack of the diagnostic

species *Lanipustula patagoniensis* (A. Pagani, personal communication). Instead, the most abundant organisms in this shell bed are bivalves. Shell Bed 6 also displayed different characteristics in that there was a decrease in the epifaunal to infaunal organism ratio, though not a statistically significant decrease, although it may be important to note that this decrease in ratio may be due to the drastic reduction in number of ostracodes counted in this level. There was also the reappearance of some nektobenthic organisms, as well as other mobile fauna (e.g. *Nuculopsis* and *Phestia*; Appendix B). The lack of *Lanipustula* and an increase in mobile taxa than in the lower five shell beds is most likely due to a major change in environment as this shell bed is located above the incursion of the shelf and clinoform facies into the deeper parts of the basin. The stresses in the environment are most likely due to an unstable substrate, which has been considered to be an important factor in the distribution of brachiopods and bivalves (Sterren and Cisterna, 2010).

In addition, the sliding of large bodies of sediment, such as the slide blocks and slumps discussed in the previous chapter, would have caused periodic disruptions to the otherwise stable slope environment. There may have also been changes in the nutrient supply, oxygen levels, and temperature as the depositional environments shifted landward (Sterren and Cisterna, 2010; Badyrka et al., 2013). Bivalves and brachiopods have different metabolic demands in relation to environmental factors such as the ones previously listed (Tomasovych, 2006; Sterren and Cisterna, 2010; Badyrka et al., 2013). As the depositional environments in the basin shift, it is possible that these ambient water factors would have affected the established lower paleocommunities (Shell Beds 1-5), and this could have led to a new faunal composition at Shell Bed 6, one that would have

had the ability to adapt to the new conditions. This shell bed is also located in the section directly overlying the low stand system, and the furthest regression into the system, which could have been caused by changes in relative sea level within the basin, and may have coincided with sea ice, which tends to play a significant role in the biological productivity as well as the abundances and diversities of the faunal communities (Powell, 2005). This uppermost shell bed is also defined by Pagani et al. (2012) as being poorly diverse in comparison to previously studied shell beds in this location. In almost every respect, Shell Bed 6 is different than those in the lower five levels, which indicates that there may be a new faunal composition at this position in the basin, but further analysis is needed to determine the significance of this.

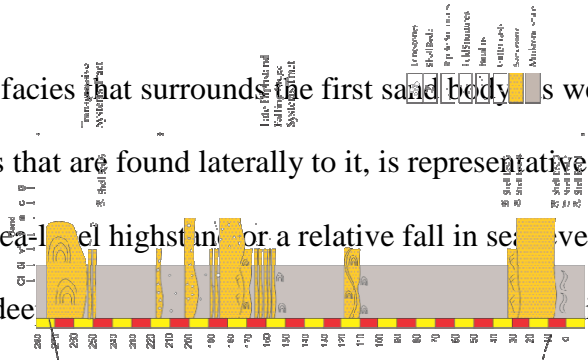
Chapter 5. Discussion

The interpretations of the depositional settings within the Tepuel Basin are still in question (Frakes and Crowell, 1969; Gonzalez Bonorino et al. 1988, 1992; López Gamundí, 1997; Gonzalez 1997, 2010). The controversy revolves around the depositional setting and the proximity of the glaciers within the basin through time. Interpretations of the Pampa de Tepuel Formation, in particular, are contentious. Originally, the formation was interpreted as a glacially-derived marine deposit (Suero, 1948). Later studies also support this interpretation (Frakes and Crowell, 1969; Page et al., 1984; López Gamundí, 1987; González Bonorino et al., 1988; González Bonorino, 1992). In contrast to these interpretations, the Pampa de Tepuel Formation has also been regarded as a more continental succession that was deposited by glaciers at the shoreline, or in the littoral zone with marine transgressions as the glaciers advanced and retreated within the basin (González, 1972, 2002; González and Glasser, 2008; González and Díaz Saravia, 2010). This study presents a closer look at the middle portion of this formation and proposes a modified interpretation of the depositional setting through the identification and subsequent interpretation of the lithofacies in this portion of the formation. This project then uses that information in order to better understand the controls on the establishment and distribution of a specific faunal zone, the *Lanipustula* Biozone.

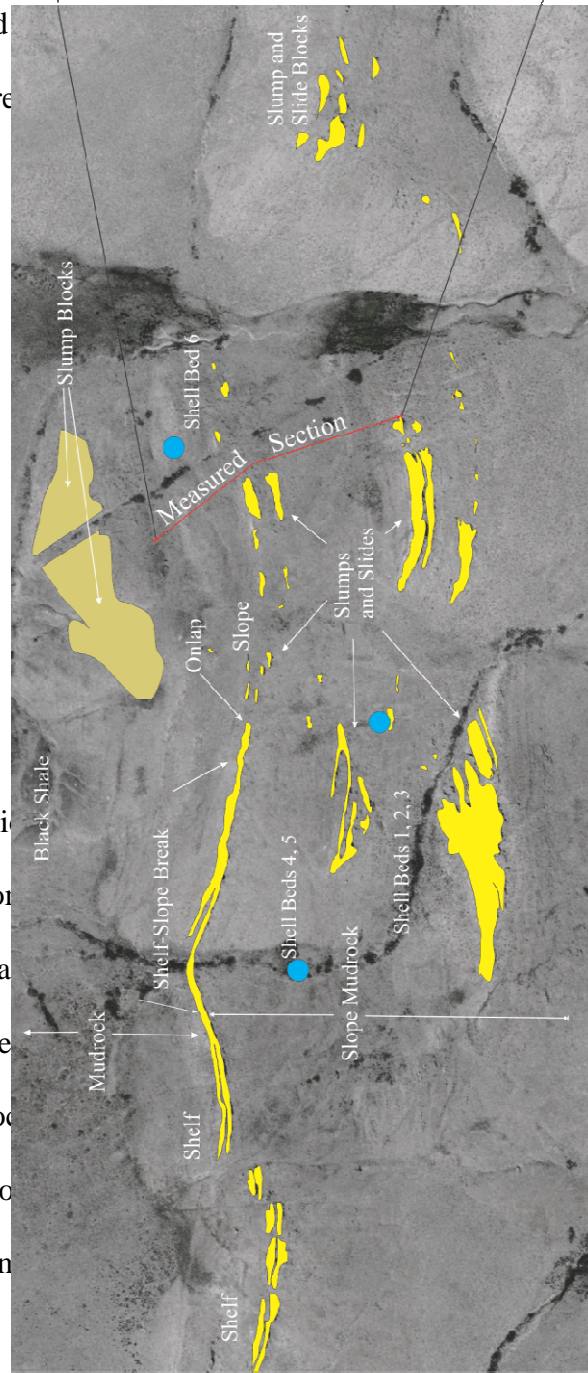
In this study, a majority of the depositional processes are interpreted to be marine-dominated in this portion of the Pampa de Tepuel Formation, and are most similar to processes found in normal shelf and slope facies, which include: settling from suspension of hemipelagic muds, wave and storm activity, sliding and slumping, as well as

deposition from turbidity currents. The measured section contains three main lenticular sand bodies (e.g. near the base, the upper middle portion, and at the very top), a set of clinoforms, as well as thick successions of mudrock, where the shell beds are located (Figure 41). At the base of the measured section is the first lenticular sand body. Lateral to this, within the lower mudrock succession, are the first five shell beds (#1-5). The upper middle portion of the section contains the second major set of lenticular sand bodies, which dips at a 1-5 degree angle (depositional dip) with respect to the sand bodies located to the north. These middle sand bodies comprise the clinoforms within this portion of the Pampa de Tepuel Formation. Another succession of mudrock separates the second set of sand bodies from the third and uppermost lenticular sand body, and the last shell bed (#6) is located within this mudrock succession. Within these deposits there is a brief (about 10-20m) coarsening-upward succession through the middle of the section, due to the progradation of the shelf into the basin (i.e. the clinoform). This is followed by a brief fining-upward succession from the middle sand body to the top of the second clinoform that abruptly changes to mudrock through the rest of the measured section. This measured section represents portions of two sequences within the basin: a late highstand, followed by a lowstand systems tract due to a regression and relative sea level fall, which is then followed by a transgressive systems tract and a second late highstand/falling stage package (Figure 41; Steel and Olsen, 2002).

The mudrock facies that surround the first sand body, as well as the other lenticular sand bodies that are found laterally to it, is representative of marine strata and likely a relative late sea-level highstand or a relative fall in sea level (falling stage systems tract) in the deep ocean basin. This is due to the landward (transgression); Figure



is due to the landward (transgression); Figure



facies, clastics periodically moved downslope from the shelf as the slide blocks during the early stages of relative sea-level fall. These clastics were deposited in Shell Beds 1-5 within the mudrock at these level, and was once again deposited in the low energy environment of the slope. This process created a mixing and nutrients to the

slope and basin floor environments, which allowed for the establishment of such a diverse fauna.

The lower five shell beds studied here consist of a relatively diverse fauna composed of dominantly epifaunal and actively mobile organisms. The most abundant organism in the lower five shell beds of this study was the ostracod *Graphiadactylloides patagoniensis*. Ostracodes are a eurytopic taxon and have the ability to live in most environments (Dodd and Stanton, 1986; Brenchley and Harper, 1998; Díaz Saravia and Jones, 1999). The species of ostracod that has been identified here, seems to indicate that these ostracodes are tolerant to a wide variety of changes and environments, as they are found near the shelf-slope break environments within basins (Benson and Collinson, 1958; Green, 1963; Blumenstengel, 1975; Gründel, 1975; Lane,

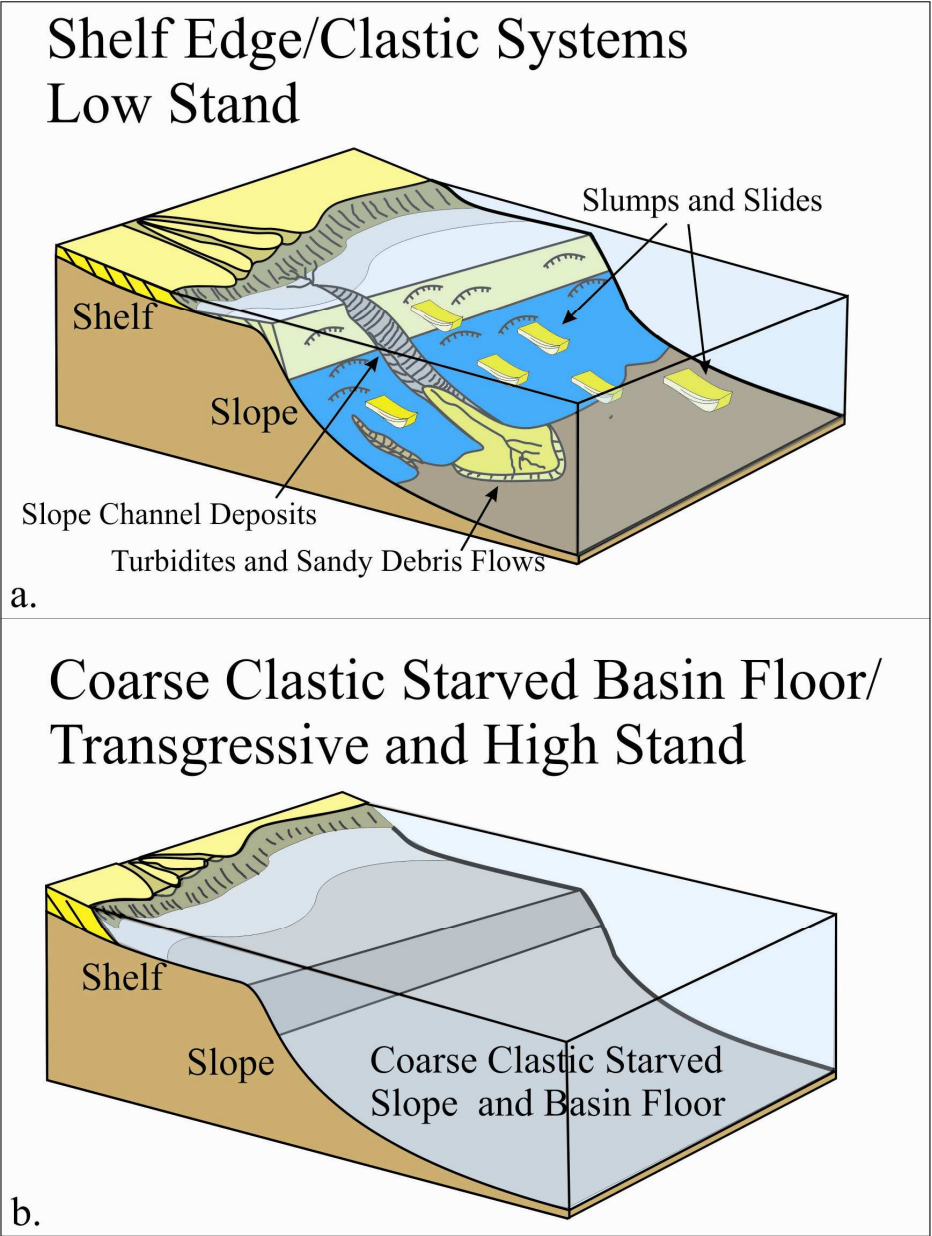


Figure 42. A model for sedimentation in this section of the Pampa de Tepuel Formation, Sierra de Tepuel, Argentina. A. Lowstand deposits consist of mass transport processes in which clastics make it into the deep basin. B. Highstand and transgressive systems tracts deposits when the slope and basin floor experience sediment starvation.

1978; Díaz Saravia and Jones, 1999; Pagani and Taboada, 2010). Two bivalve genera, *Nuculopsis* and *Phestia*, found in these lower five shell beds are considered to be generalist and opportunistic taxa that have been linked to dysaerobic and unstable substrate conditions that may indicate stressed environments (Kammer et al., 1986; Sterren and Cisterna, 2010). As there is not a predominance of either genus in the lower five shell beds, the appearance may be a reflection of the periodic disruptions introduced by the slide blocks that moved down the slope to the basin floor environments where these established and diverse paleocommunities were living. The mudrock facies association occurs upward until the fine-grained mudrock coarsens into interbedded sandstones a few tens of meters below the dipping sandstone clinoform.

The interbedded sandstone facies, here interpreted as turbidites, are deposited as the shelf-slope break progrades further basinward during a late high stand or during the falling stage of relative sea level when sediment bypass of the shelf occurs due to a lack of accommodation space (Steel et al., 2008). The clinoform is evidenced by slide/slump blocks and slope channel deposits at 175-181 meters. The appearance of the clinoform is indicative of shallower marine processes as clastics transit across the shelf to the shelf-slope break. Density-driven, sediment-laden currents draining down the slope through slope channels transported coarse sediment away from the shelf edge and into the deeper basin during a sea-level low stand (Figure 42a). The onlap onto the nodal point, as indicated in Figure 41, represents a brief aggradation of the clinoform, which indicates that the lowstand persisted through a short interval of continued relative sea level fall. The massive diamictite facies sections, here interpreted as debris flows, bounds the top of this second onlapping clinoform, and suggests continued high sedimentation rates at the

shelf-slope break. There were no body fossils found within this portion of the section as the *Lanipustula* fauna seems to be found within deeper slope environments. High rates of sedimentation and storm activity are indicated by the numerous levels of wave ripples and the occurrence of hummocky cross-stratification. Such conditions would have created stressful living conditions for a fauna that appears to occupy calmer deeper water conditions. During this time, shell beds containing *Lanipustula* fauna would most likely be found further to the south of this measured section, as that is the interpreted location of deeper basin environments.

The abrupt return to the mudrock facies above the clinoform deposits marks the occurrence of a flooding surface as a relative sea-level transgression occurred and the shoreline retreated landward allowing for a deepening upward succession (Figure 42b). Shell bed 6 is located within this upper mudrock facies, which seems to be indicative of a return to a basin floor or upper slope environment where fauna were able to establish communities. Lateral to the shell bed and located depositionally higher along the interpreted slope of the basin is a set of amalgamated slump bodies (Figure 41). These slumps, which are the third set of sand bodies located at the very top of this section, could be indicative of a destabilization of the shelf-edge as the transgression occurred causing clastics to move onto the lower slope (Noda et al., 2013). The slumps here, like the slide blocks found at the base of the measured section, are also encased in mudrock, which indicates that clastic-starved conditions persisted in the distal portion of the basin during the transgression. This upper mudrock unit grades into very black shale as the Pampa de Tepuel Formation continues above the measured section. This mudrock unit is several hundred meters thick and ends in another laterally continuous sandstone horizon, which

is proposed to be another incursion of shelf into the deep basin and the start of a new depositional sequence.

The paleocommunity of Shell Bed 6 in this study, though showing no statistical taxonomic difference, displays a slightly different faunal composition from the lower five beds, as evidenced by the multivariate analysis results. The most notable difference in the fauna of this shell bed is that there was a distinct lack of the diagnostic brachiopod species *Lanipustula patagoniensis*, which suggest that the shell bed is no longer located within the *Lanipustula* Biozone (A. Pagani, personal communication). The most abundant organisms in this bed are bivalves, which is also a change from the lower shell beds that are dominated by *Graphiadactylloides*. There was also the reappearance of some nektobenthic organisms, as well as other mobile fauna (e.g. *Streblochondria*, *Nuculopsis* and *Phestia*; Appendix B). The lack of *Lanipustula* and an increase in mobile taxa over what was contained in the lower five shell beds is most likely due to a major change in environment as this shell bed is located above the incursion of the shelf and clinoform facies into the deeper parts of the basin.

Shifts in community composition after periods of stress have been introduced into the marine system are not uncommon (Brenchley and Harper, 1998; Badyrka et al., 2013). As the relative sea level rose, there may have been changes in oxygen concentrations, the nutrient supply, and possibly water temperature as the water depths, and therefore the depositional environments, shifted landward during the transgression (Sterren and Cisterna, 2010; Badyrka et al., 2013). Bivalves and brachiopods have different metabolic demands in relation to environmental factors such as the ones previously listed, and can potentially tolerate stresses such as low oxygen concentrations

and unstable substrates, which could account for the dominance of bivalves in this paleocommunity (Tomasovych, 2006; Sterren and Cisterna, 2010; Badyrka et al., 2013). As the depositional environments in the basin shift from a late highstand to lowstand into a transgressive sequence, it is possible that these ambient water factors would have affected the established lower paleocommunities (Shell Beds 1-5) of the *Lanipustula* fauna. The shifting of the shelf and basin floor as relative sea level fell and subsequently rose again potentially creating inhospitable conditions that led to a possible different faunal composition at Shell Bed 6, but further analysis and data is needed in order to determine if this is a significant trend.

The stratigraphic section described in this thesis from the middle portion of the Pampa de Tepuel Formation is most easily related to normal marine processes acting along the outer shelf, shelf slope break, slope and basin floor in the Tepuel Basin. Despite having been deposited at a high paleo-latitude during the late Paleozoic Ice Age (LPIA), these strata record only a minimal glacial influence. Rare outsized clasts contained within mudstones are the only evidence suggesting a possible glacial origin. However, such clasts also can be rafted by sea ice, vegetation, or be transported by mass transport processes (Thomas and Connell, 1985; Gilbert, 1990; Lisitzin, 2002; Isbell et al., 2013). Elsewhere in the Pampa de Tepuel Formation, thick massive diamictites and striated, bullet-shaped dropstones are common, which attest to deposition in a glaciomarine setting or in a glacially influenced marine setting.

Originally, numerous studies determined that glaciation in Gondwana shifted from west to east during the LPIA, as the super continent drifted over the South Pole (Caputo and Crowell, 1985; López Gamundí, 1997; Isbell et al., 2003). Although it was

previously thought that there were three major glacial phases (e.g. López Gamundí and Martínez, 2000; Isbell et al., 2003; Fielding et al., 2008a, 2008b), it now appears that the timing and location of glaciation waxed and waned diachronously across the supercontinent (Visser, 1997; Isbell et al., 2003, 2012; Fielding et al., 2008a, 2008b; Gulbranson et al., 2010). Therefore, localized near-field projects, such as this one, are important in understanding the bigger picture of the LPIA. The findings from this project show that there was not always glaciation within the polar basins during the LPIA, and that the sequences recorded in these basins can also be due to changes in relative sea level with little to no influence from local glaciers.

Because of the Tepuel Basin's location within the South Polar Circle during deposition, it is important to consider how paleocommunities responded to changing conditions within different environments. The paleoecology of the *Lanipustula* fauna is still not well understood. The data presented here attempts to create a more thorough analysis of the paleoecology, but there is still much to be done. As there is only one shell bed in this section that is different compositionally, and has been interpreted to have existed in a different sequence, more sampling needs to be done in order to corroborate the findings here. The sampling should include more shell beds that are stratigraphically higher than Shell Bed 6 in order to determine in further detail how this new faunal composition reacted as the basin ultimately deepened before shallowing again at the top of the second sequence. Questions to be addressed include: Is there really a new fauna? Are there similarities between the new fauna and that of the *Lanipustula* fauna that lived in the Tepuel Basin? What types of trends are there, if any, for the duration of the *Lanipustula* fauna in the basin? Does the *Lanipustula* fauna mirror the trends published

in Sterren and Cisterna (2010), with a post-glacial faunal composition and an intra-glacial faunal composition, and does that explain the differences seen here in this study as compared to the previously published study by Dineen (2010)?

Chapter 6. Conclusion

The Pampa de Tepuel Formation records Mississippian to Permian depositional history within the Tepuel Basin. Based on current age models for the basin, the depositional section reported here occurs in the upper portion of the *Lanipustula* biozone likely from the late Bashkirian to the early Moscovian. This particular section of the Pampa de Tepuel Formation in the Sierra de Tepuel is representative of at least two depositional sequences. The mudrock units of this section contains evidence of open marine conditions on the upper slope environments of either a non-glacial interval or in an environment distal to an active ice front. However, the presence of rare dropstones suggest that limited glacial activity was still present along basin margins shedding ice into the basin. The mudrock unit grades into a coarsening-upward succession, which contains the appearance of massive slump and slide blocks as well as the clinoform in the middle of the section. This middle portion has been interpreted here as a regression, and a progradation of the shelf-slope break basinward likely do to a fall in relative sea level and during a relative sea-level lowstand. The clinoform is overlain by an abrupt return to mudrock and another massive slump at the top of the section. The upper portion of the section is interpreted here as a transgression and a return to open marine conditions, similar to conditions seen in the lower part of the section with major retrogradation of coarse clastics landward across the shelf leaving the study area starved of such sediment. At that time, the study area would have been located in a lower slope-basin floor setting. Continued deposition allowed for progradation of another shelf edge succession ~300 m higher in the section.

The fauna in this area records established paleocommunities followed by a shift in the faunal composition of the uppermost shell bed in the section. At the base of this section, the paleocommunities represent a diverse faunal composition that is indicative of the *Lanipustula* biozone, and consisted of ostracodes, brachiopods, bivalves, hyoliths, crinoids, gastropods, bryozoans, and corals. The lowermost paleocommunities (1-5) show little difference to one another compositionally and ecologically. The paleocommunities were relatively diverse and contained abundant fauna. It is interpreted here that these were stable and established communities living on lower slope and basin floor environments that may have experienced some disturbances due to the sliding bodies.

Some of the more notable differences, though not statistically significant, were recorded in upper shell beds (4 and 5) with the appearance of more opportunistic and mobile fauna, such as the ostracod *Graphiadactylloides*, and the bivalves *Phestia* and *Nuculopsis*. These changes in faunal composition may be early indicators of the shifting depositional environments, as the clinoform prograded into the basin, although this trend needs to be further tested. The uppermost shell bed (6) may indicate shift to a new fauna, one that is not as diverse as the *Lanipustula* fauna and contains more mobile taxa, but the significance of this needs to be further analyzed. It also does not contain the diagnostic brachiopod species, *Lanipustula patagoniensis*, and therefore cannot be at this time regarded as part of the *Lanipustula* biozone. Regardless, this paleocommunity would have existed after the retreat of the clinoform during what is interpreted here in this study to be a transgression. The fauna here may indicate that the environment was not as

hospitable as the one that the lower fauna was living in, which may or may not account for the reported lower diversity and the higher number of mobile and opportunistic taxa.

The conclusions from this project contribute to understanding the complex relationship the depositional environments of near-field basins have with the establishment and diversification of the faunal communities that live within them. The data also contribute to defining the complex nature of the LPIA, and how the timing and duration of the glacial intervals occurring across Gondwana affected the paleoecology. The paleoecology of the marine fauna during the LPIA seems to be dependent upon the localized environmental factors, including turbidity, water depth and ice proximity.

References

- Allen, J. R. L., 1985. Sedimentary structures: Their character and physical basis
Amsterdam, Elsevier, 663 p.
- Amos, A. J., Antelo, B., González, C. R., Mariñelarena, M. P., and Sabattini, N., 1973.
Síntesis sobre el conocimiento bioestratigráfico del Carbónico y Pérmico de
Argentina: Actas 5° Congreso Geológico Argentino, Carlos Paz, v. 3, p. 3–20.
- Amos, A. J., and Rolleri, E. O., 1965. El Carbónico Marino en el Valle Calingasta–
Uspallata (San Juan–Mendoza): Boletín de Informaciones Petroleras, v. 368, p. 50–71.
- Anderson, J. B., Brake, C., Domack, E., Myers, N., and Wright, R., 1983, Development
of a polar glacial-marine sedimentation model from Antarctic quaternary deposits and
glaciological information, in Molina, B. F., ed., Glacial Marine Sedimentation: New
York, Plenum Press, p. 233-264.
- Andreis, R. R., Archangelsky, S., Gonzalez, C. R., Lopez Gamundi, O., Sabattini, N.,
Acenolaza, F. G., Azcuy, C. L., Cortinas, J., Cuerda, A., and Cuneo, R., 1987. Cuenca
Tepuel-Genoa, *in* Archangelsky, S., ed., El Sistema Carbonifero en la República
Argentina, Academia Nacional De Ciencias de Cordoba, p. 169-196.
- Andreis, R. R., Cúneo, R., López Gamundi, O., Sabattini, N., and González, C. R., 1996.
Cuenca Tepuel–Genoa., *in* Archangelsky, S., ed., El Sistema Pérmico en la República
Argentina y en la República Oriental del Uruguay, Academia Nacional de Ciencias de
Córdoba, p. 65–92.

- Archangelsky, S., and Marrquez Toigo, M., 1980. La palinología y el límite Carbónico–Pérmico en el Gondwana sudamericano, *in* Proceedings Actas 2do. Congreso Argentino de Paleontología y Bioestratigrafía y 1er. Congreso Latinoamericano de Paleontología, v. 4, p. 221–229.
- Azcuy, C., Beri., A., Bernardes-de-Oliveira, M.E.C., Carrizo, H.A., Pasquo, M., Saravia, P.D., Gonzalez, C.R., Iannuzzi, R., Lemos, V.B., Melo, J.H., Pagani, A., Rohn, R., Amenabar, C.R., Sabattini, N., Souza, P.A., Taboada, A.C., Vergel, M.M., 2007. Bioestratigrafía del Paleozoico Superior de América del Sur: Primera Etapa de Trabajo Hacia una Nueva Propuesta Cronoestratigráfica: Asociación Geológica Argentina Serie D: Publicación especial, v. 11, p. 9–64.
- Badyrka, K., Clapham, M.E., López, S., 2013. Paleoeology of brachiopod communities during the late Paleozoic ice age in Bolivia (Copacabana Formation, Pennsylvanian–Early Permian): *Palaeogeography, Palaeoclimatology, Palaeoecology*, v. 387, p. 56–65.
- Baird, D. M., 1962, Ripple Marks: *Journal of Sedimentary Petrology*, v. 32, no. 2, p. 332–334.
- Basilici, G., Luca, P.H.V.d., and Poiré, D.G., 2012, Hummocky cross-stratification-like structures and combined-flow ripples in the Punta Negra Formation (Lower-Middle Devonian, Argentine Precordillera): A turbiditic deep-water or storm-dominated prodelta inner-shelf system?, *Sedimentary Geology*, v. 267–268, p. 73–92.
- Benn, D.I., Evans, D.J.A., 1998. *Glaciers and Glaciation*. Arnold, London. 734 p.

- Bennett, M.R., Glasser, N.F., 1996. *Glacial Geology: ice sheets and landforms*, New York, John Wiley & Sons, 364 p.
- Benson, R.H., and Collinson, C., 1958. Three ostracode fauna from lower and middle Mississippian strata of southern Illinois: *Illinois Geological Survey Circular*, v. 255, p. 1-26.
- Blumenstengel, H., 1975. Zur biostratigraphischen und faziellen Bedeutung der Ostracoden des Dinant von Rugen und Hiddensee: *Zeitschrift Geologie Wissenschaften*, v. 3, no. 7, p. 951-969.
- Bonelli, J.R., and Patzkowsky, M.E., 2011. Taxonomic and ecologic persistence across the onset of the late Paleozoic Ice age: evidence from the Upper Mississippian (Chesterian Series), Illinois basin, United States: *PALAIOS*, v. 26, p. 5–17.
- Bonelli, J.R., and Patzkowsky, M.E., 2008. How Are Global Patterns of Faunal Turnover Expressed at Regional Scales? Evidence from the Upper Mississippian (Chesterian Series), Illinois Basin, USA. *PALAIOS*, v.23, p.760-772.
- Boulton, G.S., 1990. Sedimentary and sea level changes during glacial cycles and their control on glacial marine facies architecture, in Dowdeswell, J.A., and Scourse, J.D., eds., *Glacial marine environments: processes and sediment*, Volume Special Publication 53, Geological Society, p. 15-52.
- Brenchley, P.J., Harper, D., 1998. *Palaeoecology: ecosystems, environments and evolution*: New York, Chapman & Hall, 402 p.

- Bryn, P., Kjell, B., Forsberg, C.F., Solheim, A., Kvalstad, T.J., 2005. Explaining the Storrega Slide: *Marine & Petroleum Geology*, v. 22, p. 11-19.
- Caputo, M. V., and Crowell, J. C., 1985. Migration of glacial centers across Gondwana during Paleozoic Era: *Geological Society of America Bulletin*, v. 96, p. 1020-1036.
- Carto, S.L., and Eyles, N., 2012. Identifying glacial influences on sedimentation in tectonically-active, mass flow dominated arc basins with reference to the Neoproterozoic Gaskiers glaciation (c. 580 Ma) of the Avalonian-Cadomian orogenic belt: *Sedimentary Geology*, v. 261-262, p. 1-14.
- Cisterna, G.A., and Sterren, A.F., 2010. "Levipustula Fauna" in central-western Argentina and its relationships with the Carboniferous glacial event in the southwestern Gondwanan margin, *in* López-Gamundí, O., and Buatois, L.A., eds., *Late Paleozoic glacial events and postglacial transgressions in Gondwana*: Boulder, Geological Society of America Special Paper 468, p. 133-147.
- Clapham, M.E., Bottjer, D.J., Powers, C.M., Bonuso, N., Fraiser, M.L., Marengo, P.J., Dornbos, S.Q., Pruss, S.B., 2006. Assessing the ecological dominance of Phanerozoic Marine Invertebrates. *Palaios*, vol. 21, p. 431-441.
- Clapham, M.E., and Bottjer, D.J., 2007. Prolonged Permian-Triassic ecological crisis recorded by molluscan dominance in Late Permian offshore assemblages. *Proceedings of the National Academy of Sciences* 104, 12971-12975.

- Clapham, M.E. and James, N.P., 2008. Paleocology of Early-Middle Permian Marine Communities in eastern Australia: Response to global climate change in the aftermath of the Late Paleozoic Ice Age. *Palaios*, vol.23, no.11, p.738-750.
- Clapham, M.E., Shen, S., Bottjer, D.J., 2009. The double mass extinction revisited: reassessing the severity, selectivity, and causes of the end-Guadalupian biotic crisis (Late Permian): *Paleobiology*, v. 35, no. 1, p. 32-50.
- Clifton, H.E., 2006. A reexamination of facies models for clastic shorelines: Special Publication - Society for Sedimentary Geology, v. 84, p. 293-337.
- Collinson, J.D., and Thompson, D.B., 1989. *Sedimentary Structures*, London, Chapman & Hall, 207 p.:
- Cowan, E.A., and Powell, R.D., 1991, Ice-proximal sediment accumulation rates in a temperate glacial fjord, south-eastern Alaska, in Anderson, J. B., and Ashley, G. M., eds., *Glacial marine sedimentation; paleoclimatic significance*, Volume Geological Society of America Special Publication 261: Boulder, Colorado, p. 61-73.
- Crowell, J.C., and Frakes, L.A., 1970. Ancient Gondwana glaciations. in *Proceedings and Papers of the Second Gondwana Symposium*, South Africa, ed. S. H. Haughton Pretoria: CSIR, 469-76.
- Dalla Salda, L., Cingolani, C., Varela, R., 1990. The origin of Patagonia. *Comunicaciones* 41, 55–61.
- Damuth, J. E., 1978. Echo character of the Norwegian-Greenland Sea: relationship to Quaternary sedimentation: *Marine Geology*, v. 281, p. 36.

- Davies, S.J., 2008. The record of Carboniferous sea-level change in low-latitude sedimentary successions from Britain and Ireland during the onset of the late Paleozoic ice age: Special Paper - Geological Society of America, v. 441, p. 187-204.
- Díaz Saravia, P., and Jones, P. J., 1999. New Carboniferous (Namurian) glacial marine ostracods from Patagonia, Argentina: *Journal of Micropalaeontology*, v. 18, p. 97–109.
- Dimakis, P., Elverhoi, A., Hoeg, K., Solheim, A., Harbitz, C., Laberg, J. S., Vorren, T. O., and Marr, J., 2000. Submarine slope stability on high-latitude glaciated Svalbard-Barents Sea margin: *Marine Geology*, v. 162, no. 2-4, p. 303-316.
- Dineen, A.A., Fraiser, M.L., and Isbell, J.L., 2012. Palaeoecology and Sedimentology of Carboniferous Glacial and Postglacial Successions in the Paganzo and Rio Blanco Basins of Northwestern Argentina, in Slowakiewicz, M., ed., *Late Palaeozoic Climate Cycles: Their Evolutionary, Sedimentological and Economic Impact*: London, Geological Society Special Publication.
- Dineen, A.A., 2010. Regional paleoecology of near-field marine faunas during the late Paleozoic Ice Age, western Argentina [MS: University of Wisconsin-Milwaukee.
- Dodd, J.R., and Stanton, R. J., Jr., 1981, *Paleoecology, Concepts and Applications*, John Wiley and Sons, 559 p.
- Dott Jr., R. H., 1961. Squantum "tillite", Massachusetts—evidence of glaciation or subaqueous mass movements?: *Geological Society of America Bulletin* v. 72, p. 1289–1305.

- Dott, R. H. J., and Bourgeois, J., 1982, Hummocky stratification: significance of its variable bedding sequences: *Geological Society of America Bulletin*, v. 93, p. 663-680.
- Dowdeswell, J.A., Whittington, R. J., Jennings, A.E., Andrews, J.T., Mackensen, A., and Marienfeld, P., 2000. An origin for laminated glacial marine sediments through sea-ice build-up and suppressed iceberg rafting: *Sedimentology*, v. 47, no. 557-576.
- Dykstra, M., Kneller, B., and Milana, J. P., 2006. Deglacial and postglacial sedimentary architecture in a deeply incised paleovalley-paleofjord; the Pennsylvanian (Late Carboniferous) Jejenes Formation, San Juan, Argentina: *Geological Society of America Bulletin*, v. 118, no. 7-8, p. 913-937.
- Elliott, C. G., and Williams, P. F., 1988. Sediment slump structures: a review of diagnostic criteria and application to an example from Newfoundland: *Journal of Structural Geology*, v. 10, no. 2, p. 171-182.
- Evans, J., and Pudsey, C. J., 2002. Sedimentation associated with Antarctic Peninsula ice shelves; implications for palaeoenvironmental reconstructions of glacial marine sediments: *Journal of the Geological Society of London*, v. 159, no. 3, p. 233-237.
- Eyles, C.H., and Eyles, N., 2000. Subaqueous mass flow origin for Lower Permian diamictites and associated facies of the Grant Group, Barbwire Terrace, Canning Basin, Western Australia: *Sedimentology*, v. 47, p. 343-356.
- Eyles, C.H., Eyles, N., and Miall, A. D., 1985. Models of glacial marine sedimentation and their application to the interpretation of ancient glacial sequences: *Palaeogeography, Palaeoclimatology, Palaeoecology*, v. 51, no. 1-4, p. 15-84.

Eyles, N., and Eyles, C. H., 1992. Glacial depositional systems, in Walker, R. G., and James, N. P., eds., *Facies models: response to sea level change*: St. John's, Newfoundland, Geological Association of Canada, p. 73-100.

Fielding, C.R., Frank, T.D., Birgenheier, L.P., Rygel, M.C., Jones, A.T., Roberts, J., 2008a. Stratigraphic imprint of the Late Paleozoic Ice Age in eastern Australia: a record of alternating glacial and nonglacial climate regime. *Journal of the Geological Society of London* 165, 129–140.

Fielding, C.R., Frank, T.D., Isbell, J.L., 2008b. The late Paleozoic ice age — a review of current understanding and synthesis of global climate patterns. In: Fielding, C.R., Frank, T.D., Isbell, J.L. (Eds.), *Resolving the Late Paleozoic Ice Age in Time and Space: Geological Society of America Special Paper*, 441, pp. 343–354.

Forcino, F.L., 2012. Multivariate assessment of the required sample size for community paleoecological research. *Palaeogeography, Palaeoclimatology, Palaeoecology* 315-316, 134-141.

Frakes, L.A., and Crowell, J.C., 1969. Late Paleozoic glaciation: I, South America: *Geological Society of America Bulletin*, v. 80, p. 1007-1042.

Frakes, L. A., and Crowell, J. C., 1969. Late Paleozoic glaciation: I, South America: *Geological Society of America Bulletin*, v. 80, p. 1007-1042.

Franchi, M., and Page, R., 1980. Los basaltos Cretácicos y la evolución magmática del Chubut occidental: *Revista de la Asociación Geológica Argentina*, v. 35, p. 208–229.

- Freytes, E., 1971. [Informe geológico preliminary sobre la Sierra de Tepuel (Deptos. Languiñeo y Tehuelches, prov. de Chubut). Informe YPF. Inédito.]
- Gani, M. R., 2004. From Turbid to Lucid: A Straightforward Approach to Sediment Gravity Flows and Their Deposits.: *The Sedimentary Record.*, v. 2, no. 3, p. 4-8.
- Gastaldo, R.A., DiMichele, W.A., Pfefferkorn, H.W., 1996. Out of the icehouse into the greenhouse; a late Paleozoic analog for modern global vegetational change. *GSA Today*, 6, 1-7.
- Gilbert, R., 1990. Rafting in glacial marine environments, in Dowdeswell, J. A., and Scourse, J. D., eds., *Glacial marine environments: processes and sediments*, Volume 53, Geological Society Special Publications, p. 105-120.
- González Bonorino, G., Rafine, G., Veega, V., Guerin, D., 1988. Ambientes de plataforma nerítica dominada por tormentas en la sección glaciogénica del Grupo Tepuel, Chubut. *Revista de la Asociación Geológica Argentina* 43, 239-252.
- González Bonorino, G., 1992. Carboniferous glaciation in Gondwana. Evidence for grounded marine ice and continental glaciation in southwestern Argentina. *Palaeogeography, Palaeoclimatology, Palaeoecology* 91, 363-375.
- González, C.R., 1972. La Formación Las Salinas, Paleozoico superior de Chubut (República Argentina); Parte I, Estratigrafía, facies y ambientes de sedimentación. *The Las Salinas Formation, upper Paleozoic of Chubut, Argentina; part I, Stratigraphy, facies and depositional environment: Revista de la Asociación Geológica Argentina*, v. 27, no. 1, p. 95-115.

- González, C.R., 1978. *Orbiculopecten* gen. nov. (Aviculopectinidae, Bivalvia), from the Upper Carboniferous of Patagonia, Argentina: *Journal of Paleontology*, v. 52, no. 5, p. 1086-1092.
- González, C. R., 1981. Pavimento glaciario en el Carbonico de la Precordillera. Glacial pavement in the Carboniferous of the Precordillera: *Revista de la Asociacion Geologica Argentina*, v. 36, no. 3, p. 262-266.
- Gonzalez, C.R., 1993. Late Paleozoic Faunal Succession in Argentina: *Compte Rendus XII Congr s International de la Stratigraphie et G ologie du Carbonifere et Permien*, v. 1, p. 537-550.
- González, C.R., 2002. Bivalves from Carboniferous glacial deposits of western Argentina: *Pal ontologische Zeitschrift*, v. 76 no. 1, p. 127–148.
- González, C.R., 2006. Lower Permian bivalves from central Patagonia, Argentina: *Pal ontologische Zeitschrift*, v. 80, p. 130–155.
- González, C.R., and Glasser, N. F., 2008. Carboniferous glacial erosional and depositional features in Argentina: *Geologica et Palaeontologica*, v. 42, p. 39-53.
- González, C.R., and D az Saravia, P., 2010. Bimodal character of the Late Paleozoic glaciations in Argentina and bipolarity of climatic changes. *Palaeogeography, Palaeoclimatology, Palaeoecology* 298, 101-111.
- Green, R., 1963. Lower Mississippian Ostracodes from the Banff Formation, Alberta: *Research Council of Alberta Bulletin*, v. 11, p. 1-201.

- Gründel, J., 1975. Neues Ostracoden der Healdiaceae und Quasillitaceae aus dem Dinant der Insel Rugen: *Zeitschrift Geologie Wissenschaften*, v. 3, p. 971-983.
- Gulbranson, E., Montañez, I. P., Schmitz, M. D., Limarino, C.O., Isbell, J.L., Marensi, S. A., and Crowley, J. L., 2010. High-precision U-Pb calibration of Carboniferous glaciation and climate history, Paganzo Group, NW Argentina: *Geological Society of America Bulletin*, v. 122, no. 9, p. 1480-1498.
- Hammer O., Harper, D., 2006. *Paleontological Data Analysis*: Malden, MA, Blackwell Publishing, 351 p.
- Heckel, P.H., 1994. Evaluation of evidence for glacio-eustatic control over marine Pennsylvanian cyclothems in North America and consideration of possible tectonic effects, *in* Dennison, J. M., and Ettensohn, F. R., eds., *Tectonic and eustatic controls on sedimentary cycles, Volume Concepts in Sedimentology and Paleontology Volume 4*: Tulsa, SEPM (Society of Sedimentary Geology), p. 65-87.
- Heckel, P.H., 2008. Pennsylvanian cyclothems in Midcontinent North America as far-field effects of waxing and waning of Gondwana ice sheets: *Special Paper - Geological Society of America*, v. 441, p. 275-289.
- Heim, N.A., 2009. Stability of regional brachiopod diversity structure across the Mississippian/Pennsylvanian boundary: *Paleobiology*, v. 35, p. 393-412.
- Henriksen, S., Hampson, G.J., Helland-Hansen, W., Johannessen, E.P., Steel, R.J., 2009. Shelf edge and shoreline trajectories, a dynamic approach to stratigraphic analysis: *Basin Research*, v. 21, p. 445-453.

- Henriksen, S., Helland-Hansen, W., and Bullimore, S. A., 2011. Relationships between shelf-edge trajectories and sediment dispersal along depositional dip and strike: a different approach to sequence stratigraphy: *Basin Research*, v. 23, no. 1, p. 3-21.
- Henry, L.C., 2007. Carboniferous glaciogenic deposits of the Hoyada Verde and Tramojo Formations of the Calingasta-Uspallata Basin, west central Argentina [MS: University of Wisconsin-Milwaukee.
- Henry, L.C., Isbell, J.L., and Limarino, C.O., 2007. Short duration glaciation of limited extent in western Gondwana: the Carboniferous glaciogenic deposits of the Protoprecordillera of west central Argentina: *Geological Society of America Abstracts with Programs*, v. 39, no. 3, p. 55.
- Horton, D.E., and Poulsen, C. J., 2009. Paradox of late Paleozoic glacioeustasy: *Geology*, v. 37, no. 8, p. 715-718.
- IPCC, 2007. *Climate Change 2007 – Mitigation of Climate Change, Contribution of Working Group III to the Fourth Assessment Report of the Intergovernmental Panel on Climate Change*, Cambridge University Press.
- Isbell, J.L., 2010, Environmental and paleogeographic implications of glaciotectonic deformation of glaciomarine deposits within Permian strata of the Metschel Tillite, southern Victoria Land, Antarctica, in López-Gamundí, O. R., and Buatois, L. A., eds., *Late Paleozoic Glacial Events and Postglacial Transgressions in Gondwana*: Boulder, CO, Geological Society of America Special Publication 468, p. 81-100.

Isbell, J.L., Miller, M.F., Wolfe, K.L. & Lenaker, P.A., 2003. Timing of late Paleozoic glaciation in Gondwana: was glaciation responsible for the development of northern hemisphere cyclothems? in *Extreme depositional environments: mega end members in geologic time*, eds. M. A. Chan & A. W. Archer Boulder, Colorado: Geological Society of America Special Paper, 5-24.

Isbell, J.L., Fraiser, M.L., and Henry, L.C., 2008. Examining the complexity of environmental change during the late Paleozoic and early Mesozoic: *PALAIOS*, v. 23, p. 267-269.

Isbell, J.L., Henry, L.C., Limarino, C.O., Koch, Z.J., Ciccioli, P.L., and Fraiser, M.L., 2011. The equilibrium line altitude as a control on Gondwana Glaciation during the late Paleozoic Ice Age, in Hakansson, E., and Trotter, J., eds., *Programme & Abstracts, XVII International Congress on the Carboniferous and Permian Perth 3-8, July 2011*, Volume Record 2011/20, Geological Survey of Western Australia, p. 74.

Isbell, J.L., Henry, L.C., Gulbranson, E.L., Limarino, C.O., Fraiser, M.L., Koch, Z.J., Ciccioli, P.L., Dineen, A.A., 2012. Glacial paradoxes during the late Paleozoic ice age: Evaluating the equilibrium line altitude (ELA) as a control on glaciation. *Gondwana Research* 22, 1-19.

Isbell, J.L., Henry, L.C., Reid, C.M., Fraiser, M.L., 2013a. Sedimentology and palaeoecology of lonestone-bearing mixed clastic rocks and cold-water carbonates of the Lower Permian Basal Beds at Fossil Cliffs, Maria Island, Tasmania (Australia): Insight into the initial decline of the late Palaeozoic ice age, in Gasiewicz, A., Słowakiewicz, M., ed., *Palaeozoic Climate Cycles: Their Evolutionary and*

- Sedimentological Impact, Volume 376: London, Geological Society, Special Publications, p. 307–341.
- Isbell, J.L., Taboada, A.C., Gulbranson, E.L., Pagani, M.A., Pauls, K.N., Limarino, C.O., Ciccioli, P.L., Fraiser, M.L., 2013b. Carboniferous and Permian glacigenic and non-glacial strata of the Tepuel-Genoa Basin, Patagonia, Argentina: A near-continuous, deep-water record of South Polar Gondwana during the late Paleozoic Ice Age: Geological Society of America Abstracts with Programs, v. 45, no. 7.
- Kammer, T. W., Brett, C. E., Boardman, D. R., and Mapes, R. H., 1986. Ecologic Stability of the dysaerobic biofacies during the Late Paleozoic: *Lethaia*, v. 19, p. 109–121.
- Keidel, J., 1922. Sobre la distribución de los depósitos glaciares del Pérmico conocidos en la Argentina y su significación para la estratigrafía de la Serie de Gondwana y la paleogeografía del hemisferio austral.: *Boletín de la Academia Nacional de Ciencias*, v. 25, p. 239–368.
- Laberg, J. S., Vorren, T.O., 1995. Late Weichselian submarine debris flow deposits on the Bear Island Trough Mouth Fan: *Marine Geology*, v. 127, p. 45-72.
- Lane, H. R., 1978. The Burlington Shelf (Mississippian, north-central United States): *Geologica et Palaeontologica*, v. 12, p. 165-176.
- Lawver, L.A., Dalziel, I.W.D., Norton, I.O., Gahagan, L.M., 2008. The Plates 2007 Atlas of Plate Reconstructions (750 Ma to Present Day), Plates Progress Report No. 305–0307. University of Texas Technical Report No. 195. 160 pp.

- Lee, H., Edwards, B., 1986. Regional method to assess offshore slope stability: *Journal of Geotech. Eng., ASCE*, v. 112, p. 489-509.
- Lee, H. J., Locat, J., Desgagnes, P., Parsons, J. D., McAdoo, B. G., Orange, D. L., Puig, P., Wong, F. L., Dartnell, P., and Boulanger, E., 2007. Submarine mass movements on continental margins: Special Publication of the International Association of Sedimentologists, v. 37, p. 213-274.
- Lesta, P. J., and Ferello, R., 1972. Región extrandina de Chubut y Norte de Santa Cruz, *in* Leanza, A. F., ed., *Geología Regional Argentina*, Academia Nacional de Ciencias de Córdoba, p. 601–654.
- Limarino, C.O., Spalletti, L.A., 2006. Paleogeography of the upper Paleozoic basins of southern South America: an overview. *Journal of South American Earth Sciences* 22, 134–155.
- Lisitzin, A. P., 2002, *Sea-ice and iceberg sedimentation in the ocean*, Berlin, Springer-Verlag, 800 p.
- López-Gamundí, O. R., 1987. Depositional models for the glaciomarine sequences of Andean late Paleozoic basins of Argentina: *Sedimentary Geology*, v. 52, p. 109–126.
- López-Gamundí, O. R., 1989. Postglacial transgressions in late Paleozoic basins of western Argentina; a record of glacioeustatic sea level rise: *Palaeogeography, Palaeoclimatology, Palaeoecology*, v. 71, no. 3-4, p. 257-270.
- López Gamundí, O.R., 1991. Thin-bedded diamictites in the glaciomarine Hoyada Verde Formation (Carboniferous), Calingasta-Uspallata Basin, western Argentina; a

discussion on the emplacement conditions of subaqueous cohesive debris flows.

Sedimentary Geology 73, 247–255.

López Gamundí, O.R., 1997. Glacial–postglacial transition in the late Paleozoic basins of

Southern South America. In: Martini, I.P. (Ed.), *Late Glacial and Postglacial*

Environmental Changes: Quaternary, Carboniferous–Permian, and Proterozoic.

Oxford University Press, Oxford, U.K., pp. 147–168.

López-Gamundí, O.R., and Martínez, M., 2000. Evidence of glacial abrasion in the

Calingasta-Uspallata and western Paganzo basins, mid-Carboniferous of western

Argentina. *Palaeogeography, Palaeoclimatology, Palaeoecology*, 159, 145–165.

Maejima, W., 1988. Marine transgression over an active alluvial fan: the early Cretaceous

Arida Formation, Yuasa-Aridagawa Basin, southwestern Japan, *in* Nemeč, W., Steel,

R.J., ed., *Fan Deltas: Sedimentology and Tectonic Settings*, Volume 303-317: London,

Blackie.

Moncrieff, A.C. M., Hambrey, M. J. , 1990, Marginal-marine glacial sedimentation in the

late Precambrian succession of East Greenland, *in* Dowdeswell, J. A., Scourse, J. D.,

ed., *Glacimarine Environments: Processes and Sediments*, Volume 53: London,

Geological Society, Special Publication, p. 397–410.

Montañez, I., and Soreghan, G. S., 2006. Earth's fickle climate; lessons learned from

deep-time ice ages: *Geotimes*, v. 51, no. 3, p. 24-27.

- Montañez, I.P., Tabor, N.J., Niemeier, D., DiMichele, W.A., Frank., T.D., Fielding, C.R., Isbell, J.L., Birgenheier, L.P., and Rygel, M.C., 2007. CO₂-Forced Climate and Vegetation Instability During Late Paleozoic Deglaciation. *Science*, v.315, p.87-91.
- Montañez, I.P., and Poulsen, C. J., 2013, The late Paleozoic ice age: an evolving paradigm: *Annual Review of Earth & Planetary Sciences*, v. 41, no. 24, p. 1-28.
- Mulder, T., and Alexander, J., 2001. The physical character of subaqueous sedimentary density flows and their deposits: *Sedimentology*, v. 48, no. 2, p. 269-299.
- Mulder, T.J., Cochonat, P., 1996. Classifications of offshore mass movements: *Journal of Sedimentary Research*, v. 66, p. 43-57.
- Murray, K. T., Miller, M. F., and Bowser, S. S., 2013, Depositional processes beneath coastal multi-year sea ice: *Sedimentology*, v. 60, no. 2, p. 391-410.
- Noda, A., TuZino, T., Masato, J., Goto, S., 2013. Mass transport-diminated sedimentation in a foreland basin, the Hidaka Trough, northern Japan: *Geochemistry, Geophysics, Geosystems*, v. 14, no. 8, p. 2638-2660.
- Norem, H., Locat, J., Schieldrop, B., 1990. An approach to the physics and the modelling of submarine landslides: *Marine Geology*, v. 20, p. 129-173.
- Pagani, M.A., and Sabbatini, N., 2002. Biozonas de moluscos del Paleozoico superior de la Cuenca Tepuel–Genoa (Chubut, Argentina): *Ameghiniana*, v. 39, p. 351–366.
- Pagani, M.A., Taboada, A.C., 2010. The marine upper Paleozoic in Patagonia (Tepuel-Genoa Basin, Chubut Province, Argentina): 85 years of work and future prospects. *Palaeogeography, Palaeoclimatology, Palaeoecology* 298, 130-151.

- Pagani, M.A., Taboada, A.C., Isbell, J.L., Fraiser, M.L., Dineen, A.A., and Pauls, K.N., 2012. The Lanipustula Biozone in Patagonia: stratigraphic extension, faunal changes, paleoclimatology and paleoecology, *in* Proceedings Asociación Paleontológica Argentina Annual Meeting General Roca.
- Page, R. F.N., Limarino, C.O., Lopez Gamundi, O., and Page, S., 1984. Estratigrafía del Grupo Tepuel en su perfil tipo y en la región de El Molle, provincia del Chubut.: 9° Congreso Geológico Argentino (S. C. de Bariloche), v. Actas 1, p. 619-632.
- Pankhurst, R.J., Rapella, C.W., Fanning, C.M., Márquez, M., 2006. Gondwanide continental collision and the origin of Patagonia. *Earth-Science Reviews* 76, 235–257.
- Peck, L.S., Webb, K.E., Bailey, D.M., 2004. Extreme sensitivity of biological function to temperature in Antarctic marine species: *Functional Ecology*, v. 18, p. 625-630.
- Piatnitzky, A., 1933. Rético y Liásico de los valles de los ríos Genoa y Tecka y sedimentos continentales de la sierra de San Bernardo, *Boletín de Informaciones Petroleras*, v. 10, p. 151–182.
- Piatnitzky, A., 1936. Estudio geológico de la región del Río Chubut y del Río Genoa, *Boletín de Informaciones Petroleras*, v. 13, p. 83–118.
- Pörtner, H.O., 2001. Climate change and temperature-dependent biogeography: oxygen limitation of thermal tolerance in animals: *Naturwissenschaften*, v. 88, p. 137-149.
- Posamentier, H.W., and Walker, R.G., 2006. Deep-water turbidites and submarine fans, *in* Posamentier, H. W., and Walker, R. G., eds., *Facies models revisited: Tulsa, SEPM Special Publication* 84, p. 397-520.

- Poulsen, C. J., Horton, D. E., Pollard, D., and Anonymous, 2007. Glacial-interglacial climate change during the late Paleozoic; a climate modeling perspective: Abstracts with Programs - Geological Society of America, v. 39, no. 6, p. 354.
- Powell, M.G., 2005. Climatic basis for sluggish macroevolution during the late Paleozoic ice age: *Geology (Boulder)*, v. 33, no. 5, p. 381-384.
- Powell, M.G., 2008. Timing and selectivity of the late Mississippian mass extinction of brachiopod genera from the Central Appalachian Basin: *PALAIOS*, v. 23, p. 525-534.
- Powell, R.D., 1984. Glacimarine processes and inductive lithofacies modeling of ice shelf and tidewater glacier sediments based on Quaternary examples: *Marine Geology*, v. 57, p. 1-52.
- Powell, R.D., 1990, Glacimarine processes at grounding-line fans and their growth to ice contact deltas, in Dowdeswell, J. A., and Scourse, J. D., eds., *Glacimarine Environments: processes and sediments, Volume 53*: London, Geological Society Special Publication, p. 53-73.
- Powell, R.D., 2005. Subaquatic landsystems: Fjords. *Glacial landsystems*. D. J. A. Evans, A Hodder Arnold Publication: 313-347.
- Powell, R.D., and Cowan, E.A., 1986. Depositional processes at McBride Inlet and Riggs glacier. In: Anderson, P.G., Goldthwait, R.P., McKenzie, G.D. (Eds.), *Observed processes of glacial deposition in Glacier Bay, Alaska*: Ohio State University, Institute of Polar Studies, Miscellaneous Publications, 256, pp. 140–156.

- Powell, R., and Domack, E., 1995. Modern glaciomarine environments, in Menzies, J., ed., *Modern glacial environments: processes, dynamics and sediments*, Volume Glacial environments: Volume 1: Oxford, Butterworth-Heinemann Ltd., p. 445-486.
- Powell, R.D., and Cooper, J. M., 2002. A glacial sequence stratigraphic model for temperate, glaciated continental shelves: *Geological Society Special Publication*, no. 203, p. 215-244.
- Powell, R.D., and Domack, E., 2002. Modern glaciomarine environments. *Modern and past glacial environments*. J. Menzies. Oxford, Butterworth-Heinemann Ltd.: 361-389.
- Prior, D. B., 1984. Submarine landslides, in *Proceedings The IV International Symposium on Landslides, Toronto, Volume 2*, p. 179-196.
- Prior, D.B., Bornhold, B.D., Wiseman, W.J., and Lowe, D.R., 1987. Turbidity current activity in a British Columbia fjord: *Science*, v. 237, no. 4820, p. 1330–1333.
- Ramos, V.A., 2008. Patagonia: a Paleozoic continent adrift? *Journal of South American Earth Sciences* 26, 235–251.
- Rapalini, A.E., López de Luchi, M., Martínez Dopico, C., Lince Klinger, F., Giménez, M., Martínez, P., 2010. Did Patagonia collide with Gondwana in the Late Paleozoic? Some insights from a multidisciplinary study of magmatic units of the North Patagonian Massif. *Geologica Acta* 8, 349–371.
- Reineck, H. E., and Singh, I. B., 1980. *Depositional sedimentary environments*, Berlin, Springer-Verlag, 551 p.:

- Ricci Lucchi, F., 1995. *Sedimentographica: a photographic atlas of sedimentary structures*, New York, Columbia University Press, 255 p.:
- Rise, L., Ottesen, D., Berg, K., Lundin, E., 2005. Large-scale development of the mid-Norwegian shelf and margin during the last 3 million years: *Marine and Petroleum Geology*, v. 22.
- Rocha Campos, A.C., dos Santos, P.R., Canuto, J.R., 2008. Late Paleozoic glacial deposits of Brazil: Paraná Basin. In: Fielding, C.R., Frank, T.D., Isbell, J.L. (Eds.), *Resolving the Late Paleozoic Ice Age in Time and Space: Geological Society of America Special Paper*, 441, pp. 97–114.
- Royer, D. L., Berner, R. A., Montañez, I. P., Tabor, N. J., and Beerling, D. J., 2004. CO₂ as a primary driver of Phanerozoic climate: *GSA Today*, v. 14, no. 3, p. 4-10.
- Rygel, M. C., Fielding, C. R., Frank, T. D., and Birgenheier, L. P., 2008. The magnitude of late Paleozoic glacioeustatic fluctuations: a synthesis: *Journal of Sedimentary Research*, v. 78, p. 500-511.
- Scotese, C.R., Boucot, A. J., and McKerrow, W.S., 1999. Gondwanan palaeogeography and palaeoclimatology: *Journal of African Earth Sciences*, v. 28, p. 99-114.
- Shanmugam, G., 2006. *Deep-water processes and facies models: implications for sandstone petroleum reservoirs*, Amsterdam, Elsevier, 475 p.
- Shanmugam, G., Lehtonen, L. R., Straume, T., Syvertsen, S.E., Hodgkinson, R. J., and Skibeli, M., 1994. Slump and debris-flow dominated upper slope facies in the Cretaceous of the Norwegian and northern North Seas (61-67 degrees N): implications

- for sand distribution, *American Association of Petroleum Geologists Bulletin*, v. 78, no. 6, p. 910-937.
- Shannon, C.E., 1948. A mathematical theory of communication, *Bell System Technical Journal* v. 27, p. 466-467.
- Shi, G. R., and Waterhouse, J. B., 2010. Late Palaeozoic global changes affecting high-latitude environments and biotas: An introduction, *Environmental processes and biotic responses at high latitudes: a study of Late Palaeozoic sequences, biotas and palaeoenvironmental changes in Gondwana and northern Eurasia*, Volume 298, *Palaeogeography, Palaeoclimatology, Palaeoecology*, p. 1-16.
- Simanauskas, T., 1996. Una nueva especie de *Lanipustula* (Productoidea, Brachiopoda) del Paleozoico superior de Patagonia, Argentina: *Ameghiniana* v. 33, p. 301-305.
- Simanauskas, T., Sabattini, N., 1997. Bioestratigrafía del Paleozoico superior marino de la Cuenca Tepuel-Genoa, Provincia del Chubut, Argentina: *Ameghiniana*, v. 34, p. 49-60.
- Simpson, E. H., 1949. Measurement of diversity, *Nature*, v. 189.
- Solheim, A., Riis, F., Elverhoi, A., Faleide, J.I., Jensen, L.N., and Cloetingh, S., 1996. Impact of glaciations on basin evolution: Data and models from the Norwegian margin and adjacent areas, *Global and Planetary Change*, Volume 12, p. 1-9.
- Solheim, A., Berg, K., Forsberg, C.F., Bryn, P., 2005. The Storegga Slide Complex: repetitive large scale sliding with similar cause and development: *Marine and Petroleum Geology*, v. 22.

- Soreghan, G.S., 2004, Déjà-Vu All Over Again: Deep Time (Climate) Is Here To Stay: *Palaios*, v. 19, no. 1, p. 1-2.
- Stanley, S.M., Powell, M.G., 2003. Depressed rates of origination and extinction during the late Paleozoic ice age: a new state for the global marine ecosystem. *Geology* 31, 877–880.
- Steel, R., and Olsen, T., 2002. Clinofolds, Clinofold Trajectories and Deepwater Sands, *Sequence Stratigraphic Models for Exploration and Production: Evolving Methodology, Emerging Models, and Application Histories: 22nd Annual, Volume 22*, Society of Economic Paleontologists and Mineralogists, p. 367-380.
- Steel, R., Porębski, S.J., Plink-Bjorklund, P., Mellere, D., and Schellpeper, M., 2003. Shelf-Edge Delta Types and Their Sequence-Stratigraphic Relationships, Shelf Margin Deltas and Linked Down Slope Petroleum Systems: 23rd Annual, Volume 23, Society of Economic Paleontologists and Mineralogists, p. 205-230.
- Steel, R.J., Carvajal, C., Petter, A.L., and Uroza, C., 2008. Shelf and shelf-margin growth in scenarios of rising and falling sea level: Special Publication - Society for Sedimentary Geology, v. 90, p. 47-71.
- Sterren, A.F., and Cisterna, G. A., 2010. Bivalves and brachiopods in the Carboniferous - Early Permian of Argentine Precordillera: Diversification and faunal turnover in Southwestern Gondwana: *Geologica Acta*, v. 8, no. 4, p. 501-517.

- Strachan, L. J., 2002. Slump-initiated and controlled syndepositional sandstone remobilization: an example from the Namurian of County Clare, Ireland: *Sedimentology*, v. 49, no. 1, p. 25-41.
- Suero, T., 1948. Descubrimiento de Paleozoico superior en la zona extraandina de Chubut. *Boletín de Informaciones Petroleras* 287, 31-48.
- Suero, T., 1953. Las sucesiones sedimentarias suprapaleozoicas de la zona extraandina del Chubut: *Revista de la Asociación Geológica Argentina*, v. 8, no. 1, p. 37-63.
- Suero, T., 1958. Datos geológicos sobre el Paleozoico superior en la zona de Nueva Lubecka y alrededores (Chubut extraandino, prov. de Chubut): *Revista Museo de La Plata (N.S.)* 5, *Geología*, v. 30, p. 1-28.
- Swift, D.J.P., Hudelson, P. M., Brenner, R.L., and Thompson, P., 1987. Shelf construction in a foreland basin: storm beds, shelf sandbodies, and shelf-slope depositional sequences in the Upper Cretaceous Mesaverde Group, Book Cliffs, Utah: *Sedimentology*, v. 34, p. 423-457.
- Swift, D.J.P., Thorne, J.A., 1991. Sedimentation on continental margins, 1: a general model for shelf sedimentation: *IAS Special Publication* v. 14, p. 3-31.
- Syvitski, J.M., Burrell, D. C., and Skei, J. M., 1987. *Fjords: processes and products*, New York, Springer-Verlag, 379 p.
- Taboada, A.C., 2001. Bioestratigrafía del Neopaleozoico del Valle de Tres Lagunas, sierra de Tepuel, Provincia de Chubut: *Acta Geológica Lilloana* v. 18, p. 291-304.

- Taboada, A.C., 2008. First record of the Late Palaeozoic brachiopod *Verchojania* Abramov in Patagonia, Argentina: Proceedings of the Royal Society of Victoria, v. 120, no. 1, p. 305–319.
- Taboada, A.C. , 2010. Mississippian-Early Permian brachiopods from western Argentina: Tools for middle- to high-latitude correlation, paleobiogeographic and paleoclimatic reconstruction. *Palaeogeography, Palaeoclimatology, Palaeoecology* 298, 152-73.
- Taboada, A.C., Archbold, N. W., González, C. R., and Sabbattini, N., 2005. The Late Carboniferous–Early Permian Tepuel fauna of Patagonia: updated brachiopods records, *in* Pankhurst, R. J., and Veiga, G. D., eds., *Gondwana 12: Geological and Biological Heritage of Gondwana, Mendoza, Argentina.: Córdoba, Argentina, Academia Nacional de Ciencias*, p. 349.
- Taboada, A.C., and Pagani, M.A., 2010, The coupled occurrence of *Cimmeriella-Jakutproductus* (Brachiopoda: Productidina) in Patagonia: implications for Early Permian high to middle paleolatitudinal correlations and paleoclimatic reconstruction: *Geologica Acta*, v. 8, no. 4, p. 513-534.
- Taboada, A.C., Shi, G.R., 2011. Taxonomic review and evolutionary trends of *Levipustulini* and *Absenticostini* (Brachiopoda) from Argentina; palaeobiogeographic and palaeoclimatic implications. *Memoirs of the Association of Australian Palaeontologists* 41, 87–114.

- Talling, P.J., Masson, D.G., Sumner, E.J., and Malgesini, G., 2012. Subaqueous sediment density flows: Depositional processes and deposit types: *Sedimentology*, v. 59, no. 7, p. 1937-2003.
- Thomas, G.S.P., and Connell, R. J., 1985. Iceberg drop, dump, and grounding structures from Pleistocene glacio-lacustrine sediments, Scotland: *Journal of Sedimentary Petrology*, v. 55, no. 2, p. 243-249.
- Tomasovych, A., 2006., Brachiopod and bivalve ecology in the Late Triassic (Alps, Austria): onshore-offshore replacements caused by variations in sediment and nutrient supply: *Palaios*, v. 21, p. 344-368.
- Visser, J.N.J., 1997, Deglaciation sequences in the Permo-Carboniferous Karoo and Kalahari basins of southern Africa: a tool in the analysis of cyclic glaciomarine basin fills: *Sedimentology*, v. 44, p. 507-521.
- Vorren, T.O., Vorren, K.D., Alm, T., Gulliksen, S., Lovlie, R., 1988. The last deglaciation (20,000 to 11,000 bp) on Andøya, Northern Norway: *Boreas* v. 17, p. 41-77.
- Vorren, T., Lebesbye, E., Andreassen, K., Larsen, K-B., 1989. Glacigenic sedimentation on a passive continental margin as exemplified by the Barents Sea, in Powell, R. D., Elverhøi, A., ed., *Modern Glaciomarine Environments: Glacial and Marine Controls of Modern Lithofacies and Biofacies*, Volume 85, *Marine Geology*, p. 251-272.
- Waterhouse, J.B., Shi, G.R., 2010. Evolution in a cold climate. *Palaeogeography, Palaeoclimatology, Palaeoecology* 298, 17-30.

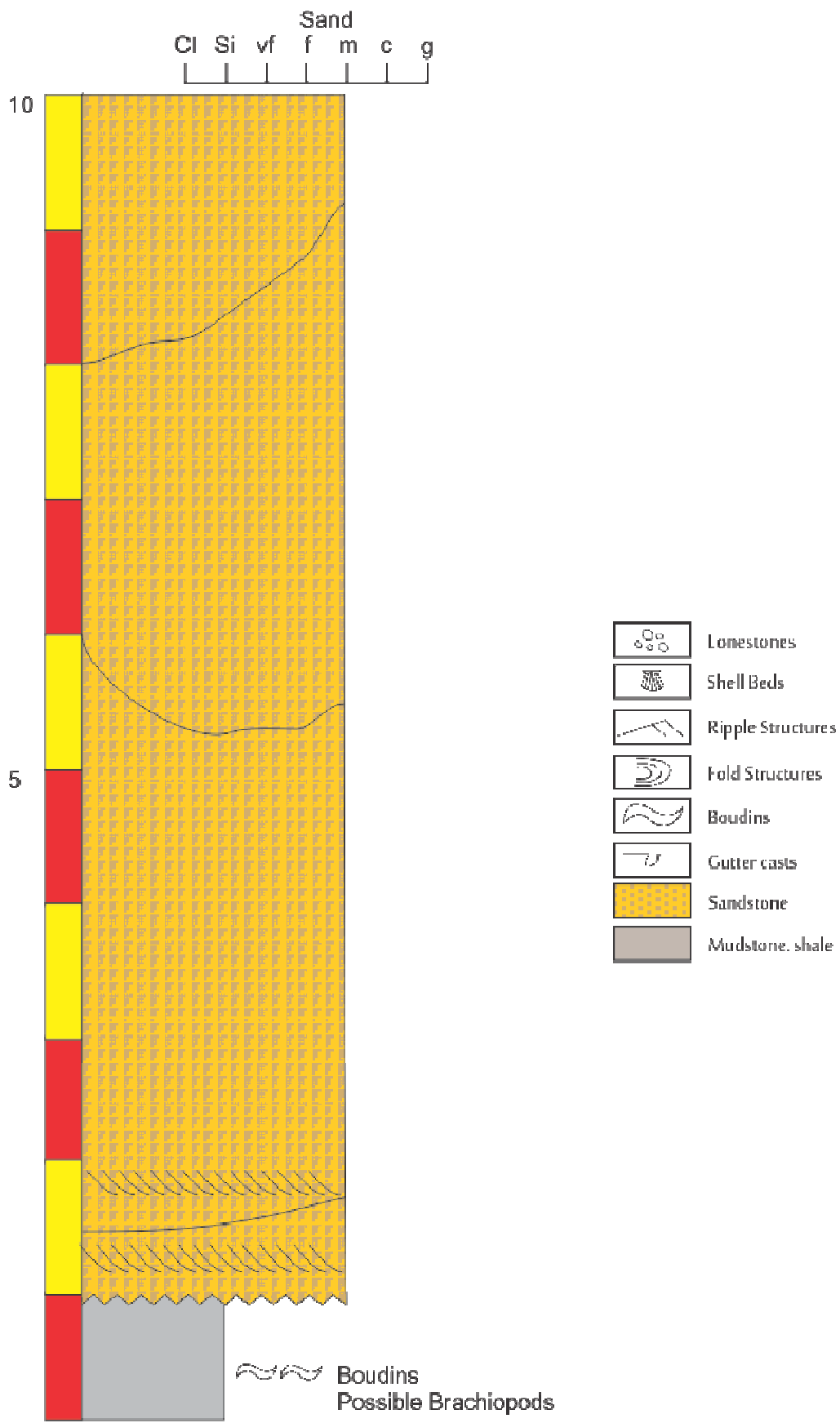
Wignall, P.B., 1994. *Black Shales*, New York, Oxford University Press.

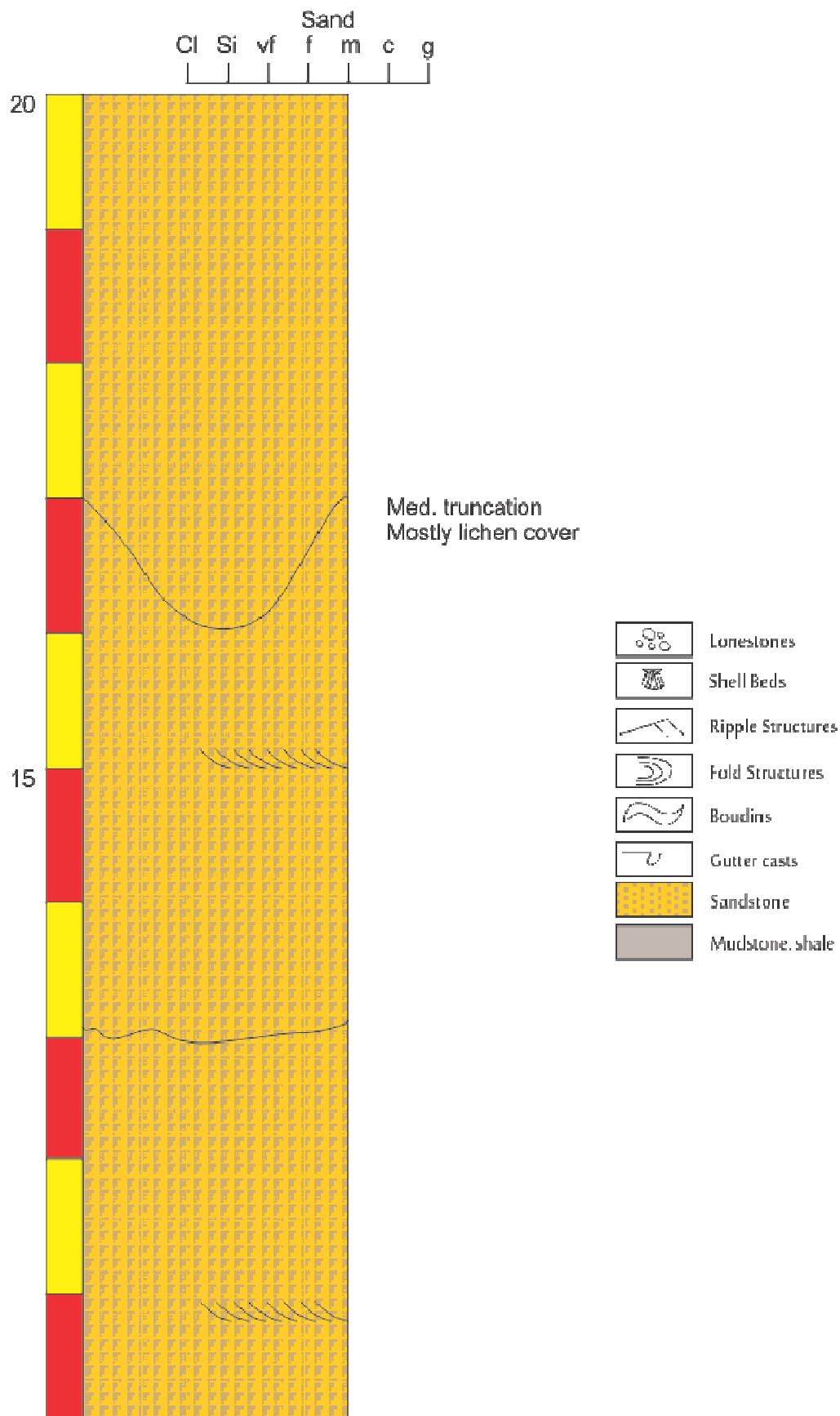
Wild, R., Flint, S.S., and Hodgson, D. M., 2009. Stratigraphic evolution of the upper slope and shelf edge in the Karoo Basin, South Africa: *Basin Research*, v. 21, no. 5, p. 502-527.

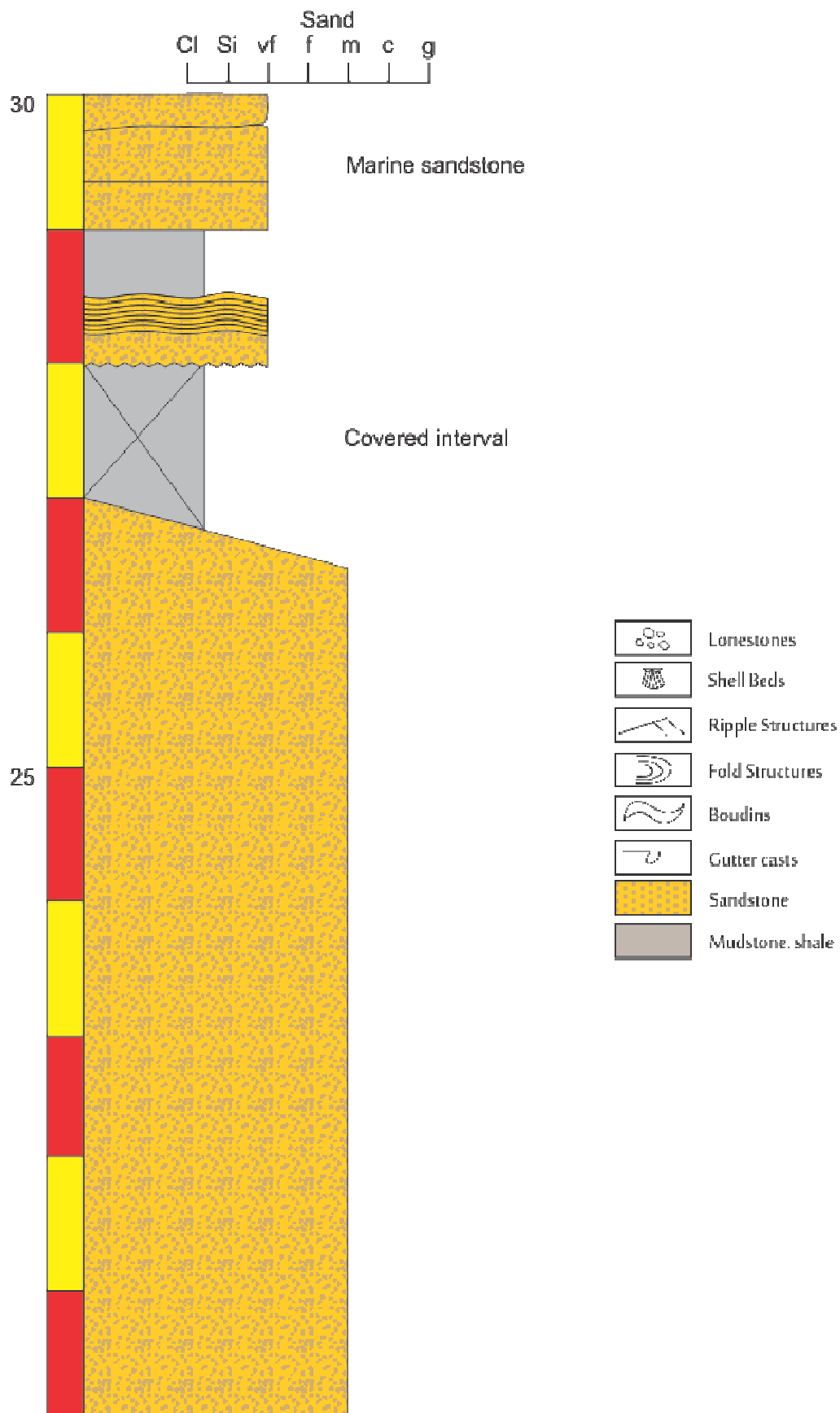
Winsemann, J., Asprion, U., Meyer, T., and Schramm, C., 2007. Facies characteristics of Middle Pleistocene (Saalian) ice-margin subaqueous fan and delta deposits, glacial Lake Leine, NW Germany.: *Sedimentary Geology*, v. 193, p. 105-129.

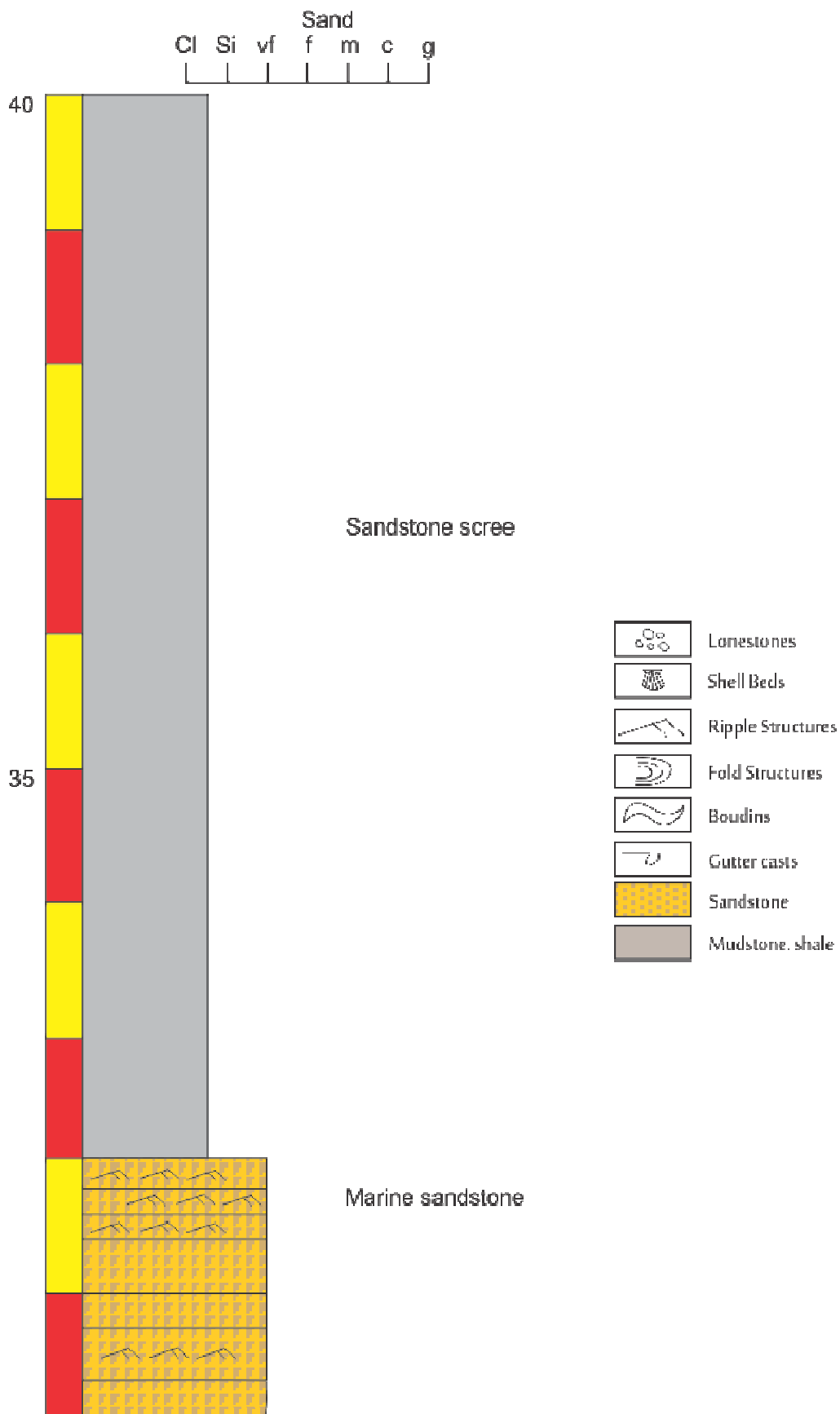
Woodworth-Lynas, C. M. T., and Dowdeswell, J. A., 1994. Soft-sediment striated surfaces and massive diamicton facies produced by floating ice, in Deynoux, M., Miller, J. M. G., Domack, E. W., Eyles, N., Fairchild, I. J., and Young, G. M., eds., *Earth's Glacial Record*: Cambridge, U.K., Cambridge University Press, p. 241-259.

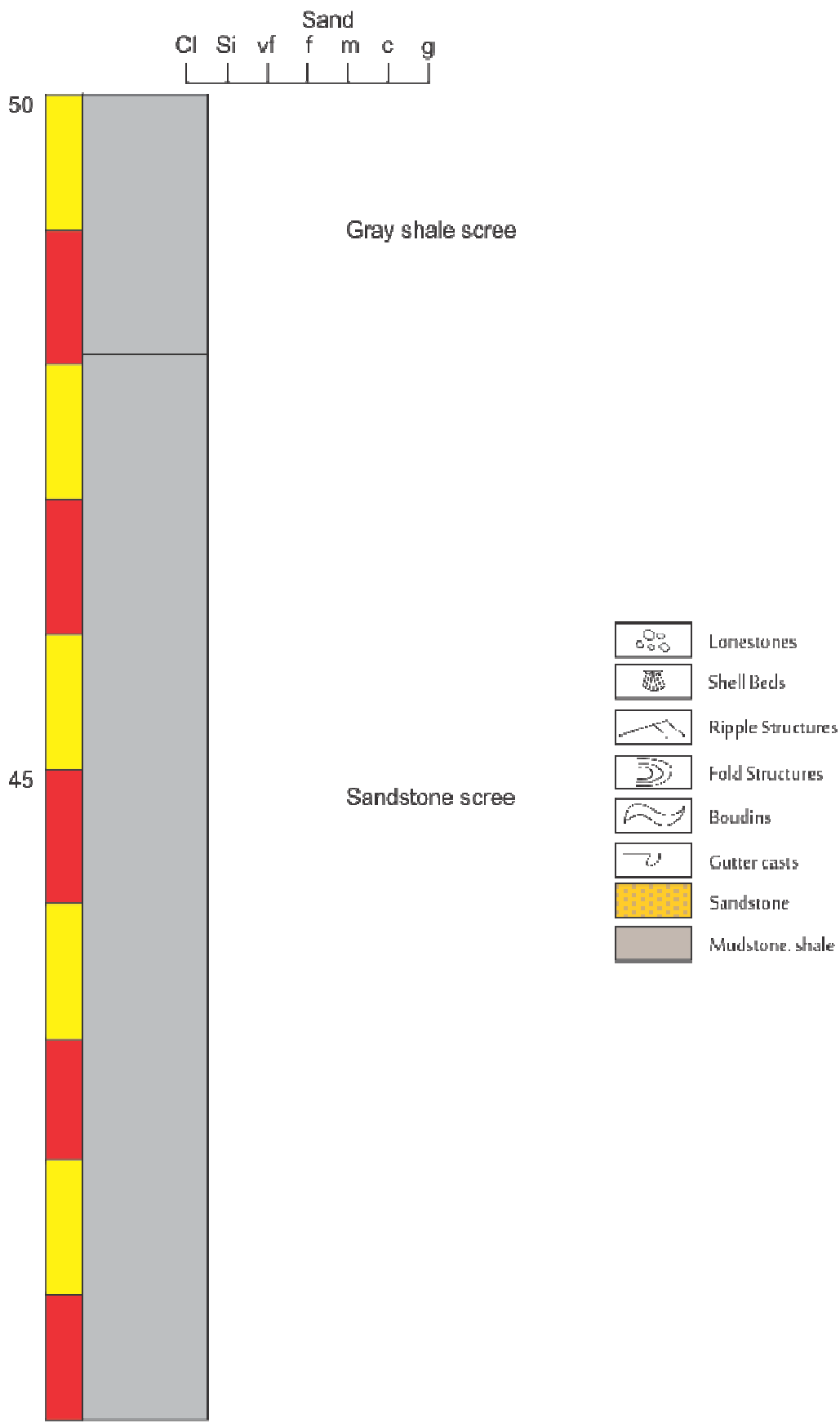
Appendix A
Pampa de Tepuel Formation
Stratigraphic Columns

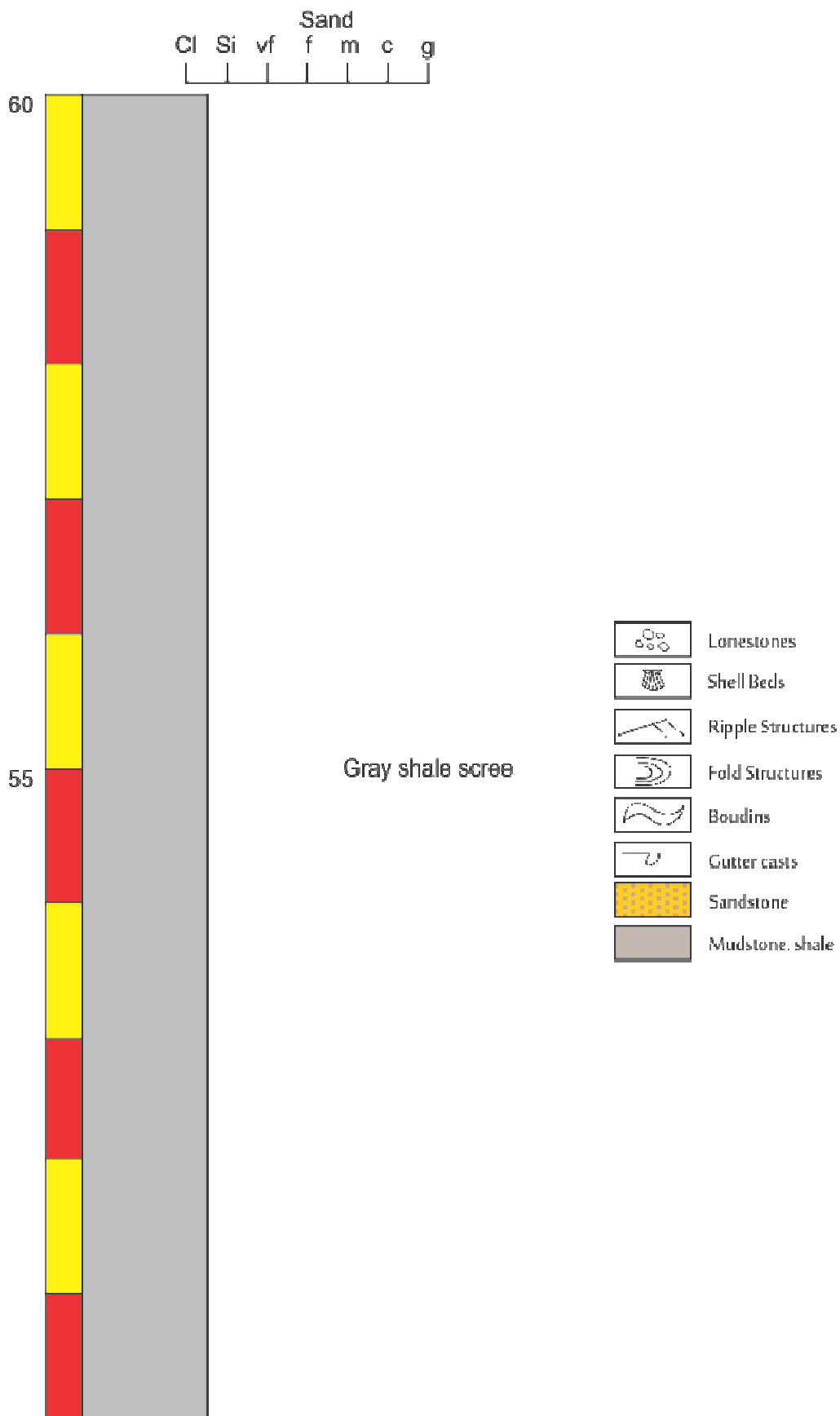


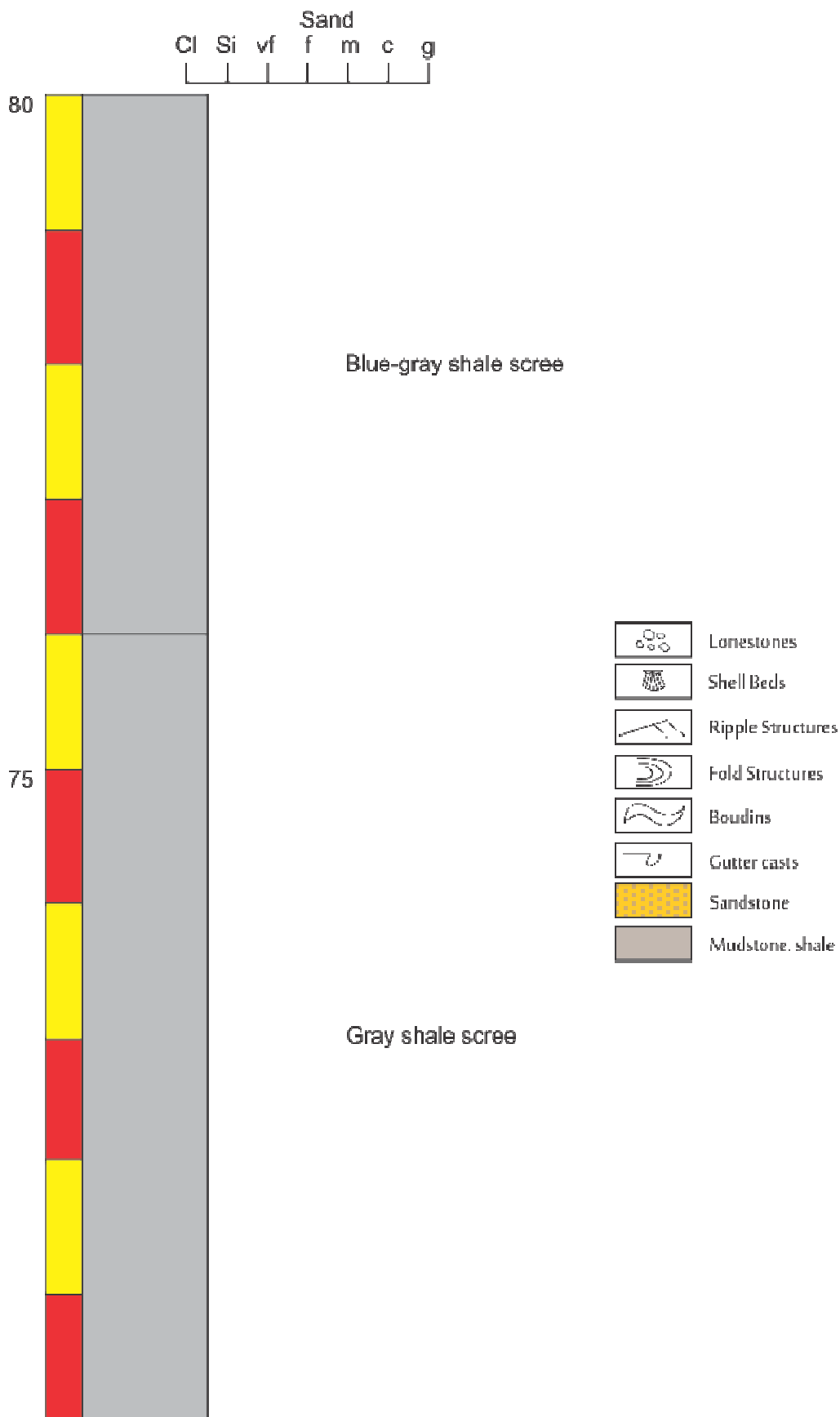


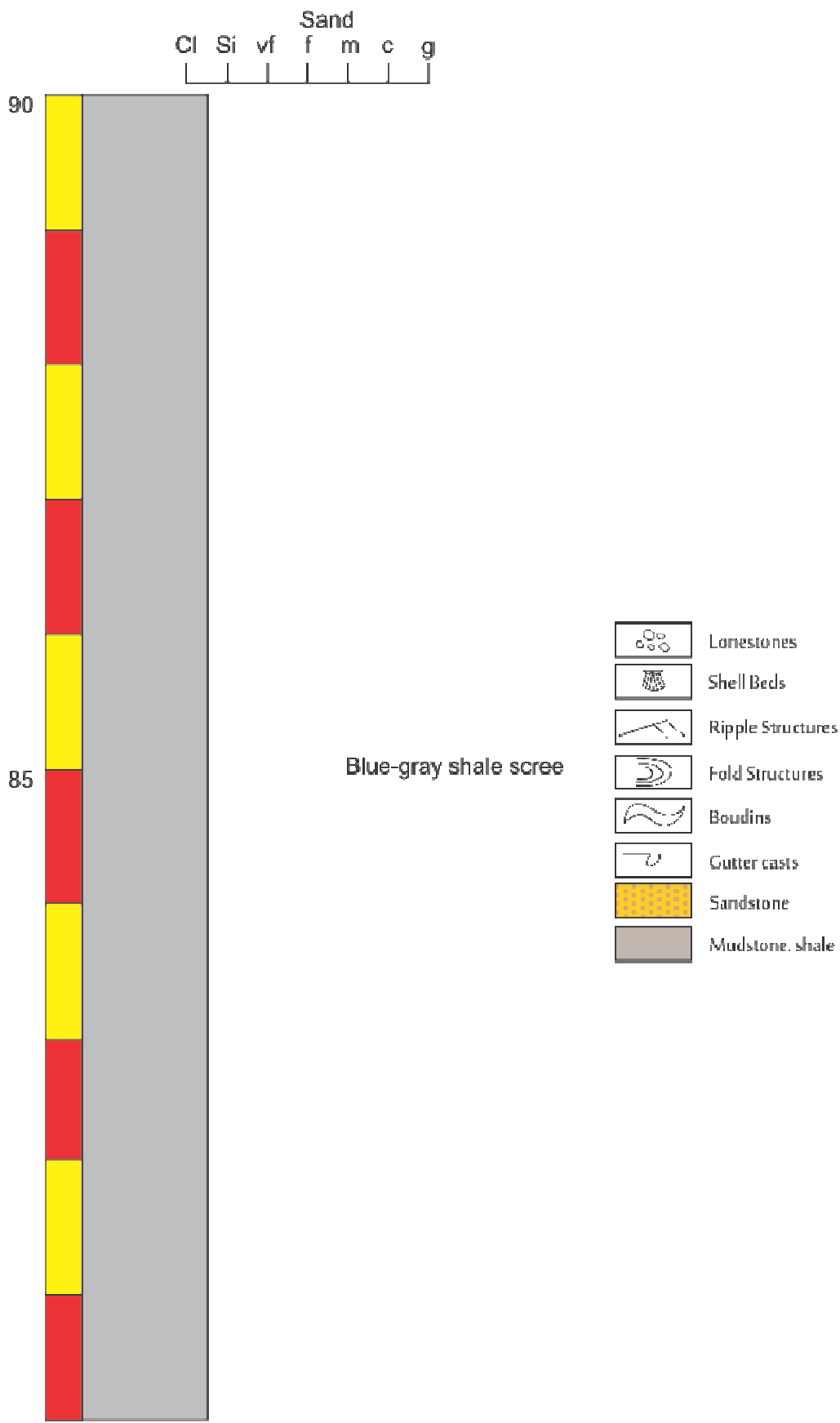


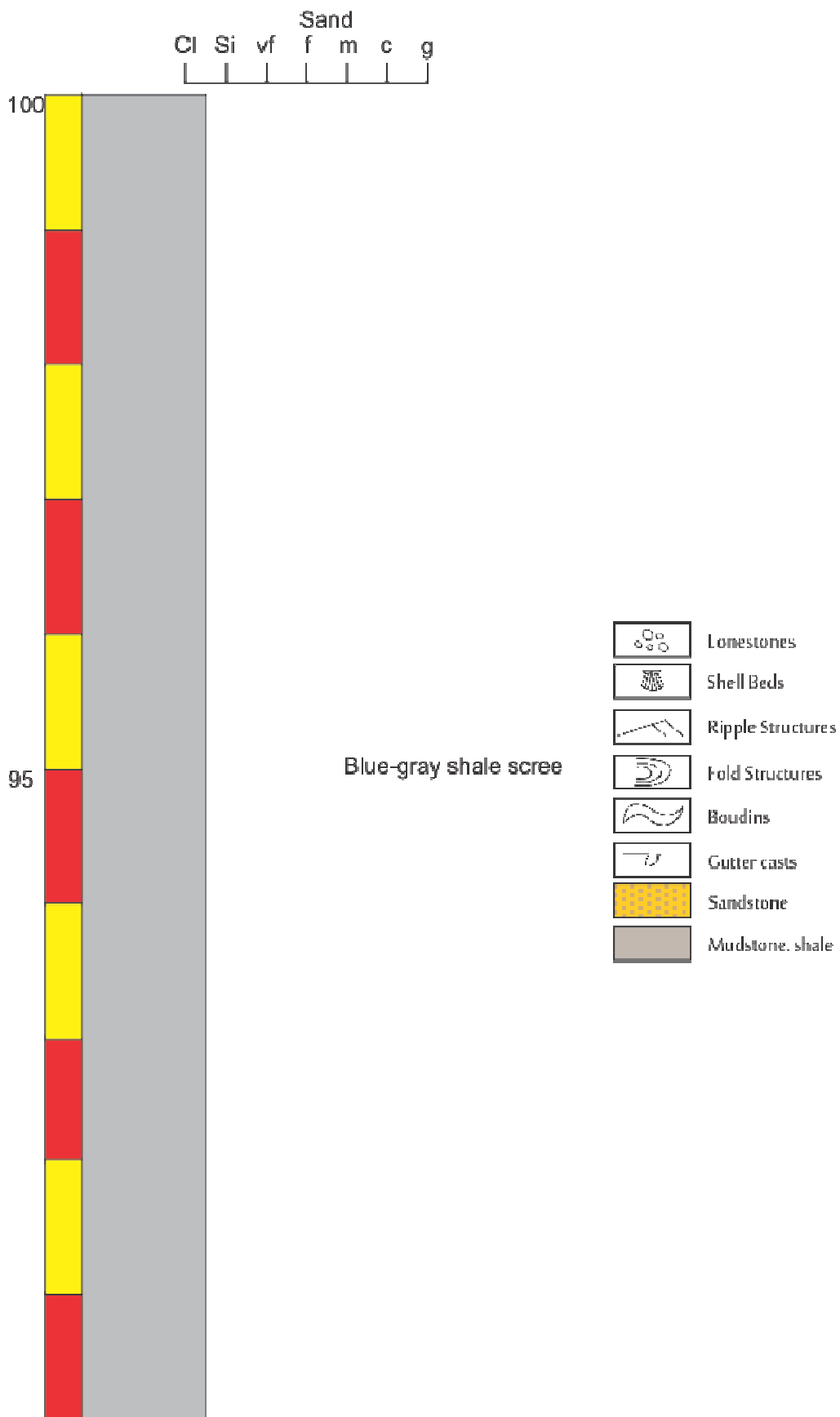


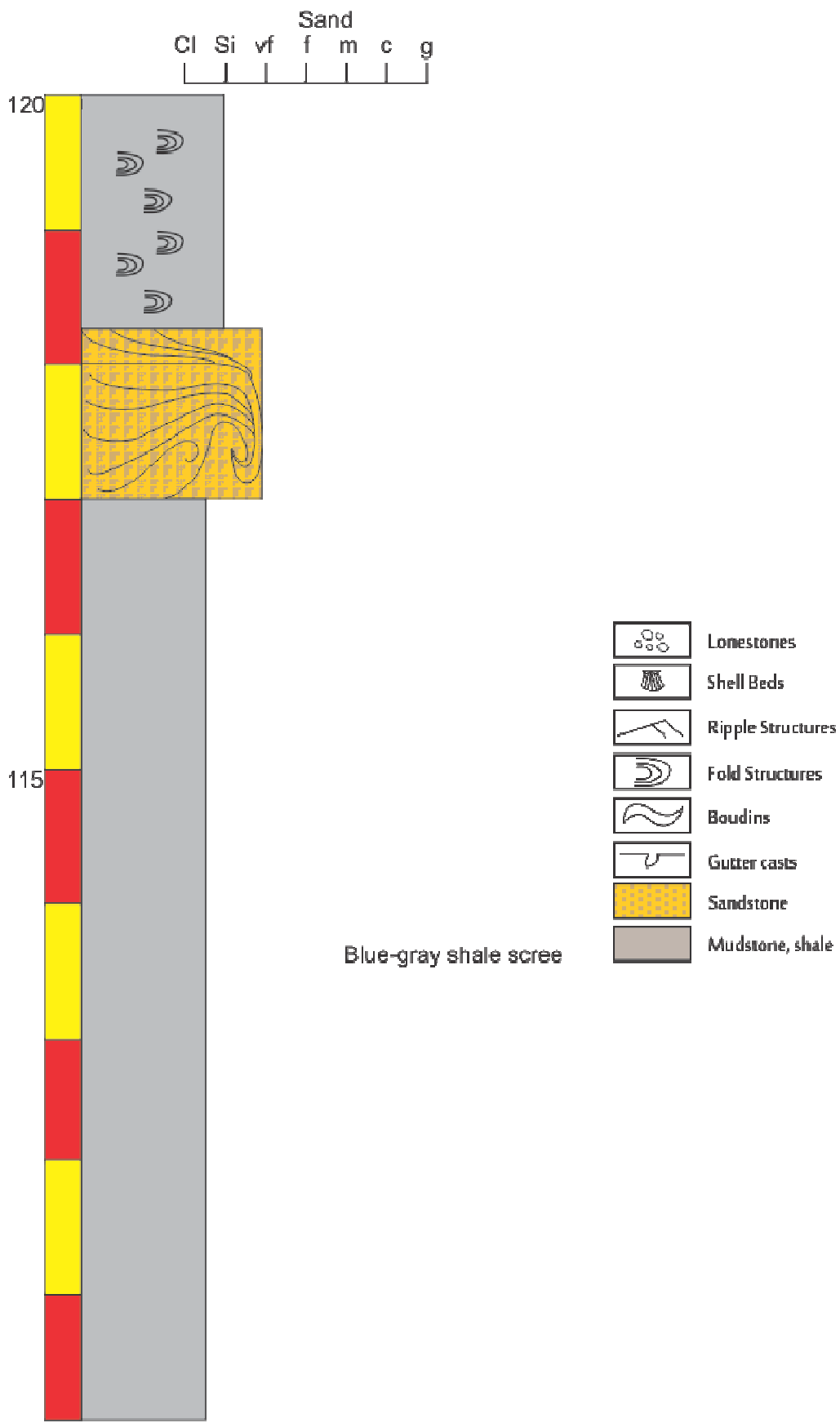


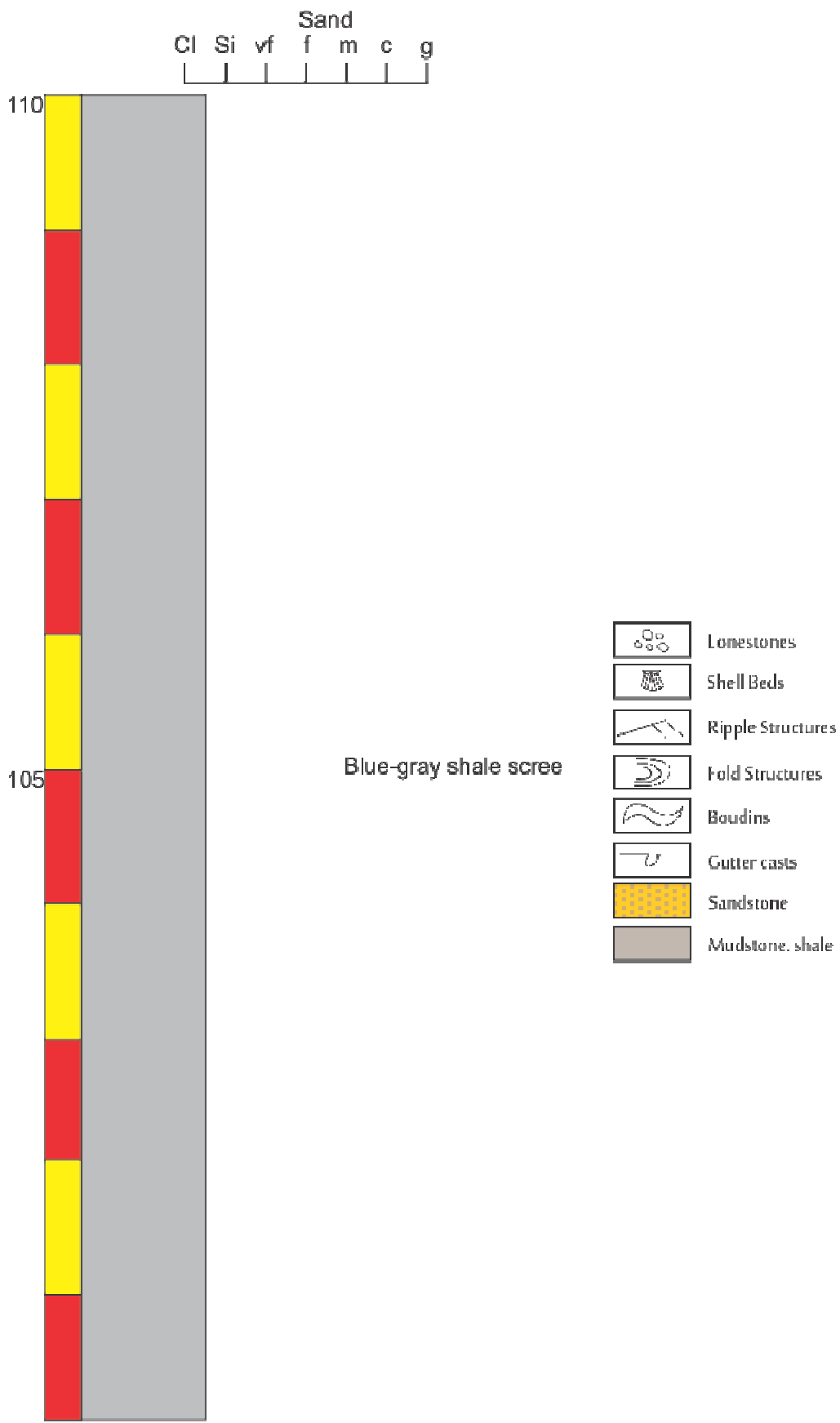


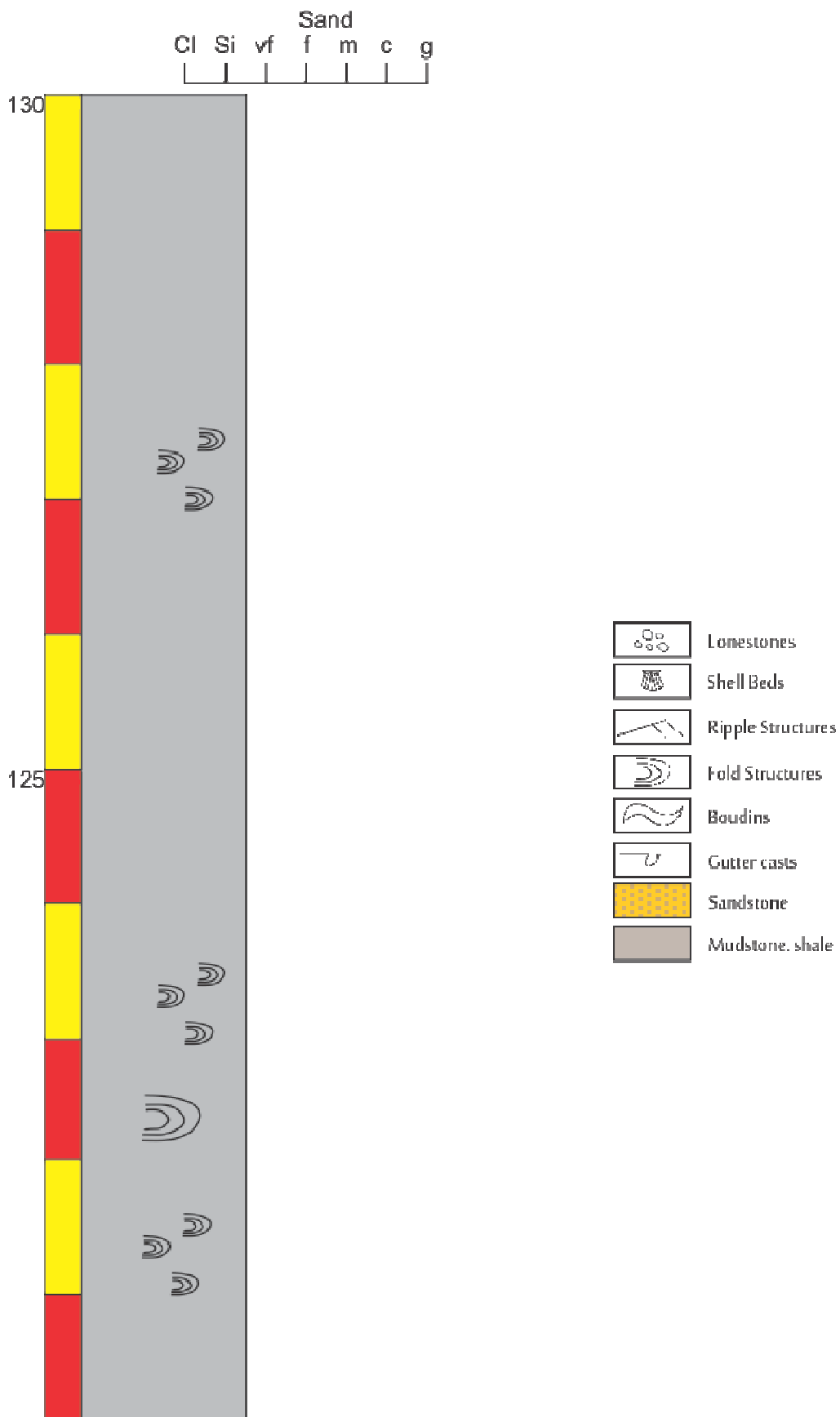


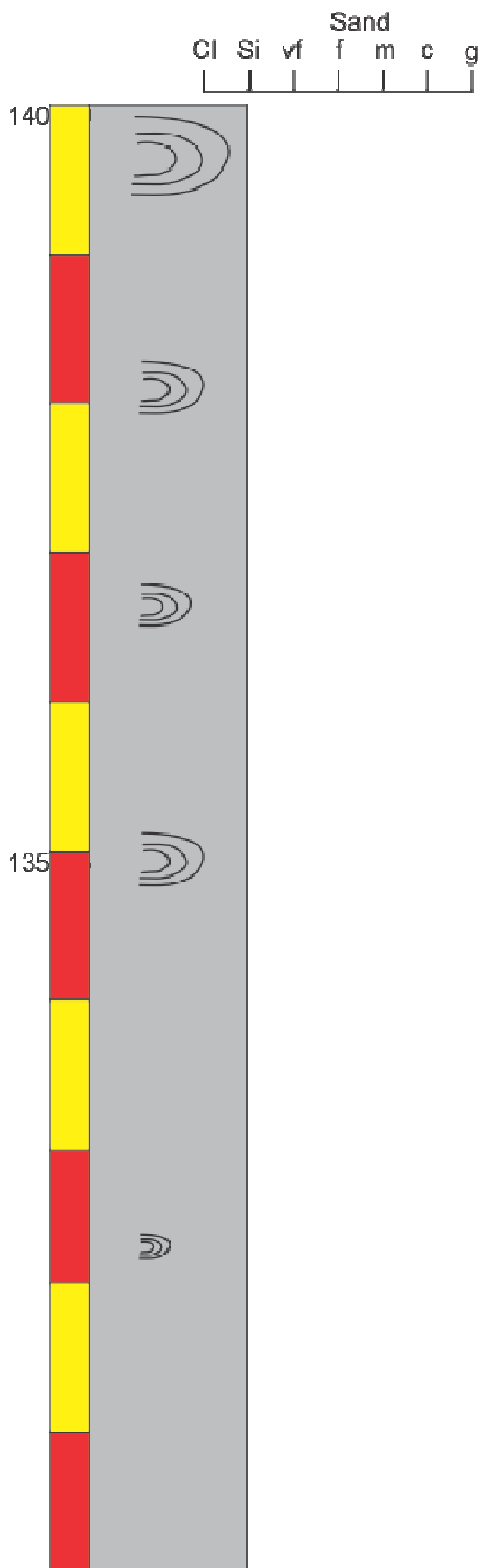












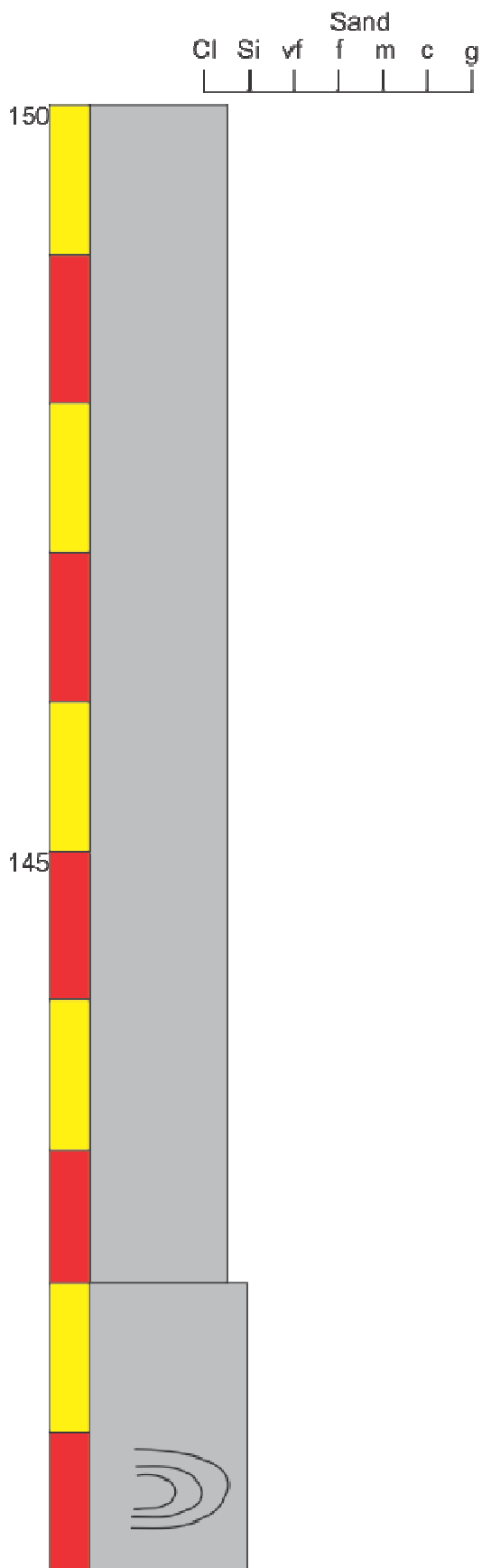












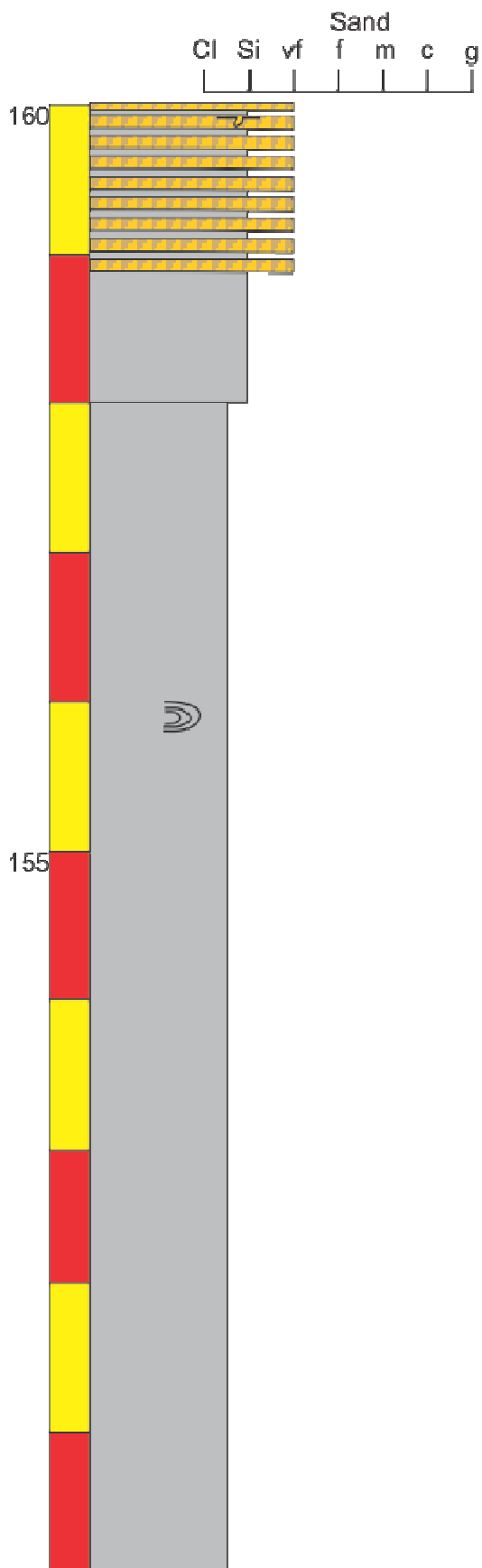












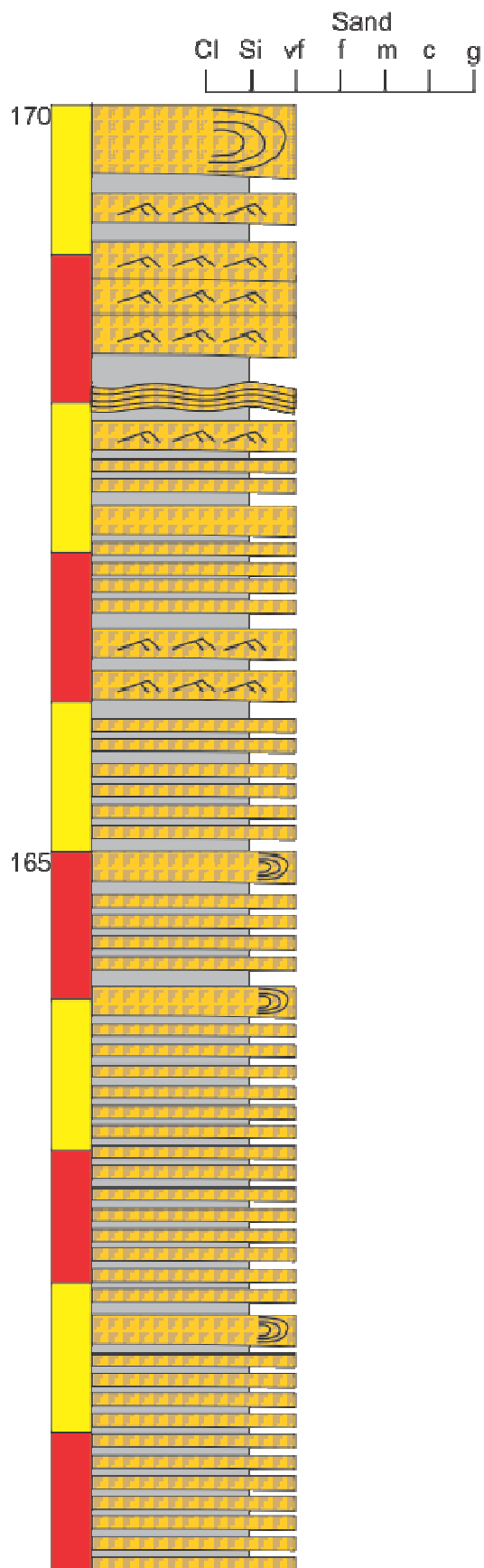
-  Limestones
-  Shell Beds
-  Ripple Structures
-  Fold Structures
-  Boudins
-  Gutter casts
-  Sandstone
-  Mudstone, shale











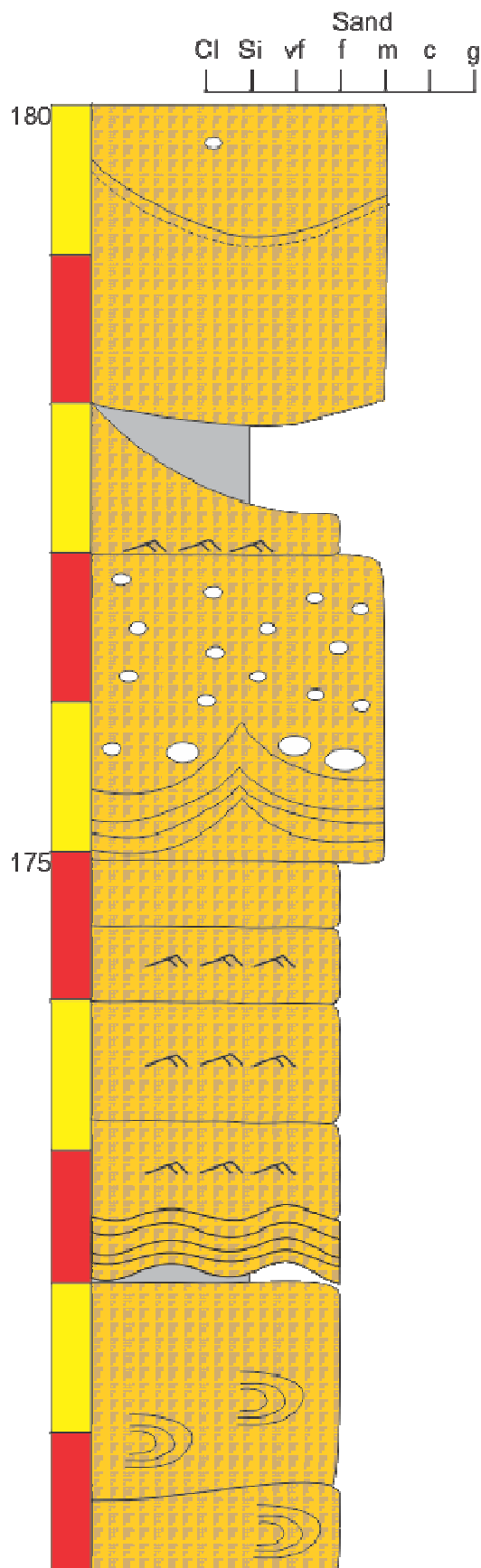
-  Limestones
-  Shell Beds
-  Ripple Structures
-  Fold Structures
-  Boudins
-  Gutter casts
-  Sandstone
-  Mudstone, shale



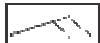







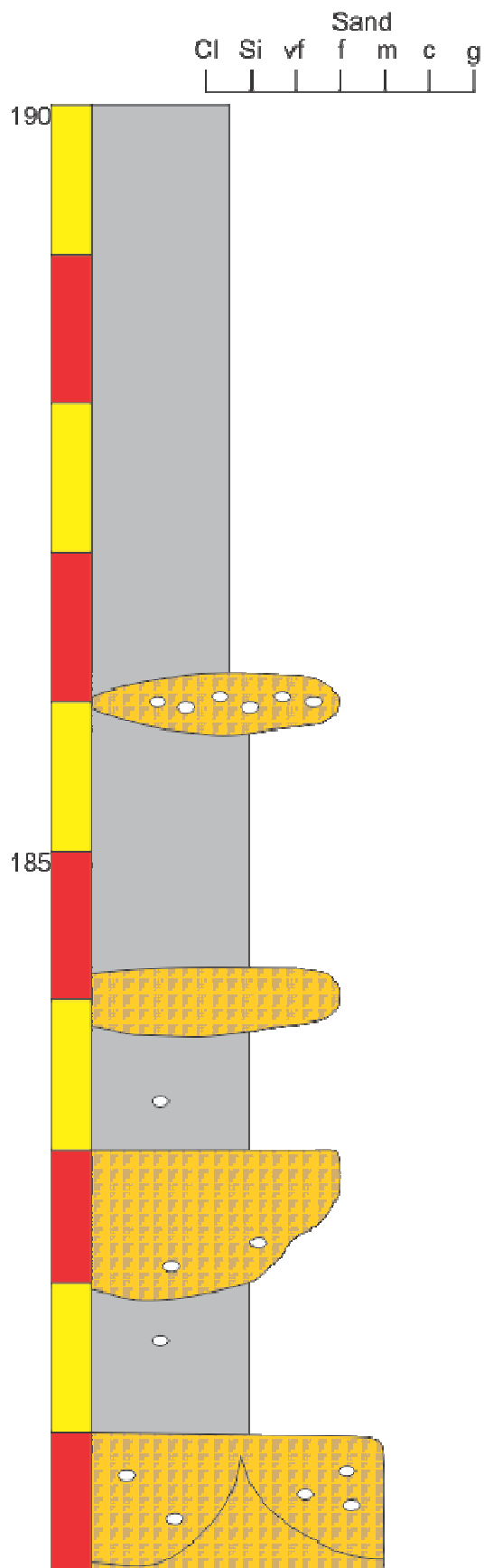
-  Limestones
-  Shell Beds
-  Ripple Structures
-  Fold Structures
-  Boudins
-  Gutter casts
-  Sandstone
-  Mudstone. shale





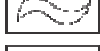





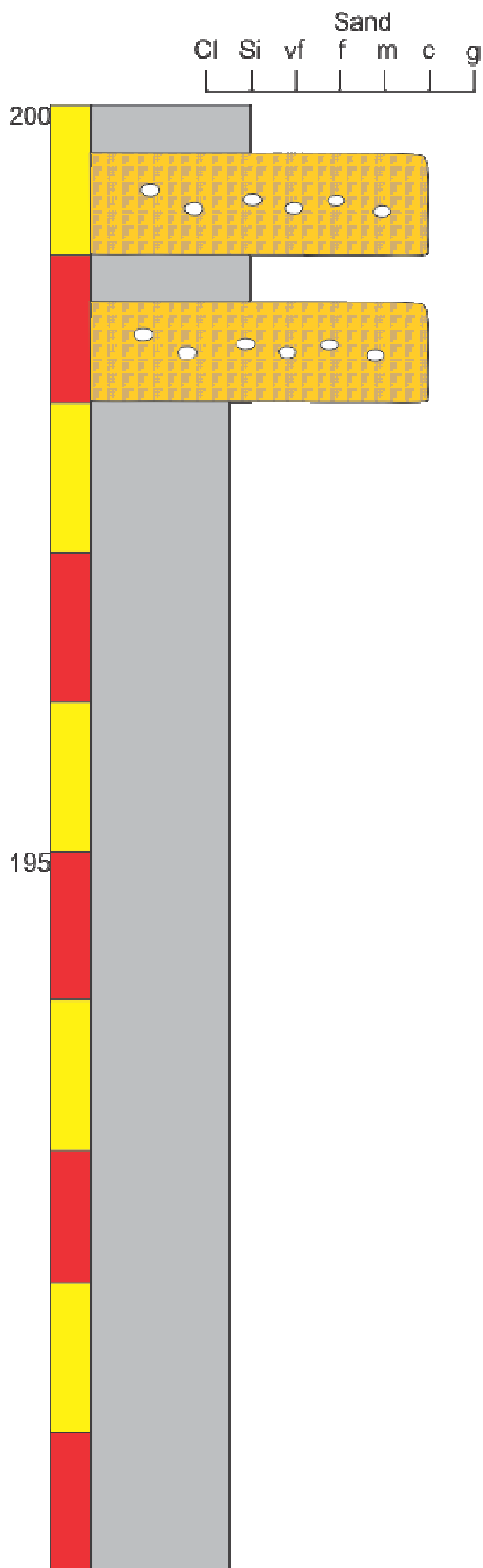
-  Limestones
-  Shell Beds
-  Ripple Structures
-  Fold Structures
-  Boudins
-  Gutter casts
-  Sandstone
-  Mudstone, shale



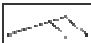







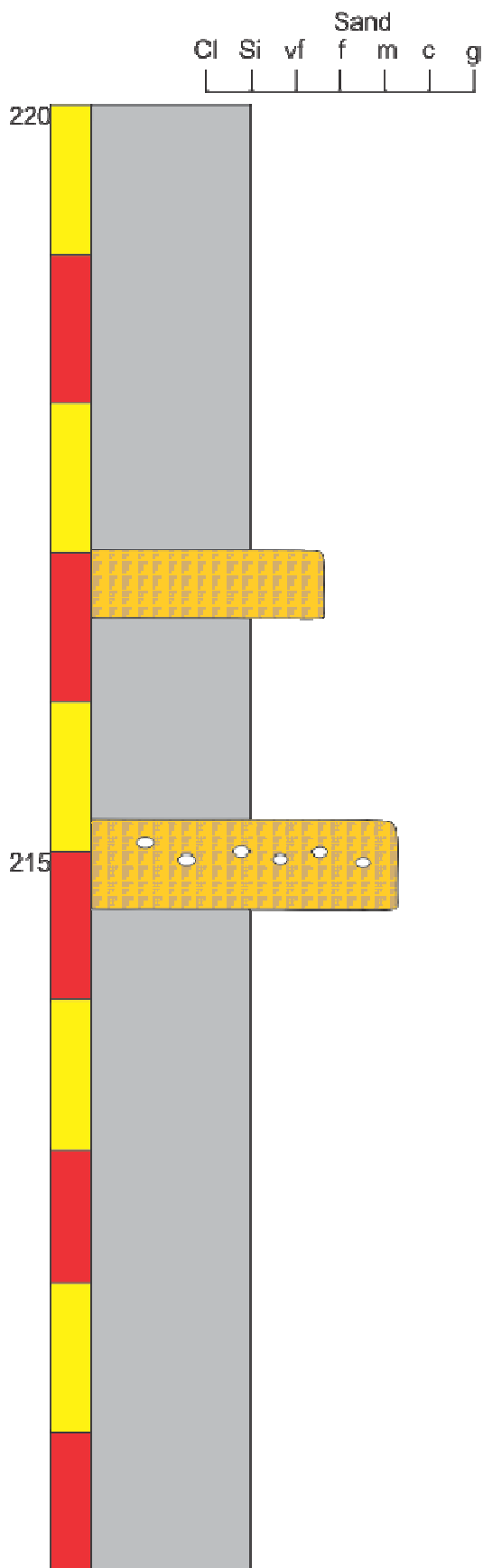
-  Limestones
-  Shell Beds
-  Ripple Structures
-  Fold Structures
-  Boudins
-  Gutter casts
-  Sandstone
-  Mudstone, shale







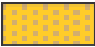



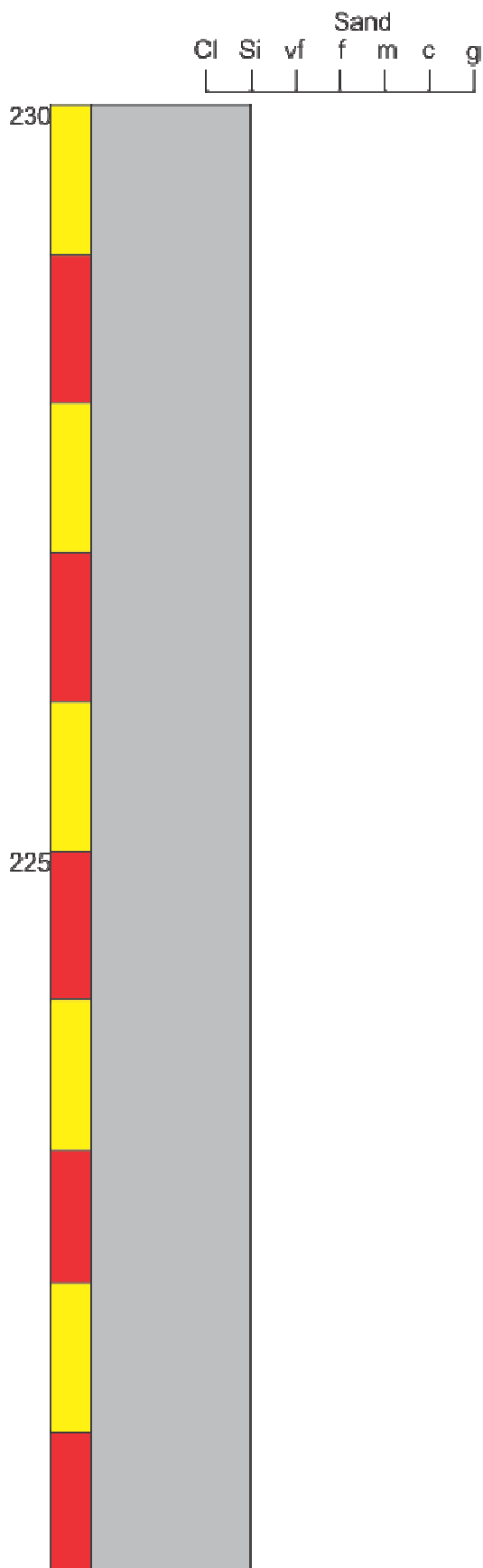
-  Limestones
-  Shell Beds
-  Ripple Structures
-  Fold Structures
-  Boudins
-  Gutter casts
-  Sandstone
-  Mudstone. shale



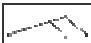







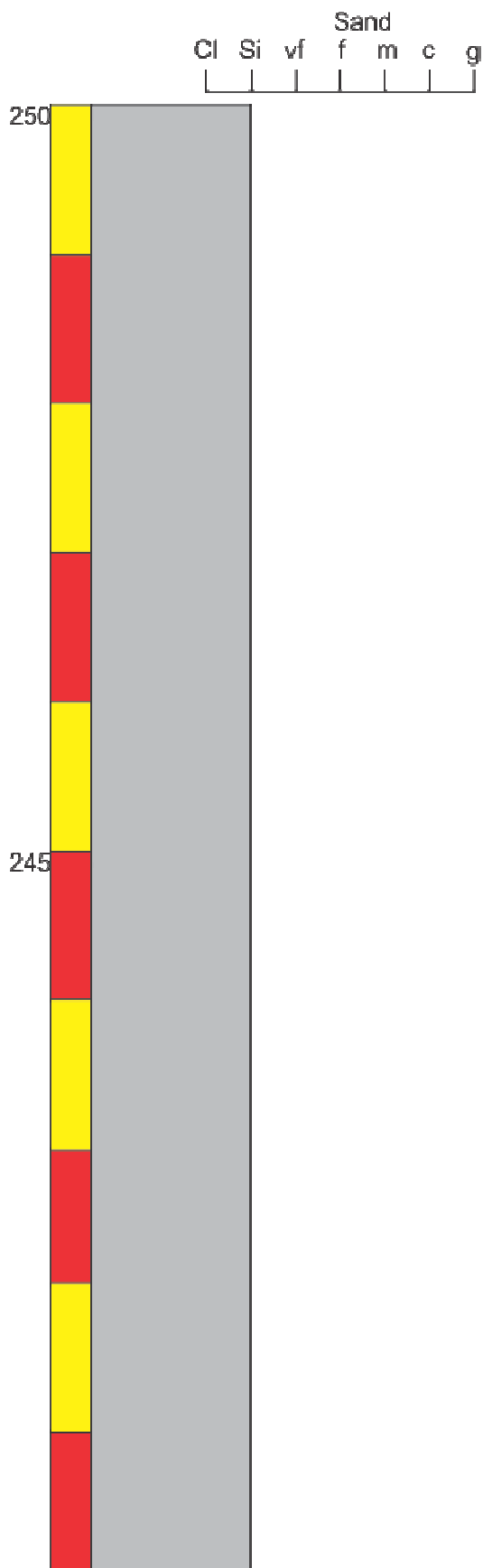
-  Limestones
-  Shell Beds
-  Ripple Structures
-  Fold Structures
-  Boudins
-  Gutter casts
-  Sandstone
-  Mudstone, shale



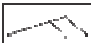







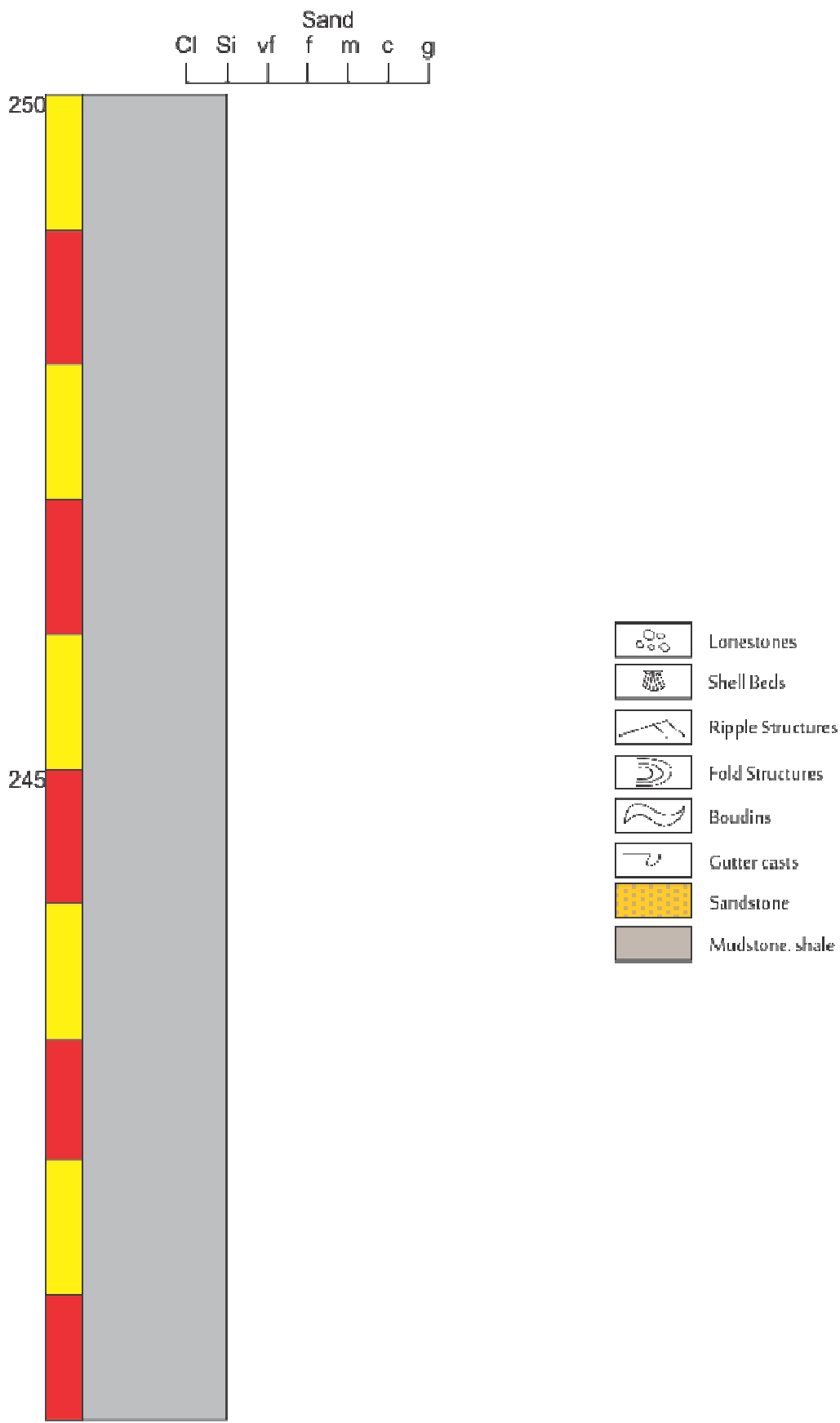
-  Lonestones
-  Shell Beds
-  Ripple Structures
-  Fold Structures
-  Boudins
-  Gutter casts
-  Sandstone
-  Mudstone, shale

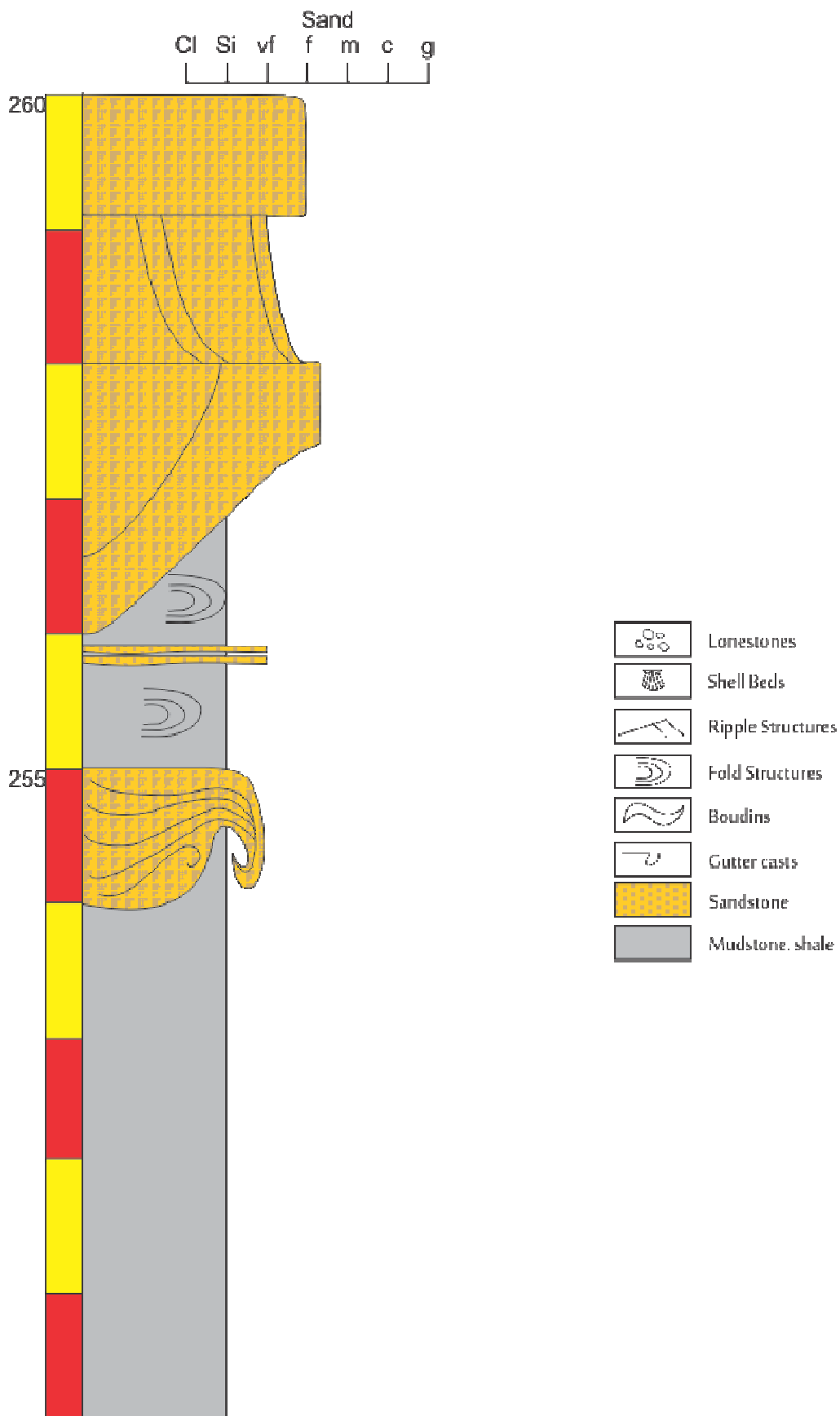


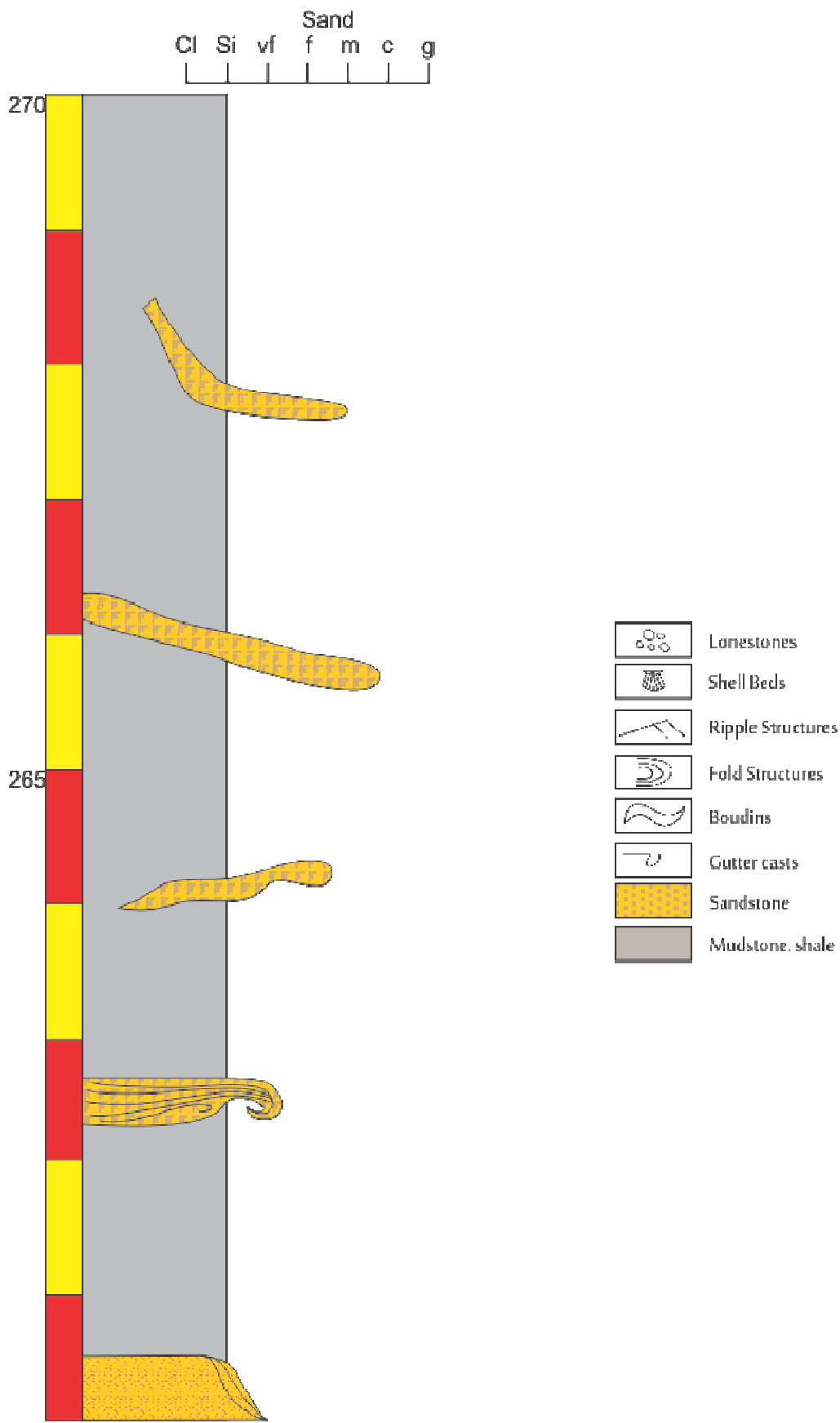
-  Lonestones
-  Shell Beds
-  Ripple Structures
-  Fold Structures
-  Boudins
-  Gutter casts
-  Sandstone
-  Mudstone. shale

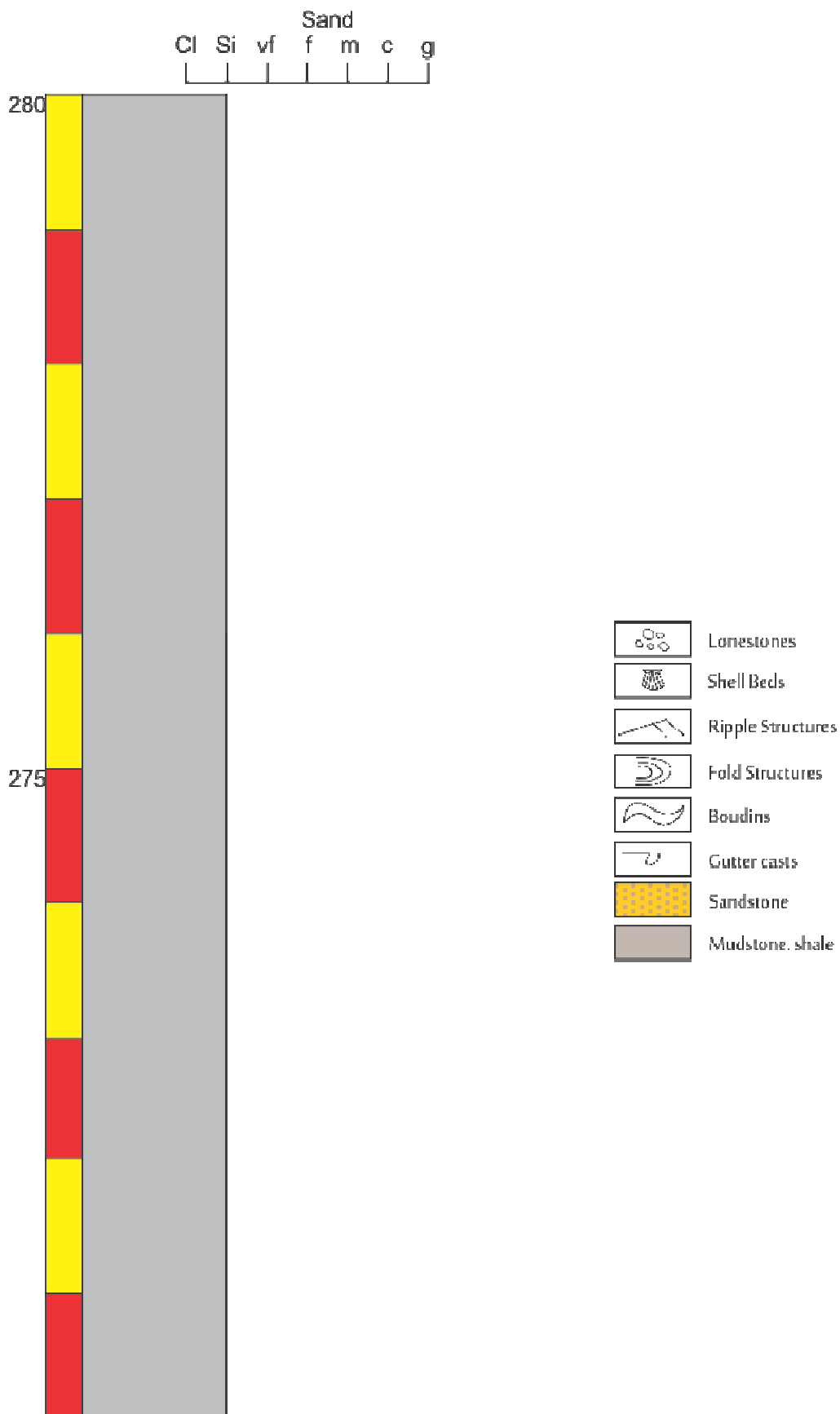


-  Lonestones
-  Shell Beds
-  Ripple Structures
-  Fold Structures
-  Boudins
-  Gutter casts
-  Sandstone
-  Mudstone, shale









Appendix B
Pampa de Tepuel Formation
Paleoecological Data

Z-test with p values	# Genera	# Total	# Genera	# Total	p	1-p
Shell bed 1 v. Shell Bed 2	8.1287	50	8.77213	50	0.169008	0.830992
Shell bed 1 v. Shell Bed 3	8.1287	50	6.69058	50	0.148193	0.851807
Shell bed 1 v. Shell Bed 4	8.1287	50	10.9322	50	0.190609	0.809391
Shell bed 1 v. Shell Bed 5	8.1287	50	9.5737	50	0.177024	0.822976
Shell bed 1 v. Shell Bed 6	8.1287	50	9	50	0.171287	0.828713
Shell Bed 2 v. Shell Bed 3	8.77213	50	6.69058	50	0.154627	0.845373
Shell Bed 2 v. Shell Bed 4	8.77213	50	10.9322	50	0.197043	0.802957
Shell Bed 2 v. Shell Bed 5	8.77213	50	9.5737	50	0.183458	0.816542
Shell Bed 2 v. Shell Bed 6	8.77213	50	9	50	0.177721	0.822279
Shell Bed 3 v. Shell Bed 4	6.69058	50	10.9322	50	0.176228	0.823772
Shell Bed 3 v. Shell Bed 5	6.69058	50	9.5737	50	0.162643	0.837357
Shell Bed 3 v. Shell Bed 6	6.69058	50	9	50	0.156906	0.843094
Shell Bed 4 v. Shell Bed 5	10.9322	50	9.5737	50	0.205059	0.794941
Shell Bed 4 v. Shell Bed 6	10.9322	50	9	50	0.199322	0.800678
Shell Bed 5 v. Shell Bed 6	9.5737	50	9	50	0.185737	0.814263

Table 1. A z-test using the rarefied taxonomic data in order to determine for statistically significant differences in faunal compositions from one shell bed to another. Statistical significance is determined when $p < 0.05$. The p values in this study remain well above 0.05 and are therefore not statistically significant.

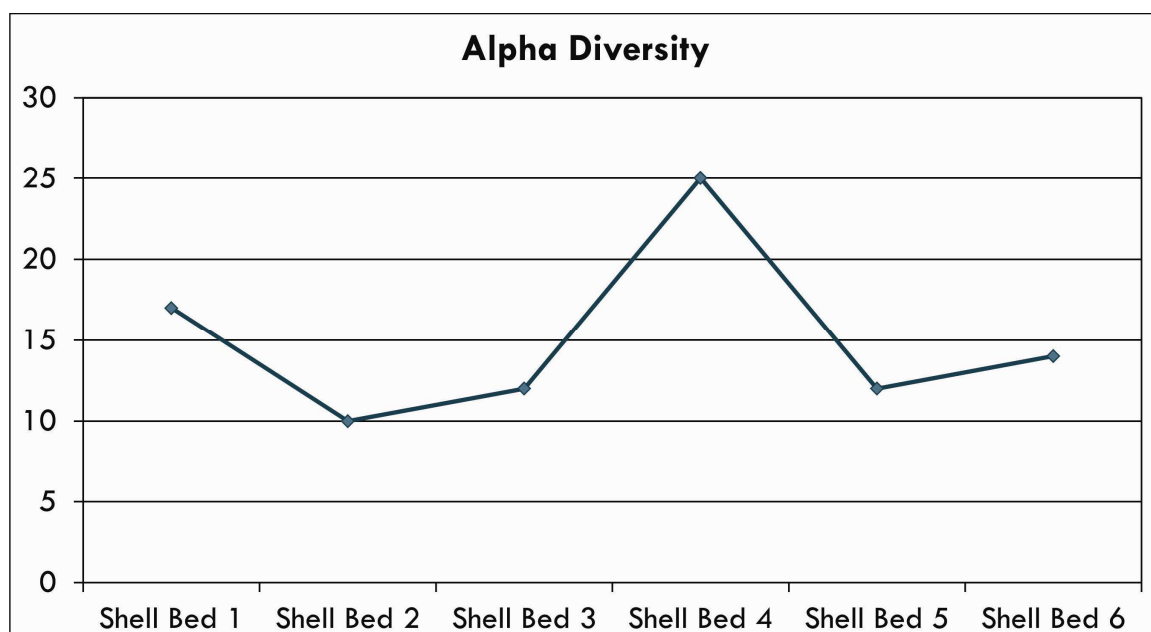


Figure 1. Alpha Diversity, or the total number of species per shell bed, as the shell beds (#1-6) progress through the section stratigraphically for the upper portion of the Pampa de Tepuel Formation.

	Ostracode	Brachiopod	Hyalolith	Bivalve	Gastropod	Crinoid	Coral	Scaphopod	Bryozoan
Mean Rank-Order	1.17	3.17	4.00	2.83	5.83	3.50	6.00	6.00	6.17
Breadth of Distribution	1.00	0.83	0.83	1.00	0.50	1.00	0.50	0.50	0.50

Table 2. Mean rank-order and Breadth of distribution values of the different faunal Classes recorded in Shell Beds #1-6 in the Pampa de Tepuel Formation. Mean rank-order allows for the ordering of the taxa according to their general abundances. Breadth of distribution values measure the proportions of shell beds in which the taxon was present.

Shell Bed 1	Locomotion:	Life Habit:	Diet:	Environment	#
Graphiadactylloides?	actively mobile	epifaunal	detritivore, grazer	hypersaline, marine, brackish, freshwater	165
Crinoids	stationary	upper-level epifaunal	suspension feeder		83
Lanipustula	stationary	low-level epifaunal	suspension feeder		19
Hyalolithids	facultatively mobile	epifaunal	suspension feeder	marine	6
Krotovia?	stationary	low-level epifaunal	suspension feeder		6
Nuculopsis	facultatively mobile	infaunal	deposit feeder-suspension feeder		6
Scaphopod	slow-moving	shallow infaunal	deposit feeder		5
Orbiculopecten	stationary	low-level epifaunal	suspension feeder	marine, brackish	3
small bivalve pieces					2
Schizodus	facultatively mobile	infaunal	suspension feeder		2
Paleoneilo	facultatively mobile	infaunal	deposit feeder		2
Unidentified spirifer	stationary	epifaunal	suspension feeder		2
Rugose	stationary	epifaunal	suspension feeder		1
Fenestra	stationary	epifaunal	suspension feeder		1
Costuloplica	stationary	epifaunal	suspension feeder		1
Euchondria	stationary	epifaunal	suspension feeder		1
Calcareous					1
Atomodesmata	facultatively mobile	infaunal	suspension feeder		1
Unidentified brachiopod	stationary	epifaunal	suspension feeder		1

Shell Bed 2	Locomotion:	Life Habit:	Diet:	Environment	#
Graphiadactylloides?	actively mobile	epifaunal	detritivore, grazer	hypersaline, marine, brackish, freshwater	36
Paleoneilo	facultatively mobile	infaunal	deposit feeder		19
Crinoid	stationary	upper-level epifaunal	suspension feeder		13
Lanipustula	stationary	low-level epifaunal	suspension feeder		9
Beecheria? (Vercheria)	stationary	epifaunal	suspension feeder		3
Unidentified Spiriferiid	stationary	epifaunal	suspension feeder		3
Hyalolith	facultatively mobile	epifaunal	suspension feeder		2
Shell Bed 3	Locomotion:	Life Habit:	Diet:	Environment	#
Graphiadactylloides?	actively mobile	epifaunal	detritivore, grazer	hypersaline, marine, brackish, freshwater	250
Crinoid	stationary	upper-level epifaunal	suspension feeder		24
Hyalolith	facultatively mobile	epifaunal	suspension feeder	marine	17
Paleoneilo	facultatively mobile	infaunal	deposit feeder		11
Rugose	stationary	epifaunal	suspension feeder		9
Lanipustula	stationary	low-level epifaunal	suspension feeder		9
Streblochondria	actively mobile, swimming	nektobenthic	suspension feeder	marine	4
Unidentified Brachiopod	stationary	epifaunal	suspension feeder		2
Spiriferiid?	stationary	epifaunal	suspension feeder		1
Beecheria? (Vercheria)	stationary	epifaunal	suspension feeder		1
Pecteniid?	actively mobile	epifaunal	suspension feeder	marine, brackish	1
Bivalve?					1

**Note that “#” indicates the number of individuals counted.

Shell Bed 4	Locomotion:	Life Habit:	Diet:	Environment	#
Graphiadactyloides?	actively mobile	epifaunal	detritivore, grazer	hypersaline, marine, brackish, freshwater	224
Hyalolith	facultatively mobile	epifaunal	suspension feeder	marine	43
Lanipustula	stationary	low-level epifaunal	suspension feeder		26
Crinoid	stationary	upper-level epifaunal	suspension feeder		19
Spiriferidellidae (big)	stationary	epifaunal	suspension feeder		15
Beecheria? (Vercheria)	stationary	epifaunal	suspension feeder		7
Paleoneilo	facultatively mobile	infaunal	deposit feeder		7
Spiriferinella	stationary	low-level epifaunal	suspension feeder		7
Orbiculopecten	stationary	low-level epifaunal	suspension feeder	marine, brackish	6
Phestia tepuelensis	facultatively mobile	infaunal	deposit feeder-suspension feeder	coastal, inner, outer shelf, deep ocean	5
Spiriferidae indet.	stationary	epifaunal	suspension feeder		4
Gastropod	actively mobile	epifaunal			4
Unidentified brachs	stationary	epifaunal	suspension feeder		3
Rugose	stationary	epifaunal	suspension feeder		3
Unidentified bivalves					3
Streblochondria	actively mobile, swimming	nektobenthic	suspension feeder	marine	2
Paraconularia	stationary	epifaunal	suspension feeder		1
Euchondria	stationary	epifaunal	suspension feeder		1
Paleolima	stationary	epifaunal	suspension feeder	marine, brackish	1
Euchondria indet.	stationary	epifaunal	suspension feeder		1
Paleotaxodont indet.	stationary	epifaunal	suspension feeder		1
Unidentified (little) spir.	stationary	epifaunal	suspension feeder		1
Branching bryozoan	stationary	epifaunal	suspension feeder		1
Nuculopsis	facultatively mobile	infaunal	deposit feeder-suspension feeder		1
Scaphopod	slow-moving	shallow infaunal	deposit feeder		1

Shell Bed 5	Locomotion:	Life Habit:	Diet:	Environment	#
Graphiadactyloides?	actively mobile	epifaunal	detritivore, grazer	hypersaline, marine, brackish, freshwater	55
Lanipustula	stationary	low-level epifaunal	suspension feeder		13
Hyalolith	facultatively mobile	epifaunal	suspension feeder	marine	5
Beecheria? (Vercheria)	stationary	epifaunal	suspension feeder		4
Spiriferellina	stationary	low-level epifaunal	suspension feeder		4
Unidentified Spiriferid	stationary	epifaunal	suspension feeder		3
Gastropod	actively mobile	epifaunal			2
Phestia	facultatively mobile	infaunal	deposit feeder-suspension feeder	coastal, inner, outer shelf, deep ocean	2
Euchondriidae Unident. Bvalve	stationary	epifaunal	suspension feeder		1
Paleoneilo	facultatively mobile	infaunal	deposit feeder		1
Krotovia?	stationary	low-level epifaunal	suspension feeder		1
Crinoid	stationary	upper-level epifaunal	suspension feeder		1

**Note that “#” indicates the number of individuals counted.

Shell Bed 6	Locomotion:	Life Habit:	Diet:	Environment	#
Leptodesma?	stationary	epifaunal	suspension feeder	marine, brackish	9
Graphiadactylloides?	actively mobile	epifaunal	detritivore, grazer	hypersaline, marine, brackish, freshwater	8
Nuculopsis (patagoniensis?)	facultatively mobile	infaunal	deposit feeder-suspension feeder		7
Unidentified bivalve3					6
Crinoid	stationary	upper-level epifaunal	suspension feeder		6
Phestia tepuelensis	facultatively mobile	infaunal	deposit feeder-suspension feeder	coastal, inner, outer shelf, deep ocean	4
Scaphopod	slow-moving	shallow infaunal	deposit feeder		3
Unidentified gastro	actively mobile	epifaunal			3
Unidentified fossil					3
Plant remains					2
Unidentified bivalve1					1
Unidentified bivalve2					1
Nuculopsis nuculanella	facultatively mobile	infaunal	deposit feeder-suspension feeder		1
Streblochondria	actively mobile, swimming	nektobenthic	suspension feeder	marine	1

**Note that “#” indicates the number of individuals counted.